

# **Topology and Function of the Inner Envelope Protein Tic110**

Dissertation der Fakultät für Biologie  
der  
Ludwig-Maximilians-Universität München

vorgelegt von  
**Inga Sjuts**  
aus Leer

München, Januar 2018

Diese Dissertation wurde angefertigt unter der Leitung von Prof. Dr. Jürgen Soll an der Fakultät für Biologie der Ludwig-Maximilians-Universität München.

Erstgutachter: Prof. Dr. Jürgen Soll

Zweitgutachter: Prof. Dr. Marc Bramkamp

Tag der Abgabe: 30.01.2018

Tag der mündlichen Prüfung: 11.4.2018

## Summary

Chloroplasts originated from an endosymbiotic event in which a free-living cyanobacterium was engulfed by an ancestral eukaryotic host. During evolution the majority of the chloroplast genetic information was transferred to the host cell nucleus. As a consequence, proteins formerly encoded by the chloroplast genome are now translated in the cytosol and must be subsequently imported into the chloroplast. During import, proteins have to overcome the two barriers of the chloroplast envelope, namely the outer envelope membrane (OEM) and the inner envelope membrane (IEM). In the majority of cases, this is facilitated by two distinct multiprotein complexes, located in the OEM and IEM, respectively, designated TOC and TIC.

The involvement of the most abundant TIC component, Tic110, in protein import into chloroplasts is well established. However, two controversial models concerning the topology of Tic110 still persist and prevent the assignment of a clear structure-function relationship of Tic110. In this study, new complementary *in situ*, *in vivo* and *in vitro* approaches were used to provide insights into the topology and function of Tic110.

From limited proteolysis using isolated inner envelope vesicles it could be concluded that Tic110 exposes domains which are found in the intermembrane space of chloroplasts. Furthermore, using an isobaric labeling strategy, two peptides could be sequenced which have a high probability to be in one out of two loops which is protruding in the intermembrane space.

By placing the small singlet-oxygen producing protein miniSOG at positions which are predicted to be located in the intermembrane space it was aimed to locate specific domains of Tic110 at nanoscale resolution. The functionality of tagged proteins was assessed via complementation of heterozygous *TIC110/tic110* plants. So far, a strong yellowish phenotype could be observed for plants transformed with a construct that places miniSOG at one predicted intermembrane space-orientated domain.

By using a liposome leakage assay it could be confirmed that Tic110 forms a channel in liposomes, which is protein-concentration dependent and that this channel-formation ability can be blocked via oxidation and enhanced via reduction of the protein.

Constructs of Tic110 were generated that carry an amber codon at various positions within the four predicted amphipathic helices in order to generate distinct site-specific protein-fluorophore conjugations by means of co-translational amber suppression, which will be used for follow-up FRET analyses. To gain further insights into the structure and function of Tic110, preliminary pictures from electron microscopy were taken. The computational analysis of these pictures will presumably resolve the three-dimensional structure of Tic110 in the future.

## Zusammenfassung

Chloroplasten entstammen einem endosymbiotischen Ereignis, bei dem ein freilebendes Cyanobakterium von einem eukaryotischen Wirt aufgenommen wurde. Während der Evolution wurde der Großteil der genetischen Informationen der Chloroplasten auf den Zellkern der Wirtszelle übertragen. Als Konsequenz werden Proteine, die früher vom Chloroplastengenom kodiert wurden, nun im Zytosol translatiert und müssen anschließend in den Chloroplasten importiert werden. Beim Import müssen Proteine die zwei Barrieren der Chloroplastenhülle überwinden: die äußere und innere Hüllmembran. In den meisten Fällen wird dies durch zwei verschiedene Multiproteinkomplexe erleichtert, die sich in der äußeren bzw. inneren Hüllmembran befinden und als TOC und TIC bezeichnet werden.

Das innere Hüllmembranprotein Tic110 kommt am häufigsten innerhalb des TIC Komplexes vor. Seine Beteiligung beim Import von Proteinen in Chloroplasten ist gut belegt. Es bestehen jedoch immer noch zwei umstrittene Modelle bezüglich der Topologie von Tic110, die die Zuordnung einer klaren Struktur-Funktionsbeziehung von Tic110 verhindern.

In dieser Studie wurden komplementäre *in situ*-, *in vivo*- und *in vitro*-Ansätze verwendet, um weitere Einblicke in die Topologie und Funktion von Tic110 zu erhalten.

Aus Proteasebehandlung isolierter innerer Hüllmembranen konnte geschlossen werden, dass Tic110 Domänen freilegt, die ursprünglich im Intermembranraum von Chloroplasten gefunden wurden. Darüber hinaus konnten unter Verwendung einer isobaren Markierungsstrategie zwei Peptide sequenziert werden, die sich mit hoher Wahrscheinlichkeit in einer der zwei Domänen von Tic110 befinden, die in den Intermembranraum ragen.

Indem das kleine singulett-sauerstoffproduzierende Protein miniSOG an Positionen von Tic110 platziert wurde, die eine vorhergesagte Orientierung in den Intermembranraum besitzen, wurde das Ziel verfolgt, mittels Elektronenmikroskopie spezifische Domänen von Tic110 mit einer Auflösung im Nanobereich zu lokalisieren. Die Funktionalität von markierten Proteinen wurde durch Komplementation von heterozygoten *TIC110/tic110*-Pflanzen beurteilt. Bisher konnte ein stark gelblicher Phänotyp für Pflanzen beobachtet werden, die mit einem Konstrukt transformiert wurden, das miniSOG an einer vorhergesagten intermembranraum-orientierten Domäne anordnet.

Mithilfe eines Liposomen-Freisetzung Experiments konnte bestätigt werden, dass Tic110 in Liposomen einen Kanal bildet, der abhängig von der eingesetzten Proteinkonzentration ist, und dass diese Kanalbildungsfähigkeit durch Oxidation blockiert und durch Reduktion verstärkt werden kann.

Weiterhin wurden Konstrukte von Tic110 erzeugt, die ein *amber*-Codon an verschiedenen Positionen innerhalb der vier vorhergesagten amphipathischen Helices tragen, um regio-

spezifische Protein-Fluorophor-Konjugationen mittels co-translationaler *amber*-Unterdrückung zu erzeugen. Die erzeugten Protein-Fluorophor-Konjugationen können nun für nachfolgende FRET-Experimente verwendet werden, um Aufschluss über die räumliche Anordnung der kanalbildenden Helices zu bringen.

Um weitere Einblicke in die Struktur und Funktion von Tic110 zu erhalten, wurden erste Bilder aus der Elektronenmikroskopie angefertigt. Die computergestützte Analyse dieser Bilder wird vermutlich die dreidimensionale Struktur von Tic110 in Zukunft auflösen.

## Abbreviations

|         |   |
|---------|---|
| AAA     | ATPases associated with various cellular activities |
| aaRS    | aminoacyl-tRNA synthetase                           |
| ACCase  | acetyl-CoA carboxylase                              |
| ACN     | acetonitrile  |
| Apa     | acetylphenylalanine                                 |
| At      | <i>Arabidopsis thaliana</i>                         |
| BN      | blue native   |
| CB      | cacodylate buffer                                   |
| CBB     | Commassie brilliant blue                            |
| cDNA    | copyDNA   |
| CID     | collision-induced dissociation                      |
| cTP     | chloroplastic transit peptide                       |
| Cys     | cysteine  |
| DAB     | diaminobenzidine                                    |
| DAS     | dense alignment surface                             |
| DMSO    | dimethylsulfoxide                                   |
| dN      | delta N-terminus                                    |
| DSSO    | disuccinimidyl sulfoxide                            |
| DTT     | dithiothreitol                                      |
| ECL     | enhanced chemiluminescence                          |
| EM      | electron microscopy                                 |
| FMN     | flavomononucleotide                                 |
| gDNA    | genomicDNA  |
| His     | histidine-tag                                       |
| IAA     | iodoacetamide                                       |
| IEM     | inner envelope membrane                             |
| IEP     | inner envelope protein                              |
| ims     | intermembrane space                                 |
| IPTG    | isopropyl- $\beta$ -D-thiogalactopyranoside         |
| ISC     | intersystem crossing                                |
| kDa     | kilo Dalton   |
| LC      | liquid chromatography                               |
| LDAO    | lauryldimethylamine oxide                           |
| LDS     | lithium dodecyl sulfate                             |
| miniSOG | mini singlet oxygen generator                       |
| MS      | mass spectrometry                                   |
| NADPH   | nicotinamide adenine dinucleotide phosphate         |
| NHS     | N-hydroxysuccinimid                                 |
| Ni-NTA  | nickel-nitrilotriacetic acid                        |
| OEM     | outer envelope membrane                             |
| PAGE    | polyacrylamid gel electrophoresis                   |
| PBS     | phosphate buffered saline                           |
| PC      | phosphatidylcholine                                 |
| PEG     | polyethylene glycol                                 |
| Ps      | <i>Pisum sativum</i>                                |
| PVDF    | polyvinylidene fluoride                             |
| rpm     | revolutions per minute                              |
| RT      | room temperature                                    |
| s       | seconds   |
| SDS     | sodium dodecyl sulfate                              |
| smFRET  | single molecule Förster resonance energy transfer   |

|         |  |
|---------|--|
| SPP     | stromal processing peptidase                         |
| TCA     | trichloroacetic acid                                 |
| TMT     | tandem mass tag                                      |
| TOC/TIC | translocon on the outer/inner chloroplast membrane   |
| TOM/TIM | translocon on the outer/inner mitochondrial membrane |
| UAA     | unnatural amino acid                                 |
| WT      | wild type  |

## Table of contents

|   |           |
|---|-----------|
| Summary .....   | I         |
| Zusammenfassung .....   | II        |
| Abbreviations .....   | IV        |
| Table of contents .....   | VI        |
| <b>1. Introduction .....</b>  | <b>1</b>  |
| 1.1 Protein import into chloroplasts.....   | 1         |
| 1.2 Cytosolic sorting of preproteins and targeting to the organelle .....                 | 1         |
| 1.3 Crossing the outer envelope membrane via the TOC complex.....                         | 3         |
| 1.4 Crossing the intermembrane space and inner envelope membrane via the TIC complex..... | 6         |
| 1.5 Completion of the translocation process: the stromal chaperone system .....           | 10        |
| 1.6 Redox sensing at the inner envelope membrane .....                                    | 13        |
| 1.7 Aim of the study .....  | 14        |
| <b>2. Materials .....</b>   | <b>15</b> |
| 2.1 Chemicals .....   | 15        |
| 2.2 Molecular weight markers and DNA standards .....                                      | 15        |
| 2.3 Enzymes and Kits.....   | 15        |
| 2.4 Strains, constructs and oligonucleotides .....  | 15        |
| 2.5 Antibodies .....  | 18        |
| 2.6 Columns .....   | 18        |
| 2.7 Plant material .....  | 18        |
| <b>3. Methods .....</b>   | <b>19</b> |
| <b>3.1 Plant methods .....</b>  | <b>19</b> |
| 3.1.1 Growth conditions.....  | 19        |
| 3.1.2 Stable transformation of <i>Arabidopsis thaliana</i> .....                          | 19        |
| 3.1.3 Transient expression of recombinant proteins in <i>Nicotiana benthamiana</i> .....  | 19        |
| <b>3.2 Molecular biological methods .....</b>   | <b>20</b> |
| 3.2.1 DNA cloning .....   | 20        |
| 3.2.2 Sequencing .....  | 21        |
| 3.2.3 Preparation of genomic DNA from <i>Arabidopsis thaliana</i> .....                   | 21        |
| 3.2.4 Genotyping.....   | 21        |
| 3.2.5 Transformation of <i>Agrobacterium tumefaciens</i> .....                            | 21        |
| <b>3.3 Biochemical methods.....</b>   | <b>21</b> |
| 3.3.1 Isolation of crude protein extracts from plants .....                               | 22        |
| 3.3.2 Preparation of samples for electron microscopy and photooxidation .....             | 22        |



|   |    |
|---|----|
| 3.3.3 Chloroplast isolation from <i>N. benthamiana</i> .....  | 22 |
| 3.3.4 Protoplast isolation from <i>N. benthamiana</i> .....   | 23 |
| 3.3.5 Immunoblotting .....  | 23 |
| 3.3.6 Isolation of outer and inner envelope membranes from pea .....  | 24 |
| 3.3.7 Chlorophyll determination .....   | 24 |
| 3.3.8 Trypsin treatment of inner envelope membranes .....   | 24 |
| 3.3.9 Tandem Mass Tag labeling and quantification of peptides .....   | 25 |
| 3.3.10 Biotinylation of inner envelope membranes .....  | 25 |
| 3.3.11 Overexpression of proteins .....   | 25 |
| 3.3.12 Co-translational incorporation of the unnatural amino acid into dNTic110 .....   | 26 |
| 3.3.13 Purification of proteins .....   | 26 |
| 3.3.14 Reconstitution of purified dNTic110 into liposomes and flotation assay .....   | 27 |
| 3.3.15 DSSO cross-linking .....   | 27 |
| 3.3.16 Labeling of proteins .....   | 28 |
| 3.3.17 Encapsulation of carboxyfluorescein and fluorescence spectroscopy .....  | 28 |
| 3.3.18 Reduction and oxidation assay .....  | 28 |
| <b>4. Results</b> .....   | 29 |
| <b>4.1 Two topological models of Tic110</b> .....   | 29 |
| <b>4.2 <i>In situ</i> topology of the inner envelope protein Tic110</b> .....   | 32 |
| 4.2.1 Selective biotinylation of inner envelope membranes .....   | 32 |
| 4.2.2 Limited proteolysis of inner envelope membranes .....   | 34 |
| 4.2.3 Tandem Mass Tag labeling and quantification of tryptic peptides .....   | 37 |
| <b>4.3 <i>In vivo</i> topology of Tic110: use of a genetically encoded tag for light and electron microscopy</b> .....                          | 40 |
| 4.3.1 Expression and localization of transiently expressed miniSOG-tagged Tic110 proteins .....   | 42 |
| 4.3.2 Photooxidation of chloroplasts expressing transiently miniSOG-tagged Tic110 .....   | 45 |
| 4.3.3 Functional <i>in vivo</i> analysis of miniSOG-tagged Tic110 proteins in heterozygous <i>TIC110/tic110</i> <i>Arabidopsis</i> plants ..... | 47 |
| 4.3.4 Role of regulatory cysteines in Tic110 <i>in vivo</i> .....   | 50 |
| <b>4.4 Topology of Tic110 in a reconstituted proteoliposome system</b> .....  | 52 |
| 4.4.1 DSSO cross-linking of reconstituted dNTic110 in proteoliposomes .....   | 53 |
| 4.4.2 Liposome leakage assay with dNTic110-containing proteoliposomes .....   | 55 |
| 4.4.3 Incorporation of the unnatural amino acid acetylphenylalanine at specific positions of dNTic110 .....                                     | 57 |
| 4.4.3.1 Expression of dNTic110 carrying acetylphenylalanine .....   | 58 |
| 4.4.3.2 Purification of dNTic110 featuring acetylphenylalanine and reactivity test .....  | 60 |
| <b>4.5 Electron microscopy analysis of purified dNTic110</b> .....  | 62 |
| <b>5. Discussion</b> .....  | 64 |

|  |           |
|--|-----------|
| <b>5.1 <i>In situ</i> topology of Tic110.....</b>                              | <b>64</b> |
| <b>5.2 <i>In vivo</i> topology and function of Tic110.....</b>                 | <b>66</b> |
| <b>5.3 Topology of dNTic110 in a reconstituted proteoliposome system .....</b> | <b>69</b> |
| <b>5.4 Conclusions .....</b>   | <b>72</b> |
| <b>6. List of references .....</b>   | <b>73</b> |
| <b>Curriculum Vitae .....</b>  | <b>81</b> |
| <b>Eidesstattliche Versicherung .....</b>                                      | <b>83</b> |
| <b>Versicherung der Co-Autoren .....</b>                                       | <b>84</b> |
| <b>Danksagung .....</b>  | <b>85</b> |

## 1. Introduction

### 1.1 Protein import into chloroplasts

Chloroplasts are unique photosynthetic organelles that evolved through an endosymbiotic event ~1.5 billion years ago. A formerly free-living cyanobacterium was engulfed by an ancestral eukaryotic host that already contained mitochondria (Gould et al., 2008). During evolution, a dramatic reduction in the bacterial endosymbiont genome size occurred, during which 95% of the genes encoding the ~3000 proteins acting in the chloroplasts were transferred to the nucleus so that the host attained control over its new organelle. The plastid genome encodes the residual ~100 genes (Sugiura, 1989; Martin et al., 2002; Timmis et al., 2004). As a consequence, nuclear-encoded chloroplast proteins that were originally encoded on the endosymbiont genome are now translated in the cytosol and are post-translationally translocated into the allocated organelle (Leister, 2003). This process involves three steps: (i) cytosolic sorting procedures, (ii) binding to the designated receptor-equipped target organelle and (iii) the consecutive translocation process. During import, proteins have to overcome the two barriers of the chloroplast envelope, namely the outer envelope membrane (OEM) and the inner envelope membrane (IEM). In the majority of cases, this is facilitated by two distinct multiprotein complexes, located in the OEM and IEM, respectively, which are designated translocon on the outer/inner chloroplast membrane (TOC/TIC).

### 1.2 Cytosolic sorting of preproteins and targeting to the organelle

The translocation process into the organelle requires a first-sorting event of the so-called preproteins. The initial step of protein import is the accurate targeting of these newly synthesized preproteins. To avoid mistargeting, chloroplast-destined preproteins harbor an N-terminal chloroplastic transit peptide (cTP) that specifically targets them to the chloroplast outer membrane (Bruce, 2001). Unexpectedly, conserved characteristics specific to chloroplast proteins across plant species are missing and the sequences of cTPs are highly heterogeneous in their length and properties. They merely display an overall positive net charge, resulting from the lack of acidic amino acids (Bruce, 2001). Regarding the fact that mitochondrial proteins have specific and conserved features within their N-terminal targeting sequence across plant species, the lack of such a consensus sequence for chloroplast-targeted proteins is striking, thus rendering the question of how specificity for the chloroplast is achieved and mistargeting between these organelles is avoided. One potential hypothesis for the heterogeneity could be different preferences of the preproteins for plastid types, which is determined by distinct cTP features (Li and Teng, 2013).

To sustain import competency by keeping preproteins in an unfolded structure, cytosolic chaperones are involved. Up to now, the most prominent chaperone thought to facilitate appropriate recruiting of preproteins is the heat shock protein Hsp70. Both cTP and the mature part of preproteins have been shown to interact directly with this chaperone, and import activity is clearly stimulated in the presence of Hsp70 (Rial et al., 2000).

Apart from Hsp70, another component has been identified in cytosolic preprotein targeting: a 14-3-3 protein preferentially binds to phosphorylated serines or threonines within the cTP, which in association with the chaperone Hsp70 leads to increased import efficiency of preproteins. This assembly has been designated the cytosolic guidance complex (May and Soll, 2000) (Figure 1).

Phosphorylation is mediated by the recently identified STY kinases 7, 18 and 46; a knockout of two and concurrent knockdown of the third kinase led to severe phenotypes in chloroplast biogenesis during greening (Lamberti et al., 2011). However, it seemed that dephosphorylation plays a more crucial role in the actual import process than phosphorylation. It could be shown that under the applied conditions – removal of the phosphorylation site within the binding motif of the cTP for 14-3-3 proteins – the kinetics, rather than the fidelity, of targeting to chloroplasts was impaired. (May and Soll, 2000; Nakrieko et al., 2004). In contrast, phosphorylated precursors, or those containing a glutamic acid residue instead to mimic phosphorylation, are only imported very slowly (Waegemann and Soll, 1996). *In vivo* studies showed that a *Arabidopsis* mutant which mimicked the phosphorylated serine in the cTP of the photosynthetic precursor pHcf136 resulted in reduced import activity, and hence impaired photosystem II assembly, most prominent in cotyledons (Nickel et al., 2015). This is probably due to the impossibility of dephosphorylation occurring within the cTP and clearly demonstrates that import and assembly of photosynthetic proteins is highly dependent on a proper phosphorylation/dephosphorylation cycle prior to translocation. Once this process cannot be completed, the chloroplast protein homeostasis is misbalanced.

Like Hsp70, the chaperone Hsp90 is able to bind to both the cTP and mature region of a different subset of preproteins. Its presence alone stimulates protein import into isolated chloroplasts (Qbadou et al., 2006; Fellerer et al., 2011). In contrast to the Hsp70/14-3-3 guidance complex, Hsp90-bound preprotein favors a distinct docking station at the OEM, which will be defined below.

### 1.3 Crossing the outer envelope membrane via the TOC complex

After synthesis and sorting in the cytosol, the preproteins are recognized at the OEM. This is mainly mediated by the two GTP-dependent receptor proteins Toc34 and Toc159 (Kessler and Schnell, 2009). Both proteins are anchored C-terminally in the OEM and expose their GTP-binding domains towards the cytosol, in consistency with their role as preprotein receptors. Together with a third protein, Toc75, which is deeply embedded in the lipid bilayer and forms the protein conducting channel (Hinnah et al., 1997), they build up a stable complex, resulting in a heterotrimeric TOC core complex (Figure 1).

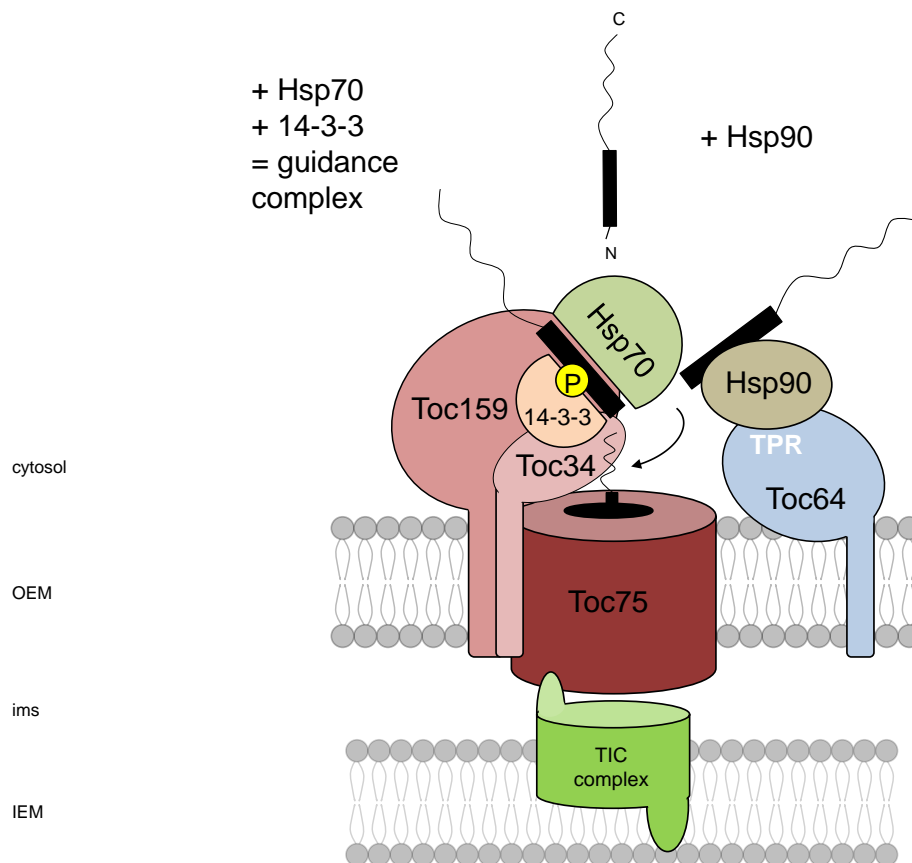


**Figure 1: Chaperone involvement in cytosolic targeting and recognition of preproteins at the outer envelope membrane of chloroplasts.** Preproteins could be chaperoned by the guidance complex or by Hsp90 alone. The guidance complex is represented by Hsp70 that binds to both mature region and cTP of the preprotein and 14-3-3 proteins which bind to the phosphorylated cTP. Hsp70-chaperoned preproteins are recognized by the GTP-dependent receptor proteins Toc159 and Toc34, followed by delivery to the import channel Toc75, whereas precursor proteins bound to Hsp90 are docked to the third receptor Toc64 via its TPR domain and are then handed over to Toc34. Picture is taken out from (Sjuts et al., 2017).

Determination of the apparent mass of 500 kDa of the pea multiprotein complex leads to a stoichiometry of 1:4:4 of Toc159/Toc34/Toc75 (Schleiff et al., 2003). Both receptors belong to a plant-specific family of eukaryotic-originated GTPases, sharing some general features. Toc159 is a tripartite protein consisting of three functional domains: an intrinsically

disordered acidic domain (A-domain), the GTPase domain (G-domain) and the membrane anchor domain (M-Domain with a mass of ~54 kDa) (Bölter et al., 1998a; Chen et al., 2000; Richardson et al., 2009). Toc34 contains a cytosolic GTPase domain and is anchored into the OEM by a single transmembrane domain. Both proteins Toc34 and Toc159 bind to distinct regions of the N-terminal cTP, hence they could act simultaneously in receiving preproteins (Becker et al., 2004).

The GTPase activity plays a central role in preprotein recognition and delivery, as non-hydrolyzable GTP analogs inhibit preprotein binding and translocation (Young et al., 1999). Interestingly each individual GTPase domain is dispensable for the plant (Agne et al., 2009; Aronsson et al., 2010), however, a viable plant lacking both domains from both receptors could not yet be isolated. The minimal structure required for sufficient assembly of the TOC complex and to support protein import is the M-domain of Toc159, which can partially complement the loss of Toc159 in *ppi2* mutant plants (Lee et al., 2003).

Toc34 is believed to exist as a homodimer in its GDP-bound state, which exhibits a preprotein-binding site in its GTPase domain (Sun et al., 2002). Upon preprotein delivery, GTPase activity is stimulated and exchanges GDP to GTP. Toc34 in its GTP-bound state binds preproteins with high affinity, which triggers not only the disruption of the Toc34-dimer but also promotes heterodimerization of Toc34 and Toc159. This GTP-heterodimer-complex is now referred to as the active TOC complex (Becker et al., 2004). GTP hydrolysis results in reduced affinity towards the preprotein, the subsequent transfer of the preprotein into the Toc75 channel and the initiation of membrane translocation (Oreb et al., 2007). Taken together, the hypothesized model clearly demonstrates that the receptors are working as GTP/GDP-regulated switches to control preprotein binding and delivery. However, there are still missing factors, such as the GTPase-activating protein or GTP-exchange factor, although it could be shown that peptides from cTPs can stimulate GTPase activity (Jelic et al., 2003).

A third component was identified to assist in receiving preproteins, named Toc64. Its potential role in protein import has been concluded from its ability to bind a precursor protein and the transient association with the other TOC components (Sohrt and Soll, 2000). In contrast to the above-mentioned receptor proteins, Toc64 serves as an initial docking station for Hsp90-bound preproteins and subsequently delivers these preproteins to Toc34 (Qbadou et al., 2006). Toc64 harbors three cytosolic tetratricopeptide repeat (TPR) domains, mediating the interaction with Hsp90 (Figure 1). This is a typical feature of proteins interacting with Hsp70/90-associated proteins (Young et al., 2003). The same holds true for a plant ER receptor TPR7 (Schweiger et al., 2012) and interestingly, a Toc64 homolog, namely OM64, was found in plant mitochondria, replacing the mitochondrial TOM70 present in mammals and fungi but absent in plants. Instead, the protein OM64 with a C-terminal TPR

domain serves as a receptor for mitochondrial-destined proteins (Chew et al., 2004). Although *in vitro* a strong interaction between Hsp90 and Toc64 could be measured with a  $K_D$  of 2.4–15.5  $\mu\text{M}$  (Schweiger et al., 2012) the essentiality of these TPR proteins *in vivo* is still under debate. Since chloroplasts lacking Toc64 sustain their import capacity, it is feasible that this docking protein rather constitutes more an additional regulatory component to the general TOC receptor complex than being an essential constituent. However, it could be shown that atToc33 and Toc64 cooperate in preprotein import, hence it is reasonable to say that atToc33 can overcome the loss of Toc64 function as preproteins are still recognized (Sommer et al., 2013), while only chaperone binding is lost.

After the preprotein has been delivered to the receptor proteins, it has to be translocated through the membrane. The preprotein-conducting channel in the OEM is represented by the beta barrel protein Toc75 (Schnell et al., 1994). The essential nature of Toc75 is demonstrated by its gene being a single copy conserved throughout all plant lineages and the embryo lethality of knockout lines (Jackson-Constan and Keegstra, 2001). The protein belongs to the Omp85 superfamily, which is exclusively found in gram-negative bacteria, mitochondria and plastids (Bölter et al., 1998b). Typically for this family, the structure of Toc75 exhibits two features: 16-18 arranged beta strands forming the C-terminal beta domain, and several POTRA domains at its N-terminus (Clantin et al., 2007). Irrespective of the fact that POTRA domains are required for Toc75 function (Paila et al., 2016), the orientation and thus exact molecular function of these POTRA domains remain a matter of debate. On the one hand, it is assumed that these domains are facing the cytosolic side of the OEM, assisting in preprotein interaction. However, a recent study proposed a localization of the POTRA domains in the intermembrane space by bimolecular fluorescence complementation analyses and immunogold labeling (Chen et al., 2016; Sommer et al., 2011).

*In vitro* analyses showed preprotein binding during import and the import process itself being inhibited with Toc75 antibodies (Tranel et al., 1995). Electrophysiological analyses revealed that reconstituted Toc75 in lipid bilayers forms a voltage-gated channel with a pore size of 14 Å at its narrowest part (Hinnah et al., 2002). In contrast to the other TOC components, Toc75 harbors an N-terminal bipartite transit peptide. One part directs the protein into the stroma where the peptidase Plsp1 cleaves off the cTP once the extreme N-terminus reaches the stroma (Inoue et al., 2005). However, the C-terminal region of the cTP spans the intermembrane space and ensures proper localization and folding at the OEM (Inoue et al., 2005).

## 1.4 Crossing the intermembrane space and inner envelope membrane via the TIC complex

Successful import requires not only the interaction between preproteins and outer membrane receptors, but also the formation of super complexes between the translocons of both OEM and IEM via contact sites that enable the preprotein to pass through both membranes simultaneously (Schnell and Blobel, 1993). Both complexes are facing the intermembrane space, thus some proteins localized in this compartment have to be involved in the import process. However, only limited knowledge about import-related factors of the intermembrane space is available. Presently, the only member identified in this compartment to be involved in protein translocation is the soluble protein Tic22. Tic22 has been shown to interact with preproteins during protein import (Kouranov et al., 1998). Structural and functional studies led to the hypothesis that Tic22 is working as a molecular chaperone, as *Arabidopsis* mutants lacking Tic22 showed growth and biogenesis defect and a decreased import activity (Kasmati et al., 2013; Rudolf et al., 2013). One potential role for Tic22 would be, like the cytosolic counterparts, to ensure proper targeting and prevent misfolding during the transfer between TOC and TIC. However, this role has not been confirmed yet.

The counterpart of the IEM to the TOC core channel, Toc75, is Tic110. Tic110 was the first TIC component described (Schnell et al., 1994) and is the second most abundant protein in the IEM (Lübeck et al., 1996). It was found in a supercomplex associated with TOC components and incoming preproteins, suggesting a functional role as the central part of the IEM translocon (Lübeck et al., 1996).

Reconstitution of a Tic110-protein lacking its two N-terminal hydrophobic transmembrane stretches (pea sequence: aa91-966, dNTic110) resulted in a cation-selective channel with a diameter of 1.7 nm, which is similar to the diameter of the channel Toc75 and hence sufficient for preprotein threading (Balsera et al., 2009; Heins et al., 2002) (Figure 2). However, two controversial models concerning the topology and function of Tic110 still persist. Undoubtedly and universally accepted is the fact that the 110-kDa protein is anchored into the membrane by its two N-terminal, highly hydrophobic helices (Inaba et al., 2003; Balsera et al., 2009). In our current topological model, we can combine the essential functions of Tic110, which has been under discussion for a long time. On the one hand, Tic110 assembles into its channel-like structure via its four amphipathic helices, substantiating its function as the main translocation pore. The four membrane-spanning helices consequently lead to the formation of two loops that are extended into the intermembrane space, which could be confirmed by limited proteolysis experiments (Lübeck et al., 1996; Balsera et al., 2009). On the other hand, a large part of the C-terminus is protruding into the stroma and thus could fulfill the additional function of Tic110 acting as a



scaffold for chaperones and co-chaperones (Inaba et al., 2005). The crystal structure of a *Cyanidioschyzon merolae* Tic110 version, which consists of the C-terminus including only the last amphipathic helix, is proposed to be too flattened and elongated to form a channel protein (Tsai et al., 2013). However, as it is unlikely that such a shortened protein can fold into its native conformational structure, it is still reasonable to assume that the full-length Tic110 protein is able to build the channel protein via its amphipathic, membrane-spanning helices.

Like Toc75, Tic110 is encoded by a single gene and constitutively expressed in all tissues. Homozygous T-DNA insertion lines are embryo-lethal, and heterozygous plants already exhibit a clear growth and greening defect, clearly emphasizing the necessity of Tic110 in chloroplast biogenesis and overall plant viability (Kovacheva et al., 2005). Import of Tic110 is achieved by targeting the protein into the stroma and after cleavage of the cTP, Tic110 is re-inserted into the lipid bilayer of the IEM (Vojta et al., 2007).

Using a cross-linking strategy, another TIC component could be directly associated to Tic110, named Tic40. Tic40 consists of a single transmembrane helix which anchors the protein at the IEM, resulting in a large stroma-facing, soluble domain. This C-terminal part harbors two Hip/Hop/Sti domains, building binding sites for Tic110 and the stromal Hsp70/93 chaperones. The main function of Tic40 is to co-chaperone the translocation process of incoming preproteins by coordinating Hsp93 activity (Chou et al., 2006) (Figure 2).

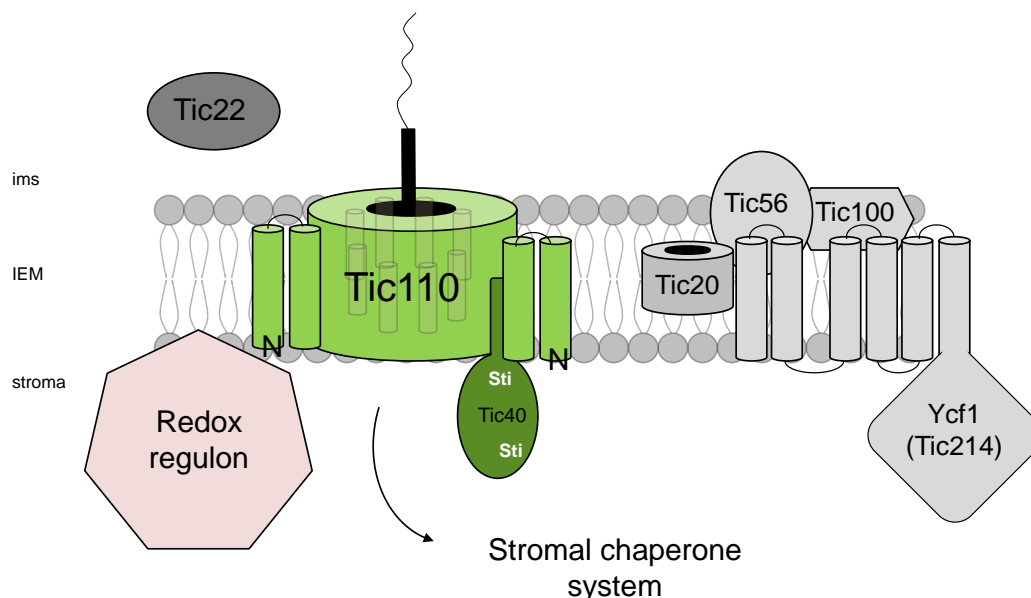


**Figure 2: Crossing the inner envelope membrane of chloroplasts via the TIC complex.** The counterpart of the outer channel protein is the IEM protein Tic110 which is a functional dimer. Two hydrophobic domains anchor the protein into the IEM whereas further eight amphipathic helices are involved in the channel formation. Tic40 is supposed to interact with Tic110 with its Sti1 domain and acts further as a scaffold for stromal chaperones. Controversial, the 1MDa-complex depicted on the right side comprises atTic20 as the channel protein, atTic56 embedded in the complex, atTic100 located at the IMS and the plastid encoded Ycf1 (atTic214) with its six transmembrane domains and a large stromal C-terminus. Picture is taken out from (Sjuts et al., 2017).

A further TIC component named Tic20 was identified by its ability to covalently cross-link with a precursor protein en route to the chloroplast (Kouranov and Schnell, 1997; Kouranov et al., 1998). Structural prediction indicated three or four hydrophobic transmembrane domains (Kouranov et al., 1998). Tic20 is essential in *Arabidopsis*. Chloroplasts isolated from Tic20 antisense lines are impaired in preprotein import (Chen et al., 2002). In addition, early phylogenetic analysis indicated a relation of Tic20 with bacterial amino acid transporter and cyanobacterial proteins of unknown function suggesting a role as a translocation channel (Reumann and Keegstra, 1999). However, a latter study with many more genomes sequences at that time was unable to reproduce these claims (Gross and Bhattacharya, 2009). Nonetheless, the important role of Tic20 in chloroplast biogenesis is evident and it was proposed early on by Keegstra and colleagues that Tic20 and Tic110 form independent preprotein translocation channels (Reumann et al., 2005). Besides this circumstantial evidence for the notion, direct support comes from electrophysiological studies using either heterologously expressed and purified Tic20 (Kovács-Bogdán et al., 2011) or a 1MDa-complex from *Arabidopsis*, of which Tic20 is one constituent (Kikuchi et al., 2009, see below), which both showed the channel-forming capacity of the applied material. Using a cleavable proteinA-tagged variant of Tic20 expressed in transgenic *Arabidopsis* plants, the authors were able to purify the 1MDa complex via affinity purification. The obtained complex contained three other proteins in addition to Tic20: atTic56, atTic100 and atTic214 (Ycf1) (Kikuchi et al., 2013) (Figure 2).

Interestingly, Ycf1 is one of the last enigmatic open-reading frames of the chloroplast genome without an assigned function (Drescher et al., 2000). It is predicted to contain at least six transmembrane helices at its N-terminus (de Vries et al., 2015). AtTic56 and atTic100 are nuclear-encoded proteins, the first deeply embedded in the holo-complex without any predicted transmembrane domain, whereas the latter is supposed to associate with the complex on the intermembrane space site (Kikuchi et al., 2013). However, major questions came up concerning the exact physiological roles of the involved proteins. So far, for the potential involvement of Tic100, no data are available. However, for atTic56, a proteomic analysis showed that most of the chloroplast proteins are still imported into the organelle in *atTic56* mutant plants, pointing towards a still functioning import machinery (Köhler et al., 2015). Furthermore, an alternative role independent from protein import for atTic56 was suggested, since Köhler and colleagues established a link between processing of plastid rRNA and the assembly of plastid ribosomes. They stated that a defect in plastid ribosome construction is responsible for the albino phenotype of *atTic56-1* mutant plants, thus leading to a potential role of atTic56 in ribosome assembly and establishment of a functional plastid translation machinery (Köhler et al., 2016). Even more importantly, since Ycf1 is missing not only in all grasses but also in a variety of dicotyledonous plants, one can

speculate about its overall significance in protein import. The critical question is: how do plants that are completely lacking this gene manage to retain their functional import machinery (de Vries et al., 2015)? Since Ycf1 is an essential protein in *Arabidopsis*, it is difficult to study protein import in knockout plants. Nonetheless, ecotypes of *Arabidopsis* can be grown on media containing spectinomycin, which is a specific inhibitor of plastid translation (Wirmer and Westhof, 2006). Under these conditions it could be shown that Ycf1 is truly absent in *Arabidopsis* plants, thus enabling to study its role in protein import (Bölter and Soll, 2016; Köhler et al., 2016). Presumably, the seed contains sufficient Ycf1 protein for the plants to germinate, and spectinomycin-induced signaling leads to compensatory mechanisms that ensure survival on the antibiotic. Interestingly, as these two studies show, precursor proteins that depend on the general protein import machinery are still efficiently imported into the plastids, thus excluding the role of Ycf1 as a constituent of the main protein channel. Furthermore, the nuclear-encoded Tic20 is also not detectable under spectinomycin treatment, implying a feedback mechanism between plastid and nucleus concerning the assembly of the 1MDa complex (Bölter and Soll, 2016). Instead of being a main translocation factor, Ycf1 could be involved in the assembly of a plastid fatty acid synthase (ACCase). Under spectinomycin, plants are also lacking the plastid-encoded subunit AccD but are able to complement for that loss by upregulating the expression and import of a nuclear-encoded and plastid-targeted protein (Acc2). This upregulation only appears if Ycf1 is strongly diminished, suggesting a functional role of Ycf1 in assembling the ACCase holoenzyme (Bölter and Soll, 2016). Recently, Ycf1 was shown to be a target of a nuclear-encoded translational activator named PBR1, which is important for thylakoid biogenesis, suggesting it could play a role in this process (Yang et al., 2016). Although a potential role of Ycf1 in protein import cannot entirely be excluded, more research is needed to clarify its functional role(s).

Beside the discrepancies concerning the main translocation machinery, additional TIC components have been identified which are called the redox regulon. This regulon includes the proteins Tic55, Tic62 and Tic32 (Stengel et al., 2009). Tic55 is a Rieske protein, while both Tic62 and Tic32 are dehydrogenases. All proteins have been found in complexes containing Tic110; specifically, Tic32 shows a direct interaction with the N-terminus of Tic110 (Hörmann et al., 2004; Stengel et al., 2009).

## 1.5 Completion of the translocation process: the stromal chaperone system

Upon reaching the stroma, the preprotein translocation proceeds by removing the cTP and subsequently folding into an active structure. Four distinct destinations for the imported proteins are possible: stroma, IEM, thylakoids and thylakoid lumen. The mature protein is either re-inserted into the IEM or, due to a bipartite transit peptide, directed to the thylakoids using different sorting mechanisms for further processing and assembly (Schünemann, 2007). The removal of the cTP is carried out by a soluble stromal processing peptidase (SPP) which is essential for plants (Richter and Lamppa, 1998; Trösch and Jarvis, 2011). Import is an energy-consuming process resulting from nucleotide-hydrolysis. Although the TOC members are able to hydrolyze GTP, this provides only the minimal energy required for the irreversible initiation of protein import and is not the driving force for sufficient and complete import, so the energy must originate from a different source. It has been shown that the energy is provided in the form of ATP, which is hydrolyzed by stromal chaperones, leading to a sufficient motor activity for preprotein crossing of the OEM and IEM of the chloroplast (Pain and Blobel, 1987). Various chaperones have been determined as being involved in the folding of proteins and/or consuming the required energy via ATP hydrolysis, mainly the chloroplast Hsp70, Hsp90, Hsp93 and Cpn60 (Akita et al., 1997; Inoue et al., 2013; Kessler and Blobel, 1996; Nielsen et al., 1997). However, Cpn60, the homolog of bacterial GroEL, is most likely exclusively involved in protein folding and assembly of the newly imported mature proteins, especially Rubisco (Goloubinoff et al., 1989).

Hsp93 (bacterial ClpC) is a member of the Hsp100 family, which itself belongs to the broader AAA+ family (ATPases associated with various cellular activities) (Moore and Keegstra, 1993). Hsp100 proteins contain one or two AAA+ domains, and are typically arranged into a hexameric structure with a central pore which is sufficient for protein threading (Rosano et al., 2011). *Arabidopsis* features two genes encoding for the isoforms Hsp93-V and Hsp93-III. Beside the putative function of providing energy coming from ATP hydrolysis, Hsp93 has been shown to be a regulatory chaperone for the Clp protease system, thus functioning in quality control and potential degradation of the incoming preproteins (Kovacheva et al., 2005).

Originally, three chloroplast Hsp70 isoforms in pea were reported. Two of them are located in the stroma whereas one is supposed to reside in the intermembrane space (Ratnayake et al., 2008). However, in *Arabidopsis* the gene coding for the latter has not yet been identified, leaving doubts about the existence or identity of such an intermembrane space chaperone. *Arabidopsis* double null mutants of the stromal Hsp70 isoforms are embryo lethal and single mutants already exhibit biogenesis and import defects (Su and Li, 2010).

CpHsp90 was identified in complexes containing import intermediates at late import stages that also contain Tic110 and Hsp93 (Inoue et al., 2013). A specific and reversible Hsp90 ATPase inhibitor arrests protein import in chloroplasts, whereas initial binding to the TOC complex is not impaired, clearly emphasizing a role of cpHsp90 in late import stages (Nakamoto et al., 2014).

Due to the complexity of the chaperone system in chloroplasts, there is an ongoing discussion about the specificity and import-related function of each individual chaperone, resulting in different models. It is still not completely clear which protein is the potential candidate to constitute the main motor protein for providing the import energy. In mitochondria and ER, the responsible driving force is believed to come from ATP hydrolysis performed by Hsp70 chaperones which are located in the matrix and lumen, respectively (Park and Rapoport, 2012; Dudek et al., 2013). Thus, it was long thought that cpHsp70s are likewise the main motor in chloroplasts. In that context, it seems logic that the responsible ATPase interacts directly with the incoming preproteins, or at least associates with the TIC translocon and for a long time, this scenario could not be shown for stromal Hsp70, hence it seemed unlikely that Hsp70 alone provides the required power. However, it could be shown in 2010 for the moss *P. patens* that Hsp70 is indeed involved in protein import into chloroplasts as a stromal Hsp70 co-immunoprecipitated with early-import intermediates, as well as with Tic40 and Hsp93 (Shi and Theg, 2010). In agreement with this, *Arabidopsis* mutants lacking the chloroplast isoforms of Hsp70 showed a reduced import level of preproteins, which could also be demonstrated in the moss *P. patens* (Su and Li, 2010; Shi and Theg, 2010). Furthermore, it was suggested that the ATP requirements correlate with the activity of moss Hsp70, emphasizing the idea that cpHsp70 is the only energy-providing motor, at least in moss (Shi and Theg, 2010). Interestingly, *Arabidopsis* double mutants of Hsp93 and Hsp70 showed an additive effect in decreased import capacity compared to the single knockout mutants, leading to the theory that both proteins are acting at least partially in parallel as independent import players (Su and Li, 2010). This idea was somewhat supported later on: it was hypothesized that Hsp70 is the motor protein whereas Hsp93 is stably associated with the Clp protease complex at the IEM, suggesting a permanent role in quality control and degradation of preproteins and not a role in powering protein translocation (Figure 3 A).

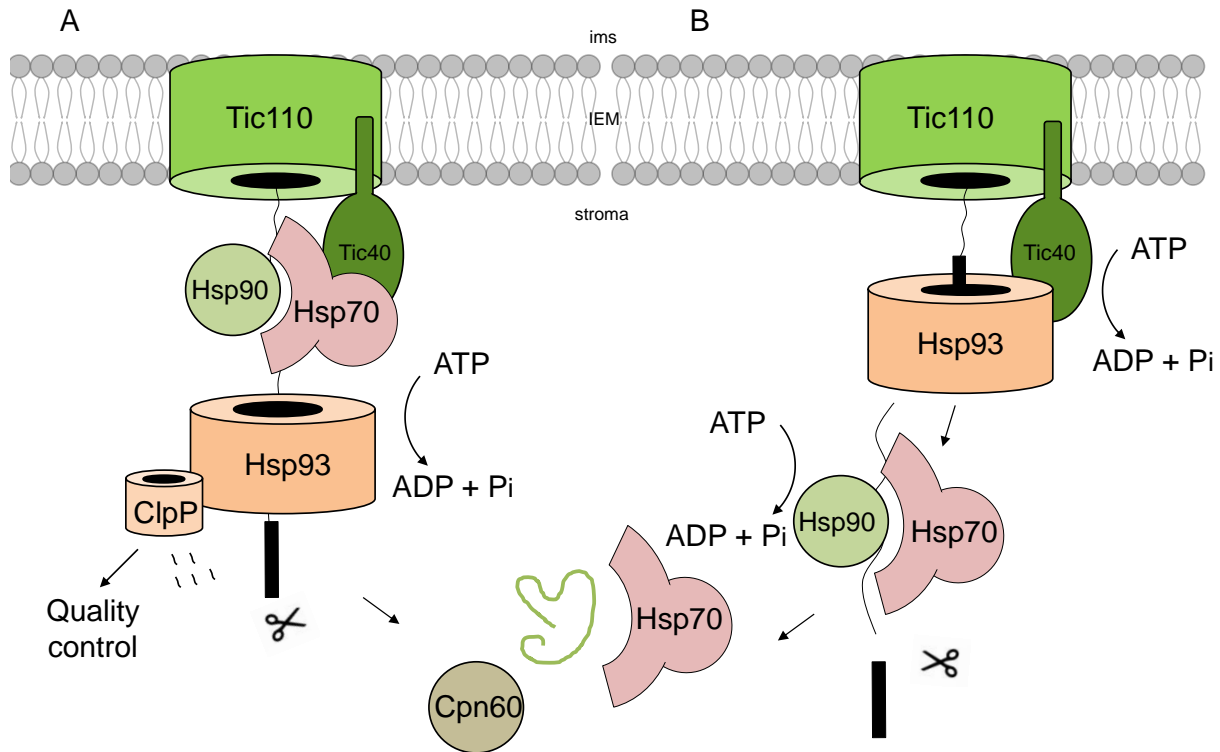


**Figure 3: The stromal chaperone system.** Two different models have been hypothesized concerning the main import motor of the chaperones. One model **(A)** involves a secondary function of Hsp93, assuming that this protein acts mainly in the quality control pathway by degrading mistargeted or wrongly folded proteins. In this model the main energy is consumed by Hsp70 and not by Hsp93 (Flores-Pérez et al., 2016). A recent study suggests that Hsp93 interacts subsequently with incoming preprotein at the N-terminal cTP, whereas Hsp70 binds to the mature parts of the protein (Huang et al., 2015). This enable the two chaperone systems to interact at least partially in parallel with the preproteins. After completing of the import by processing the cTP, proteins are folded with the help of various chaperones like Cpn60 and Hsp70 **(B)**. Picture is taken out from (Sjuts et al., 2017).

In this study, the authors used a transgenic line in which the interaction of Hsp93 with the protease ClpP was disrupted, but the protein itself was still localized to the IEM and interaction with Tic110 was also ensured (Flores-Pérez et al., 2016). This enabled the study of the role of Hsp93 in protein import independent from its role in proteolysis. However, the truncated version could not complement the *hsp93* import defective phenotype, thus excluding the possibility of Hsp93 being the main motor functioning in protein import (Flores-Pérez et al., 2016).

In remarkable contrast to the above-mentioned observations, a recent study on that topic could show that Hsp93 directly binds to both the N-terminal cTP and the mature part of incoming preproteins, thus clearly indicating a role in early-import stages and challenging the above-mentioned theory (Huang et al., 2015). These authors favor the hypothesis that both chaperones could prefer different regions of the preprotein and thus provide different modes of translocation force, which would result in additive import defects in the double mutants.

This would also hold true if Hsp93 was the primary motor for the cTP and Hsp70 for the mature region (Figure 3 B). Preprotein processing takes place during binding to Hsp93 and thus, binding to the mature protein is also detected. In their model, Hsp70 is entirely responsible for interacting with the mature protein, acting in parallel and one defined step after the action of Hsp93 (Figure 3 B).

## 1.6 Redox sensing at the inner envelope membrane

Regarding the fact that the TOC complex could be regulated in a thiol-dependent mechanism (Stengel et al., 2009), it can be supposed that this regulation is also effective for the translocase of the IEM. Indeed, a thiol-dependent interaction between Tic110 and Tic40 has been observed, but its *in vivo* role has to be clarified (Stahl et al., 1999). Tic110 itself has been found to contain one or two regulatory disulfide bridges (Balsera et al., 2009). These intramolecular bridges could have a critical influence on the structure and function of the central TIC component. Switches between reduction and oxidation of these disulfide bridges could either lead to an open or closed formation of Tic110, respectively, and thereby limit the amount of incoming preproteins (Figure 4).

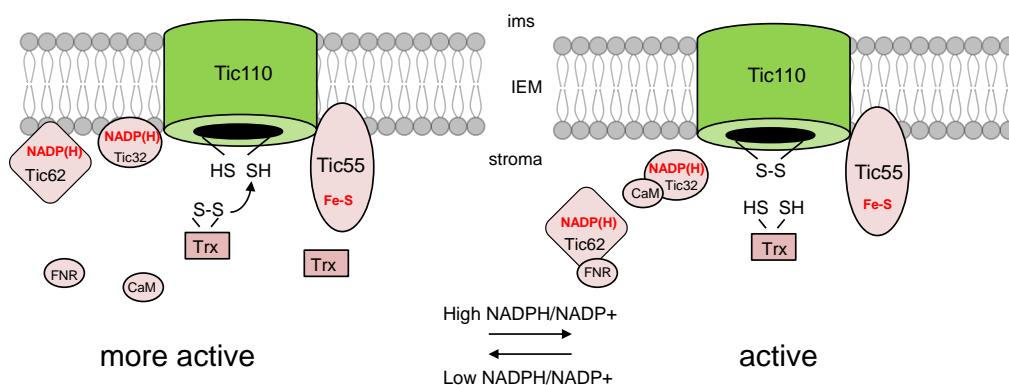


**Figure 4: Import regulation of the TIC complex from the stromal site.** Similar to the redox regulation at the OEM import of precursor proteins is accelerated under reducing conditions, suggestively due to an open conformation of the main channel, Tic110. A second regulation mechanism involves the stromal redox state, which is reflected by the NADPH/NADP<sup>+</sup> ratio. A low NADPH/NADP<sup>+</sup> ratio could be shown to enhance the import rate compared to a higher NADPH/NADP<sup>+</sup> ratio. Picture is taken out from (Sjuts et al., 2017).

The stromal thioredoxin family has been demonstrated to operate on disulfide bonds of Tic110 (Balsera et al., 2009). The redox state of thioredoxins is directly linked to both photosynthetic activity and other redox-dependent mechanisms in the organelle, thus it might act as a transport signal that eventually reaches the import machinery to regulate the chloroplast import rate. The intermembrane space protein Tic22 contains a conserved cysteine (Glaser et al., 2012), which could be involved in intramolecular disulfide bridges

leading to dimerization of Tic22. Furthermore, since Tic110 exposes one cysteine into the IMS, a possible disulfide bond between the soluble Tic22 and the pore protein Tic110 during preprotein is also a hypothesis. However, no redox-mediated modulation has been reported so far and this hypothesis has to be addressed experimentally.

[Passages of the text were taken out of a previous publication of the author (Sjuts et al., 2017)].

## 1.7 Aim of the study

The involvement of the most abundant TIC component, Tic110, in protein import into chloroplasts is well established. However, two controversial models concerning the topology of Tic110 still persist and prevent the assignment of a clear structure-function relationship of Tic110. In this study, new complementary *in situ*, *in vivo* and *in vitro* approaches were used to provide insights into the topology and function of Tic110.

The project was divided into three complementary approaches: Firstly, the *in situ* topology should be analyzed by using isolated right-side-out inner envelope as an experimental tool, secondly, the *in vivo* function and topology of Tic110 should be addressed using a novel genetically encoded tag for light and electron microscopy and thirdly, the topology of Tic110 should be analyzed applying an *in vitro* reconstituted proteoliposomal assay.



## 2. Materials

### 2.1 Chemicals

If not stated otherwise, all chemicals were purchased in high quality from Sigma-Aldrich (Taufkirchen, Germany), Roth (Karlsruhe, Germany), Merck (Darmstadt, Germany), New England BioLabs (NEB, Frankfurt am Main, Germany), ThermoFisher Scientific (Braunschweig, Germany) or Serva (Heidelberg, Germany).

### 2.2 Molecular weight markers and DNA standards

PstI digested  $\lambda$ -Phage DNA (NEB, Frankfurt am Main, Germany) was used as a molecular size marker for agarose-gel electrophoresis. For SDS-PAGE either peqGOLD protein marker I (VWR, Ismaning, Germany) or the prestained SpectraHR (NEB, Frankfurt am Main, Germany) were used.

### 2.3 Enzymes and Kits

Restriction endonucleases were purchased either from ThermoFisher Scientific or from New England BioLabs (Frankfurt am Main, Germany). T4 DNA ligase was received from Thermo Fisher Scientific, Q5 DNA polymerase from New England BioLabs, Taq DNA polymerase from Bioron (Ludwigshafen, Germany).

For DNA isolation, the NucleoSpin Plasmid Mini/Midi Kits and for purification of DNA fragments the Nucleospin Extract II Kit from Macherey and Nagel (Düren, Germany) were used.

For detection of biotinylated proteins, the VECTASTAIN ABC-HRP Kit (Vectorlabs, Cambridgeshire, UK) was used according to the manufacturer's instructions.

### 2.4 Strains, constructs and oligonucleotides

*E. coli* TOP10 cells were used for propagation of plasmid DNA. Overexpression of heterologous proteins was performed using *E. coli* BL21 (DE3) cells. For transient expression of recombinant proteins in tobacco leaves *A. tumefaciens* AGL1 strains were used. For stable transformation of *A. thaliana* plants *A. tumefaciens* GV3101 (pMP90RK) cells were used.

Table 1 lists the constructs used in this study.

**Table 1:** Constructs used in this study.

| construct                        | vector     | application                            |
|----------------------------------|------------|--|
| dNTic110                         | pET21d(+)  | overexpression                         |
| dNTic110 WT                      | pSB8.12e2  | amber suppression                      |
| dNTic110 F216amb                 | pSB8.12e2  | amber suppression                      |
| dNTic110 F222amb                 | pSB8.12e2  | amber suppression                      |
| dNTic110 F328amb                 | pSB8.12e2  | amber suppression                      |
| dNTic110 F585amb                 | pSB8.12e2  | amber suppression                      |
| dNTic110 F670amb                 | pSB8.12e2  | amber suppression                      |
| miniSOG                          | pUC        | synthetic gene template                |
| miniSOG                          | pET21d(+)  | overexpression                         |
| preTic110                        | pGEM5Zf(+) | template for site-directed mutagenesis |
| preTic110-miniSOGims1            | pK7FWG2    | overexpression, photooxidation         |
| preTic110-miniSOGims2            | pK7FWG2    | overexpression, photooxidation         |
| preTic110-miniSOGC-ter           | pK7FWG2    | overexpression, photooxidation         |
| atPro110::preTic110-miniSOGims1  | pHGW       | stable expression <i>Arabidopsis</i>   |
| atPro110::preTic110-miniSOGims2  | pHGW       | stable expression <i>Arabidopsis</i>   |
| atPro110::preTic110-miniSOGC-ter | pHGW       | stable expression <i>Arabidopsis</i>   |
| atPro110::CDS110 C190S           | pHGW       | stable expression <i>Arabidopsis</i>   |
| atPro110::CDS110 C501S           | pHGW       | stable expression <i>Arabidopsis</i>   |
| atPro110::CDS110 C526S           | pHGW       | stable expression <i>Arabidopsis</i>   |
| atPro110::CDS110 C548S           | pHGW       | stable expression <i>Arabidopsis</i>   |
| atPro110::CDS110 C562S           | pHGW       | stable expression <i>Arabidopsis</i>   |
| atPro110::CDS110 C728S           | pHGW       | stable expression <i>Arabidopsis</i>   |
| atPro110::CDS110 C944S           | pHGW       | stable expression <i>Arabidopsis</i>   |

Oligonucleotides used in this work were ordered in standard desalted quality from Metabion (Martinsried, Germany) and are listed in table 2.

**Table 2:** Oligonucleotides used in this work. Bold letters represent bases for introduced mutations. Underlined letters indicate restriction sites (uncapatalized) or attB-sites (capatalized).

| name             | Sequence (5'-3')                         | application               |
|------------------|--|---------------------------|
| Tic110F216ambfor | AAATATTGTAT <b>AG</b> GGAGATGCATCATCTTTC | site-directed mutagenesis |
| Tic110F216ambrev | GACACATATATCAACTTTTGGAAAC                | site-directed mutagenesis |
| Tic110F222ambfor | TGCATCATCTT <b>AG</b> CTTCTACCTTGG       | site-directed mutagenesis |
| Tic110F222ambrev | TCTCCAAATACAATATTTGACAC                  | site-directed mutagenesis |

|                      |   |                           |
|----------------------|---|---------------------------|
| Tic110F328ambfor     | GGTATTGTCAT <b>AGA</b> ATGATTTACTCATCTC                             | site-directed mutagenesis |
| Tic110F328ambrev     | TTTTCAAGCTCCTCAACAAC  | site-directed mutagenesis |
| Tic110F585ambfor     | GTTGATAGCTT <b>AGA</b> ATACCTTAGTTGTAAC                             | site-directed mutagenesis |
| Tic110F585ambrev     | TTCTTCAGTTCTTTTGCAGATTC   | site-directed mutagenesis |
| Tic110F670ambfor     | TTACAAGACAT <b>AG</b> TTGACTTACTGTCTAACC                            | site-directed mutagenesis |
| Tic110F670ambrev     | AGATCAGCCCTGTCTTTTC   | site-directed mutagenesis |
| 110M1XbaI_for_new2   | AAAA <u>ctaga</u> TAACGAGGGCAAAAAATGGCTA<br>GCGCACCG                | cloning into psB8.12e2    |
| 110M1AfeI6His_rev    | GATC <u>agcgct</u> TCAGTGGTGGTGGTG                                  | cloning into psB8.12e2    |
| 110EcoRI_DF_IMS1for  | TGTTGGCAGAG <b>gaattc</b> GATCTAGGAAAAC                             | site-directed mutagenesis |
| 110EcoRI_DF_IMS1rev  | GATTTCACTTGGGAAGCATAC   | site-directed mutagenesis |
| 110EcoRI_EY_IMS2for  | AGAAAGTGAA <b>gaattc</b> GAATGGGAATCAC                              | site-directed mutagenesis |
| 110EcoRI_EY_IMS2rev  | CTAATTTCTCAGGTTCTTC   | site-directed mutagenesis |
| miniSOGmitte_rev     | TAAGCTGAACAGTGATCT  | genotyping                |
| pTic110_attBsite_for | <u>GGGGACAAGTTTGTACAAAAAGCAGGCTA</u><br>TGAACCTT                    | GATEWAY cloning           |
| pTic110_attBsite_rev | <u>GGGGACCACTTTGTACAAGAAAGCTGGGT</u><br>CCATCATCATCATCATGAA         | GATEWAY cloning           |
| 110cterm_EcoRI_for   | GATGATGAT <b>Gaattc</b> GTCGACCATATGGGA<br>GAGCTC                   | site-directed mutagenesis |
| 110cterm_EcoRI_rev   | ATCATGAATACAACTTCTCTTC  | site-directed mutagenesis |
| MiniSOGcter_attB_rev | <u>GGGGACCACTTTGTACAAGAAAGCTGGGG</u><br><u>TCGAATTCATCTAACTGAAC</u> | GATEWAY cloning           |
| 110mSOGp207STOPfor   | GATGATGATG <b>TAG</b> ACCCAGCTTTC                                   | site-directed mutagenesis |
| 110mSOGp207STOPrev   | ATCATGAATACAACTTCTCTTC  | site-directed mutagenesis |
| 110mSOGctp207STOPfor | <b>TAG</b> ACCCAGCTTCTTGATC   | site-directed mutagenesis |
| 110mSOGctp207STOPrev | GAATTCATCTAACTGAACTCC   | site-directed mutagenesis |
| miniSOGNcolfor       | GATC <u>ccatgg</u> ATGGAGAAGTCTTTTGTG                               | cloning into pET21d(+)    |
| miniSOGXholrev       | GATC <u>ctcgag</u> ATCTAACTGAACTCC                                  | cloning into pET21d(+)    |
| atpTic110C190S_for   | GGCTGAGATT <b>TCT</b> GATATTTATTGCC                                 | site-directed mutagenesis |
| atpTic110C190S_rev   | TGGAATGCTTCGTCTCCT  | site-directed mutagenesis |
| atpTic110C501S_for   | TCAAAAGCT <b>TCT</b> GAAGAGCTGC                                     | site-directed mutagenesis |
| atpTic110C501S_rev   | AGGTATTTTGTCTTACTGTC  | site-directed mutagenesis |
| atpTic110C526S_for   | GCTTCAACAG <b>TCT</b> GTTACTGATG                                    | site-directed mutagenesis |
| atpTic110C526S_rev   | TTCTGCCGATAGATTTCTTC  | site-directed mutagenesis |
| atpTic110C548S_for   | AGTTATGTT <b>TCT</b> ATTCCCCAGC                                     | Site-directed mutagenesis |
| atpTic110C548S_rev   | CTTAACCTTAATAAAGCAGC  | site-directed mutagenesis |
| atpTic110C562S_for   | TGCAGAAAT <b>TCT</b> GGAACCATATTTG                                  | site-directed mutagenesis |
| atpTic110C562S_rev   | TGAGCTGTATCAACAGTTTG  | site-directed mutagenesis |
| atpTic110C728S_for   | CTTGCTCTACT <b>TCT</b> GTAAGTGGAG                                   | site-directed mutagenesis |
| atpTic110C728S_rev   | TATGTTTTGTAGAGATCTATTC  | site-directed mutagenesis |
| atp110stopforHIS_for | TTTCGTCTTT <b>TAA</b> CATCATCATCATTAAT                              | site-directed mutagenesis |

|                                |  |                           |
|--------------------------------|--|---------------------------|
| atp110stopforHIS_rev           | TTGCCCTCTTCTGCAGCA                                       | site-directed mutagenesis |
| atpTic110C944S_for             | TTTGCTTGCATCTGCACAAAGCTG                                 | site-directed mutagenesis |
| atpTic110C944S_rev             | TCATTTCAGCGACAAGACC                                      | site-directed mutagenesis |
| OL/Pro+atp110,110for           | TCAGTAGAGGGAACCATGAACCCTTCCACG                           | recombinant PCR           |
| OL/Pro+atp110,ProRev           | CGTGGAAGGGTTCATGGTTCCTCTACTGA                            | recombinant PCR           |
| Promoat110_attB_for            | <u>GGGGACAAGTTTGTACAAAAAAGCAGGCTC</u><br>TTCATACTCCACAA  | GATEWAY cloning           |
| ps110w/o6Met_attBrev           | <u>GGGGACCACTTTGTACAAGAAAGCTGGGT</u><br>CCTAGAATACAAACTT | GATEWAY cloning           |
| atTic110 T-DNA insert test rev | CTCTGCCTGAGTAATGCCACG                                    | genotyping                |
| atTic110 TDNA insert Test fwd  | GTAAGTGGAGAGGTAACAAGAATCC                                | genotyping                |
| LBa1                           | TGGTTCACGTAGTGGGCCATCG                                   | genotyping                |
| atTic110 Intron 14 rev         | CCCAGAAGCTGAAATATCCATG                                   | genotyping                |
| atTic110 Exon 7 rev            | CTCATCAGAGAGCTTGAATGATAG                                 | genotyping                |
| atTic110 Exon 2 fwd            | GTACGGTGTCAACAAAGGAG                                     | genotyping                |

## 2.5 Antibodies

Primary antisera against psTic110, atTic110, psTic62, psIEP37, psTic40 were already available in the laboratory and were diluted 1:1000 for immunodecoration in 1 % milk in TBS-T (20 mM Tris/HCl pH 7.6, 150 mM NaCl, 0.05 % Tween). Secondary antibodies coupled to horseradish peroxidase against rabbit were purchased from Sigma-Aldrich (Taufkirchen, Germany) and were used in a 1:10000 dilution. Primary antiserum against miniSOG was generated in this work. Expression and purification of the antigen is described in method section 3.3.11 and 3.3.13. 0.5 mg of the antigen was sent to Pineda (Berlin, Germany) for immunization of a rabbit. Antiserum was tested against pure protein in a 1:1000 dilution in 1 % milk in TBS-T, for antigen detection *in planta*, a 1:250 dilution in buffer containing 0.3 % casein, 0.03 % BSA, 20 mM Tris/HCl pH 7.6, 150 mM NaCl was necessary.

## 2.6 Columns

HisTrap HP 1 ml and Superdex 200 (10/300 GL) columns were supplied by GE Healthcare (München, Germany). Protein concentration columns (Amicon Ultra Filter) were purchased from Millipore (Billerica, MA, USA).

## 2.7 Plant material

Peas (*Pisum sativum*) var. "Arvica" were ordered from Bayerische Futtersaatbau (Ismaning, Germany). *Arabidopsis* line SALK\_119667 *TIC110/tic110* #5 was used for stable transformation and *Nicotiana benthamiana* was used for transient expression of recombinant proteins.

### 3. Methods

#### 3.1 Plant methods

##### 3.1.1 Growth conditions

Seeds of *Arabidopsis* were either directly grown on soil or on ½ MS-media (1 % sucrose, 0.05 % MES, 0.237 % MS salts, pH 5.7 supplemented with 0.6 % agar and for hygromycin selection supplemented with 25 µg/ml hygromycin). Before sowing on sterile ½ MS-containing petridishes, seeds were surface sterilized for 10 min using 0.05 % Triton X-100 in 70 % ethanol. To synchronize germination, plates or pots were kept at 4 °C in the dark for one to three nights. For selection of resistant plants on hygromycin-containing plates, plants were exposed to light (100 µmol photons m<sup>-2</sup> s<sup>-1</sup>) for 8 h, followed by a 48 h incubation time in the dark. After subsequent exposure to light, viable, resistant plants can be distinguished from non-resistant plants and were transferred on ½ MS-media plates without hygromycin. Finally, resistant plants were transferred onto soil for further analyses. All *Arabidopsis* plants were grown under long day conditions (16 h 100 µmol photons m<sup>-2</sup> s<sup>-1</sup>, 21 °C, 8 h dark 16 °C).

*N. benthamiana* plants for transient expression of recombinant proteins were grown in the greenhouse under long day conditions. In case of using plants for electron microscopy studies, plants were grown under short day conditions (8 h 100 µmol photons m<sup>-2</sup> s<sup>-1</sup>, 21 °C, 16 h dark 16 °C) to reduce the starch content.

##### 3.1.2 Stable transformation of *Arabidopsis thaliana*

*Arabidopsis thaliana* plants were stably transformed with *A. tumefaciens* using the floral-dip method. *A. tumefaciens* (GV3101) carrying the respective construct of interest were grown in LB (10 g/l NaCl, 10 g/l peptone, 5 g/l yeast extract) supplemented with 100 µg/ml rifampicin, 25 µg/ml gentamycin and 100 µg/ml spectinomycin overnight at 28 °C. Cells were harvested at 6000 g for 15 min and resuspended in Silwet-medium (5 % sucrose, 0.05 % silwet L-77) to a final OD<sub>600</sub> of 0.8. 6-week old flowering plants were dipped for 30 s into the *Agrobacteria* suspension and the obtained seeds were selected on ½ MS-media plates supplemented with the selection marker (25 µg/ml hygromycin).

##### 3.1.3 Transient expression of recombinant proteins in *Nicotiana benthamiana*

AGL1 strains carrying the respective plasmids were grown in LB (supplemented with 100 µg/ml carbenicillin and 100 µg/ml spectinomycin for plasmid selection) at 28 °C overnight to an OD<sub>600</sub> of 0.6-0.8. The cells were pelleted by centrifugation at 4000 rpm for 15 min. The pellet was resuspended with infiltration medium (10 mM MES pH 6, 1 mM

MgCl<sub>2</sub> and 150  $\mu$ M acetosyringone) to an OD<sub>600</sub> of 1. After 2 h incubation in the dark at 28 °C, the abaxial sides of tobacco leaves were infiltrated with the bacterial suspension using a 1 ml syringe. Expression of the recombinant protein was allowed for three days in the greenhouse or under short day conditions (8 h 100  $\mu$ mol photons m<sup>-2</sup> s<sup>-1</sup>, 21 °C, 16 h dark 16 °C) in a growth chamber (Percival Scientific). In case of using the helper plasmid p19, cultures were mixed 1:1 in infiltration medium prior to the infection of leaves.

## 3.2 Molecular biological methods

General molecular biological methods not listed below were performed as described by (Sambrook et al., 1987), with modifications to the manufacturer's recommendation.

### 3.2.1 DNA cloning

Several cloning strategies were performed in this study:

For classical cloning the genes of interests were amplified via Q5 polymerase using oligonucleotides with included appropriate restriction sites. The amplified DNA and the destination vector were digested with the respective restriction endonucleases for 2 h at 37 °C. PCR products and vectors were purified using the NucleoSpin Extract II Kit. Ligation with T4 ligase (NEB) was carried out at RT for 3 h and the reaction was eventually transformed into chemically-competent TOP10 cells. Single colonies were inoculated into 3 ml liquid LB cultures and plasmid DNA was extracted using the alkaline lysis method. Proper insertion was checked with sequencing.

Recombinant constructs were generated by overlap PCR, using appropriate oligonucleotides fusing the genes of interest. The generated fusion product was checked on an agarose gel and extracted using the Nucleospin Extract II Kit.

The GATEWAY system (Invitrogen) was used to clone genes of interest into binary plant transformation vectors. To this end, PCR products were flanked with attB sites and were subcloned into an entry vector (pDONR207) according to the manufacturer's recommendations. The gene of interest was then transferred into pK7FWG2 or pHGW (Plant Systems Biology, Zwijnaarde, Belgium) according to the manufacturer's instructions. The respective plasmids in all steps were isolated using the NucleoSpin Plasmid Kit (Macherey and Nagel) and products were verified by sequencing.

To introduce site-directed point mutations site-directed mutagenesis PCR was performed using the Q5 Site-Directed Mutagenesis Kit (NEB). Back-to-back Primers were designed according to the manufacturer's recommendations. After amplification of the entire plasmid with the Q5 polymerase, the PCR product was treated with a KLD enzyme mix (kinase, ligase and DpnI) to circularize DNA and to digest parental template DNA. Insertion of the point mutation was verified by sequencing.

### 3.2.2 Sequencing

Sequencing of plasmids was performed by the sequencing service of the Genomics Service Unit (GSU, LMU Munich) using ~150 ng of plasmid as a template and suitable oligonucleotides.

### 3.2.3 Preparation of genomic DNA from *Arabidopsis thaliana*

One leaf from 1-week-old plants was used for homogenisation in 300 µl of extraction buffer (200 mM Tris/HCl pH 7.5, 250 mM NaCl, 25 mM EDTA, 0.5 % SDS, 100 µg/ml fresh RNase). Tissue was homogenized using either the TissueLyser (Qiagen) or the Polytron mixer (Eppendorf). After a short incubation time at 37 °C for 5 min, the cell debris was pelleted for 10 min at 10000 g and 4 °C and 300 µl of the supernatant was transferred into a fresh tube. For precipitation of genomic DNA one volume of ice-cold isopropanol was added and the tubes were inverted several times. Samples were centrifuged for 10 min at 10000 g and 4 °C and the resulting pellet was washed with 500 µl 70 % ethanol. After a last centrifugation step (10 min, 10000 g, 4 °C) the pellet was dried at 37 °C and resuspended in 50 µl dH<sub>2</sub>O. For immediate use the genomic DNA was incubated at 50 °C for 10 min and 1 µl of the DNA was used for a 10 µl PCR reaction.

### 3.2.4 Genotyping

To identify successful incorporation of a construct into the genome of heterozygous *TIC110/tic110* background lines, genomic DNA of transformed plants was analyzed. To this end, primers listed in table 2 and Taq polymerase were used. With these primer pairs, it was possible to generate specific PCR products for WT (atTic110 TDNA insert Test fwd + atTic110 Intron 14 rev), for the T-DNA insertion (LBa1 + atTic110 T-DNA insert test rev) and for the insertion of the desired construct (atTic110 Exon 2 fwd + atTic110 Exon 7 rev), respectively.

### 3.2.5 Transformation of *Agrobacterium tumefaciens*

2 µg of the desired plasmid was added to a frozen aliquot of GV3101 or AGL1 cells. Cells were incubated 5 min on ice subsequently followed by incubation for 5 min in liquid nitrogen. A heat shock step was performed for 5 min at 37 °C. 800 µl LB was added and cells were incubated for 4 h at 28 °C with shaking before they were plated on LB plates with appropriate antibiotics. Cells were grown for three days at 28 °C.

## 3.3 Biochemical methods

SDS-PAGES were performed according to (Laemmli, 1970). Protein concentration was estimated with the Bradford assay for crude protein extracts using a calibration curve with defined BSA concentrations. In case of vesicular membrane proteins, the Pierce BCA

Protein Assay Kit (ThermoFisher Scientific) was used, again using defined concentration of BSA as a standard.

### 3.3.1 Isolation of crude protein extracts from plants

Leaf material was homogenized in 150  $\mu$ l isolation buffer (10 mM Tris/HCl pH 7.6, 0.1 % LDS, 0.1 mM PMSF) using a polytron mixer (Eppendorf). The homogenate was incubated on ice for 20 min and subsequently centrifuged at 10000 g for 10 min. The supernatant contained both soluble and membrane proteins. Typically, 5  $\mu$ l of the protein extract was used to estimate protein concentration with the Bradford assay.

### 3.3.2 Preparation of samples for electron microscopy and photooxidation

Leaf material was cut with a razor blade into 1x1 mm pieces which were subsequently fixed with 2.5 % glutaraldehyde in buffer containing 75 mM cacodylate pH 7.4, 2 mM  $\text{MgCl}_2$  (in the following named as CB) for one hour on ice. Several washing steps with increasing incubation times in chilled CB were carried out, followed by 15 min blocking with 50 mM glycine, 10 mM KCN, 10 mM aminotriazole in CB, again followed with washing steps with increasing incubation times. After addition of 0.5 mg/ml diaminobenzidine (DAB) in CB, leaves and solutions were transferred into glass bottom culture dishes (MatTek, Ashland, USA) and were subjected to illumination with blue light (450-490 nm) using an inverted SP5 Spectral Hybrid CLSM and a standard FITC filter (Leica, Leipzig, Germany). Illumination was carried out for 5 mins for each quarter of the dish, and the solution was changed in between to ensure optimal photooxidation. Leaves were removed from the microscope and were washed with chilled CB. Further preparation for electron microscopy studies was performed by AG Klingl (LMU Munich). In brief, samples were contrasted in 1 % osmium tetroxide, followed by extensive washing. Subsequently, samples were dehydrated with acetone, followed by infiltration with resin (1:1 resin/acetone overnight, 2:1 resin/acetone for 3 h and 100 % resin for 3 h). Fresh resin was added and samples were allowed to polymerize at 63 °C overnight. Ultrathin sections were prepared and post-stained with lead citrate. Investigation was performed on a Zeiss EM 912 with OMEGA filter at 80 kV and in zero-loss mode. For the recordings Tröndle 2k x 2k slow-scan CCD camera was used.

### 3.3.3 Chloroplast isolation from *N. benthamiana*

Leaf material of infected leaves was homogenized with a polytron mixer in 25 ml isolation buffer (300 mM sorbitol, 5 mM  $\text{MgCl}_2$ , 5 mM EDTA, 20 mM HEPES/KOH pH 8, 10 mM  $\text{NaHCO}_3$ , 50 mM ascorbic acid) and filtered through one layer of gauze. The filtrate was centrifuged at 3500 rpm for 4 min. The pellet was carefully resuspended with a brush in 1 ml isolation buffer and layered on top of a discontinuous Percoll gradient (30 % and 82 %, respectively). After centrifugation at 3500 rpm for 6 min, intact chloroplasts were collected



and washed with washing buffer (330 mM sorbitol, 50 mM HEPES/KOH pH 8, 0.5 mM  $\text{MgCl}_2$ ).

### 3.3.4 Protoplast isolation from *N. benthamiana*

Leaf material was cut with a razor blade and was vacuum-infiltrated for 30 s with 10 ml of a sterile-filtered enzyme solution (1 % cellulase R10, 0.3 % Macerozym R10 in buffer F-PIN, see below). The solution was incubated in the dark at 40 rpm for 2 h and the protoplasts were released at 80 rpm for one min. After filtration of the protoplast solution through a nylon net (100  $\mu\text{m}$  pore size), the solution was overlaid with 2 ml F-PCN (see below) and centrifuged (70 g, 10 min, 23 °C). Intact protoplasts were collected at the interface with a cut tip, washed with 10 ml W5 and collected at 50 g and 23 °C for 10 min. After resuspending in a small volume of W5 (see below), the protoplasts were used for confocal fluorescence microscopy using a SP5 Spectral Hybrid CLSM.

F-PIN (500 ml): macro MS (modified), 0.5 ml 1000x micro MS, 1 ml 500x PC vitamins, 20 mM MES/KOH pH 5.8, 55 g sucrose, osmolarity was adjusted with sucrose to 550 mOsm and the solution was filtrated (0.45  $\mu\text{m}$ ).

F-PCN (500 ml): macro MS (modified), 0.5 ml micro MS, 500x PC vitamins, 500  $\mu\text{l}$  6-benzylamino-purine (BAP, 1 mg/ml), 50  $\mu\text{l}$   $\alpha$ -naphthaleneacetic acid (NAA 1 mg/ml), 20 mM MES/KOH pH 5.8, 40 glucose, osmolarity was adjusted with glucose to 550 mOsm, and the solution was filtrated (0.45  $\mu\text{m}$ ).

2 M  $\text{NH}_4$  succinate (50 ml): 11.8 g succinic acid, 5.3 g  $\text{NH}_4\text{Cl}$ , 11 g KOH pellets, adjust pH to 5.8, and the solution was filtrated (0.45  $\mu\text{m}$ ).

Macro MS (modified): 20 mM each:  $\text{KNO}_3$ ,  $\text{CaCl}_2 \times 2 \text{H}_2\text{O}$ ,  $\text{MgSO}_4 \times 7 \text{H}_2\text{O}$ ,  $\text{KH}_2\text{PO}_4$ , 5 ml 2 M  $\text{NH}_4$  succinate.

1000x micro MS (100 ml): 83 mg KJ, 620 mg  $\text{H}_2\text{BO}_3$ , 2230 mg  $\text{MnSO}_4$ , 860 mg  $\text{ZnSO}_4$ , 25 mg  $\text{Na}_2\text{MoO}_4$ , 2.5 mg  $\text{CuSO}_4$ , 2.5 mg  $\text{CaCl}_2$ .

500x PC vitamins (100 ml): 10 g myoinositol, 100 mg pyridoxine HCl, 50 mg thiamine HCl, 100 mg nicotinic acid), 1 g biotin, 100 mg Ca panthotenate.

### 3.3.5 Immunoblotting

Separated proteins were transferred from the SDS gel onto a PVDF or nitrocellulose membrane using a semi-dry western blot apparatus. In case of PVDF, the membrane was activated by incubation in 100 % methanol. Blotting was carried out for 1-2 hours at 0.8 mA/cm<sup>2</sup> in the presence of blotting buffer (25 mM Tris/HCl pH 8.2-8.4, 192 mM glycine,

0.1% SDS, 20 % methanol). After staining with Ponceau S (5 % acetic acid, 0.3 % Ponceau S), the membrane was blocked with either 1 % milk in TBS-T or casein buffer (see 2.4) for 3 times 10 min. Primary antiserum was incubated for 2 h at RT or overnight at 4 °C in the respective blocking buffer. After three washing steps, each 10 min, a secondary antibody (horseradish peroxidase-conjugated AB anti-rabbit) was applied for 1 h at RT in the respective blocking buffer. Detection was carried out using the ECL system. For this, equal volumes of solution 1 (100 mM Tris/HCl pH 8.5, 1 % (w/v) luminol, 0.44 % (w/v) coumaric acid) and solution 2 (100 mM Tris/HCl pH 8.5, 0.018 % (v/v) H<sub>2</sub>O<sub>2</sub>) were mixed and added to the membrane. Chemiluminescence was detected after an incubation time of 2 min using Image Quant LAS 400 (GE Healthcare, Munich, Germany).

For detection of biotinylated proteins, the VECTASTAIN ABC-HRP Kit (Vectorlabs) was used according to the manufacturer's instructions.

### **3.3.6 Isolation of outer and inner envelope membranes from pea**

Isolation of separated outer and inner envelope membranes of pea chloroplasts was performed according to (Waegemann et al., 1992). For this, leaf material of 20 trays 9-day-old peas was ground in a kitchen blender in 7.5 l isolation medium (330 mM sorbitol, 20 mM MOPS, 13 mM Tris, 0.1 mM MgCl<sub>2</sub>, 0.02 % (w/v) BSA) and filtered through four layers of mull and one layer of gauze (30 µm pore size). The filtrate was centrifuged for 5 min at 1500 g, the pellet gently resuspended with a brush and intact chloroplasts reisolated via a discontinuous Percoll gradient (40 % and 80 %, respectively). Intact chloroplasts were washed twice with wash medium (330 mM sorbitol, pH 7.6), homogenized and further treated according to (Waegemann et al., 1992).

### **3.3.7 Chlorophyll determination**

For chlorophyll determination 5 µl of chloroplasts were dissolved in 5 ml of 80 % acetone. Absorbance was measured against the solvent at 645 nm, 663 nm and 750 nm and chlorophyll concentration was calculated as described in (Arnon, 1949).

### **3.3.8 Trypsin treatment of inner envelope membranes**

10 µg of isolated inner envelopes were used for protease treatments. Isolated inner envelopes were pelleted by centrifugation at 256000 g for 10 min at 4 °C and were resuspended in a trypsin-suitable buffer (25 mM Tricine pH 8.4, 0.2 mM CaCl<sub>2</sub>). Protease digestion was performed for 90 s at RT using 10 ng protease per 10 µg total membrane protein and was stopped by adding excess soybean trypsin inhibitor or 1 µg/ml α-macroglobulin. As a control for successful inhibition of proteolytic activity, samples were incubated with excess soybean trypsin inhibitor or α-macroglobulin prior to protease treatment.

### 3.3.9 Tandem Mass Tag labeling and quantification of peptides

Labeling using aminoreactive Tandem Mass Tag (TMT)-labeling reagents TMT129, TMT130 and TMT131 was carried out according to the manufacturer's recommendations (ThermoFisher Scientific) and was performed by AG Carell (LMU, Munich).

### 3.3.10 Biotinylation of inner envelope membranes

60  $\mu$ l of isolated inner envelope membranes were centrifuged for 10 min at 4 °C at 256000 g and resuspended in 1x PBS (140 mM NaCl, 2.7 mM KCl, 10 mM Na<sub>2</sub>HPO<sub>4</sub>, 1.8 mM KH<sub>2</sub>PO<sub>4</sub> pH 7.4). In a final volume of 100  $\mu$ l 2 mM NHS-PEG<sub>4</sub>-Biotin (from a 20 mM aqueous stock) or 0.5 mM Biotin-XX,SE (from a 10 mM stock in 100 % DMSO) or 0.5 mM Sulfo-NHS-Biotin (from an aqueous 10 mM stock) was added. Labeling was carried out for 10 min at 4 °C. The reaction was quenched with 10 mM Tris/HCl pH 7.4. Biotinylated membranes were centrifuged (10 min, 256000 g, 4 °C) and were washed with 1x PBS, 20 mM Tris/HCl, pH 7.4 to remove excess biotin reagent. Washed membranes were solubilized with SDS sample buffer and subjected to an 8.5 % SDS-PAGE. Bands corresponding to Tic110 protein were excised and gel pieces were further cut into 1.5x1.5 mm gel pieces. For in-gel digestion 200  $\mu$ l of 100 mM NH<sub>4</sub>HCO<sub>3</sub> pH 8/50 % ACN was added and the samples were incubated for 30 min at 37 °C until the staining solution was completely removed. Samples were reduced by adding 10 mM DTT in NH<sub>4</sub>HCO<sub>3</sub> for 10 min at 60 °C. 100 mM IAA was added, and samples were incubated for 15 at 37 °C with shaking at 600 rpm followed by two washing steps with 100 mM NH<sub>4</sub>HCO<sub>3</sub>/50 % ACN. Afterwards 50  $\mu$ l of 100 % ACN was added to the gel pieces for 15 min at RT to allow shrinkage of the gel pieces. After drying of the gel pieces 50  $\mu$ l of reconstituted trypsin (10 ng/ $\mu$ l in 100 mM NH<sub>4</sub>HCO<sub>3</sub> pH 8) was added and overlaid with 10  $\mu$ l of buffer. Digestion took place at 37 °C overnight. The digest solution was removed and added to a new tube. To extract peptides from the gel pieces, 50  $\mu$ l 50 % ACN/0.1 % TFA was added and incubated for 15 min at 37 °C. This step was repeated three times. Extracted peptides were sent to AG Carell for further analysis.

### 3.3.11 Overexpression of proteins

**miniSOG overexpression:** pET21d(+) carrying the coding sequence for miniSOG was transformed into BL21 (DE3) cells. 1 l of LB medium supplemented with 100  $\mu$ g/ml ampicillin was inoculated with a preculture and was grown to an OD<sub>600</sub> of 0.5. After addition of 1 mM IPTG expression of the protein was allowed for 3 h at 37 °C. Cells were pelleted at 6000 rpm for 15 min at 4 °C and the bacterial pellet was directly used for disrupting the cells or stored at -80 °C.

**WT dNTic110 overexpression:** pET21d(+) plasmid carrying the dNTic110 sequence was transformed into BL21 (DE3) cells. Cells were grown in LB medium (supplemented with

100 µg/ml ampicillin) at 37 °C and 120 rpm until an OD<sub>600</sub> of 0.5. Expression was induced by adding 0.5 mM IPTG and the temperature was shifted to 12 °C. Expression was allowed overnight. Cells were pelleted by centrifugation at 6000 rpm for 15 min at 4 °C and the pellet was stored at -80 °C until further use.

### 3.3.12 Co-translational incorporation of the unnatural amino acid into dNTic110

pSB8.12e2 plasmids with the respective dNTic110 constructs carrying amber codons at various positions were transformed into BL21 (DE3) cells. Cells were grown in LB medium supplemented with 30 µg/ml chloramphenicol at 30 °C until an OD<sub>600</sub> of 0.4. 1 mM acetylphenylalanine, Apa (from a 200 mM stock in 200 mM NaOH, Synchem UG & Co. KG) and 50 ng/ml anhydrous tetracycline (from a 2 mg/ml stock in DMF) was added to the cells to induce the aa-tRNA synthetase and to pre-load it with Apa. Cells were grown for 1 h at 30 °C and 0.5 mM IPTG was added to start the expression of the protein. Expression was allowed for 16-20 h at 30 °C which resulted in insoluble protein or for 36 h at 18 °C resulting in soluble protein. Cells were harvested via centrifugation at 6000 g for 20 min at 4 °C and the pellet was stored at -80 °C until further use.

### 3.3.13 Purification of proteins

**WT-110:** Since Tic110 appeared to be very degradation-prone and protease-sensitive, all following steps were carried out at 4 °C in the presence of protease-inhibitor (Roche, Penzberg) in all buffers. The bacterial pellet was resuspended in 20 mM Tris/HCl pH 8, 200 mM NaCl in the presence of 1 mM PMSF, 5 mM β-mercaptoethanol, 10 % glycerol, Roche protease inhibitor and lysed via French Press. Cell membranes were pelleted by two times centrifugation at 20000 g for 20 min at 4 °C. The clear supernatant was loaded onto a HisTrap HP column (1 ml) with an ÄKTA purifier system. For wash and elution 20 mM Tris/HCl pH 8.0, 200 mM NaCl with increasing concentrations of imidazole was used. The protein was concentrated (Amicon Ultra) to a volume of ~500 µl and was further purified using an Superdex 200 (10/300) column equilibrated with 20 mM Tris/HCl pH 8, 200 mM NaCl.

**Soluble Apa-110:** Soluble Apa-Tic110 was purified as described above, except that the protein was affinity purified in-batch on Ni-NTA agarose beads (Macherey and Nagel). Elutions were pooled and were purified without further concentration using an Superdex 200 (10/300) column equilibrated with 20 mM Tris/HCl pH 8, 200 mM NaCl.

**Insoluble Apa-Tic110:** Expression of Tic110 at elevated temperatures (30 °C) resulted in insoluble proteins. After lysis of bacterial cells and centrifugation, the inclusion body pellet was resuspended in detergent buffer (20 mM Tris/HCl pH 7.5, 200 mM NaCl, 1 % deoxycholic acid, 1 % Nonidet P-40, fresh 5 mM β-mercaptoethanol). Samples were

centrifuged at 10000 g for 10 min at 4 °C and the pellet fraction was resuspended in triton buffer (20 mM Tris/HCl pH 7.5, 0.5 % Triton X-100, fresh 5 mM  $\beta$ -mercaptoethanol). After centrifugation at 10000 g for 10 min at 4 °C, this step was repeated. The pellet was washed in Tris buffer (20 mM Tris/HCl pH 8, fresh 10 mM DTT) and centrifuged at 10000 g for 10 min at 4 °C. After a second washing step with Tris buffer, the pelleted fraction was resuspended in Urea buffer (8 M Urea, 20 mM Tris/HCl pH 8, 200 mM NaCl) and rotated at RT for 1 h to extract the protein out of the inclusion bodies. After centrifugation at 20000 g for 15 min at RT the supernatant contained the extracted protein.

**miniSOG:** The bacterial pellet was resuspended in 20 mM Tris/HCl pH 8, 150 mM NaCl and cells were cracked using a microfluidizer. After two times centrifugation (20000 g, 20 min, 4 °C) the cleared supernatant was purified with a HisTrap HP column (1 ml) and a linear gradient of imidazole was used for elution. High purity elutions were collected and subjected to gel filtration on a Superdex 200 (10/300) column to eliminate remaining contaminations.

#### **3.3.14 Reconstitution of purified dNTic110 into liposomes and flotation assay**

20 mg of phosphatidylcholine (PC) lipids (Larodan Fine Chemicals AB, Solna, Sweden) were washed with chloroform/methanol (1:1) and dried under N<sub>2</sub>. The lipids were resuspended in the indicated buffer to a concentration of 20 mg/ml. To generate liposome vesicles lipids were freeze/thawed five times. Mixed-lamellar liposomes were extruded through a membrane with 200 nm pore size to generate unilamellar vesicles. Liposomes and purified protein (~1 mg/ml) were mixed in a 1:1 volume ratio in the presence of 80 mM Nonanoyl-*N*-methylglucamide. The mixture was incubated at 4 °C for 90 min under rotation. Samples were subsequently dialysed against buffer without detergent overnight at 4 °C. Proteoliposomes were separated from free liposomes via a flotation through a sucrose gradient. To this end, samples were adjusted to 1.6 M sucrose and overlaid with 0.8 M, 0.4 M and 0.2 M sucrose in a total volume of 12 or 4 ml. After 19 h centrifugation at 100000 g at 4 °C fractions were collected and precipitated with 10 % TCA. After washing with 100 % ice-cold acetone, pellets were resuspended in SDS sample buffer and subjected to SDS-PAGE.

#### **3.3.15 DSSO cross-linking**

Proteoliposomes were described as above in 10 mM HEPES/KOH pH 7.6, 200 mM NaCl. Liposomes and freshly purified dNTic110 (~0.5 mg/ml) were mixed in a ratio 1:1 in the presence of 80 mM Nonanoyl-*N*-methylglucamide for 1.5 h at 4 °C. Detergent and residual Tris/HCl buffer from purified dNTic110 was removed by dialysis overnight at 4 °C against 10 mM HEPES/KOH, pH 7.6, 200 mM NaCl without detergent. Samples were subjected to sucrose flotation and fractions containing proteoliposomes were pooled. Sucrose was

removed by 1:8 dilution with 10 mM HEPES/KOH pH 7.6, 200 mM NaCl and pelleted proteoliposomes were resuspended in cross-linking buffer 10 mM HEPES/KOH pH 7.6, 200 mM NaCl and were subjected to cross-linking. For this, 1.5 mM of DSSO cross-linker was added two times for each 45 min at 4 °C. After this, cross-linked proteoliposomes were acetone-precipitated and the air-dried pellet containing ~250 µg of protein was resuspended, reduced, alkylated and trypsin-digested. To enrich peptides, size-exclusion was performed using a Superdex Peptide 3.2/300 column. Measurements were done on a QExactive HF and for data analysis MaxQuant software was used (AG Carell, LMU Munich).

### 3.3.16 Labeling of proteins

Labeling of acetylphenylalanine-containing dNTic110 was carried out by adding 2 µl of a 50 mM stock solution of a hydroxylamine-derivative of Alexa Fluor488 (in 100 % DMSO) to the protein solution in 20 mM Tris/HCl pH 8, 200 mM NaCl. The mixture was incubated for 16 h at 4 °C protected from light. Excess dye was removed by dialysis overnight against buffer without dye. Labeling efficiency was calculated by comparing absorbances at 494 nm ( $\text{Alexa Fluor488}\epsilon_{494} = 72000 \text{ M}^{-1} \text{ cm}^{-1}$ ) with the protein absorbance at 280 nm ( $\text{dNTic110}\epsilon_{280} = 46310 \text{ M}^{-1} \text{ cm}^{-1}$ ) after subtracting the Alexa Fluor488 contribution at 280 nm (0.15 times the absorbance at 494 nm).

### 3.3.17 Encapsulation of carboxyfluorescein and fluorescence spectroscopy

Preparation of liposomes was performed as described in 3.3.14 in 1x PBS, pH 7.4. During preparation of liposomes the fluorescent dye carboxyfluorescein was encapsulated into the liposomes. For this, 20 mM of carboxyfluorescein was added to 20 mg/ml PC lipids. This concentration is sufficient for self-quenching of the dye within the vesicles. After five freeze/thaw cycles liposomes were extruded through a membrane with 200 nm pore size to generate unilamellar vesicles. To remove non-encapsulated dye the liposomes were dialysed against 1x PBS buffer pH 7.4 overnight at 4 °C. For fluorescence measurements, 5 µl of liposomes were mixed with 995 µl 1x PBS pH 7.4 to generate a suitable fluorescent signal. After addition of purified dNTic110 protein fluorescence was recorded every millisecond for 300 or 600 s with a LS55 fluorescence spectrometer (PerkinElmer, Waltham, USA) with an excitation wavelength of 494 nm and an emission wavelength of 515 nm.

### 3.3.18 Reduction and oxidation assay

dNTic110 was incubated with 50 µM CuCl<sub>2</sub> or 10 mM DTT for 60 min at 20 °C.

## 4. Results

### 4.1 Two topological models of Tic110

Tic110 is encoded by a single gene and conserved from glaucophytes to green plants. Unfortunately, determination of the three-dimensional structure of this membrane protein at high resolution is a difficult challenge, which in general is true for a large collection of membrane proteins. So far only a low-resolution model from a truncated Tic110 variant of *Cyanidioschyzon merolae* is available (Tsai et al., 2013). However, this version of Tic110 lacks half the N-terminus and is not a reliable basis for structural analysis. Thus, information about Tic110 are mainly originating from biochemical experiments. Universally accepted is the fact that the 110-kDa protein is anchored into the membrane by its two N-terminal, highly hydrophobic helices, however, the localization of the large hydrophilic part of Tic110 has been debated for a long time. Two different theories exist:

Theory 1 suggests that the C-terminus of Tic110 mainly exists as a soluble domain in the stroma, where its unique action is to form a scaffold responsible for chaperone recruitment.

Theory 2 proposes that Tic110 forms a preprotein translocation channel, with two domains protruding into the intermembrane space which could function in interaction with TOC complexes. Tic110 is anchored into the inner envelope membrane by two hydrophobic  $\alpha$ -helical domains located in the N-terminus, while the preprotein-conducting channel is formed by four amphipathic helices. The functional protein is a dimer.

Prediction analyses were carried out using the complete amino acid sequence of the pea Tic110 protein to further analyze the presence of amphipathic regions. Dense alignment surface methods (DAS) were used to predict any transmembrane  $\alpha$ -helices in membrane proteins (Cserző et al., 1997). DAS is based on low-stringency dot-plots of the input sequence against a collection of non-homologous membrane proteins using a previously derived special scoring matrix. The result shows two segments with a high "DAS" profile score to be located at the very N-terminus (Figure 5), most probably representing the two uncontroversial N-terminal hydrophobic helices, which anchor the protein into the inner envelope membrane. Besides, four helices were identified with a lower DAS score located around residues 210-230, 470-490, 570-590 and 700-720. In parallel, investigation of the sequence by the MPEx program, based on the Wimley-White scale of hydrophobicity, revealed that the partition free energy for the region of residues 208–226, 666–684 and 697–715 makes an affiliation with the nonpolar region unfavorable. In addition, an in-depth analysis of predicted helices by helical plots shows that some have amphipathic features (numbers according to the mature pea sequence): helix 1 (L<sub>208</sub>IYVSNIVFGDASSFLLPW),

helix 2 (A<sub>311</sub>VPGVSQVVEELEKVLSFNLLI), helix 3 (K<sub>577</sub>ELKKLIAFNTLVVTKLVEDI) and helix 4 (A<sub>664</sub>DLYKTFLTYCLTGDVV). These data suggest that Tic110 contains regions with amphipathic characteristics, which however, cannot be assigned to a specific amino acid sequence. They may vary in length and involvement of amino acids. Nonetheless, if Tic110 is anchored into the inner envelope membrane by its two hydrophobic helices and further assembles or integrates into the membrane by four amphipathic helices, this consequently leads to the fact that two loops extend into the intermembrane space. That is in line with previously reported results (Balsera et al., 2009).



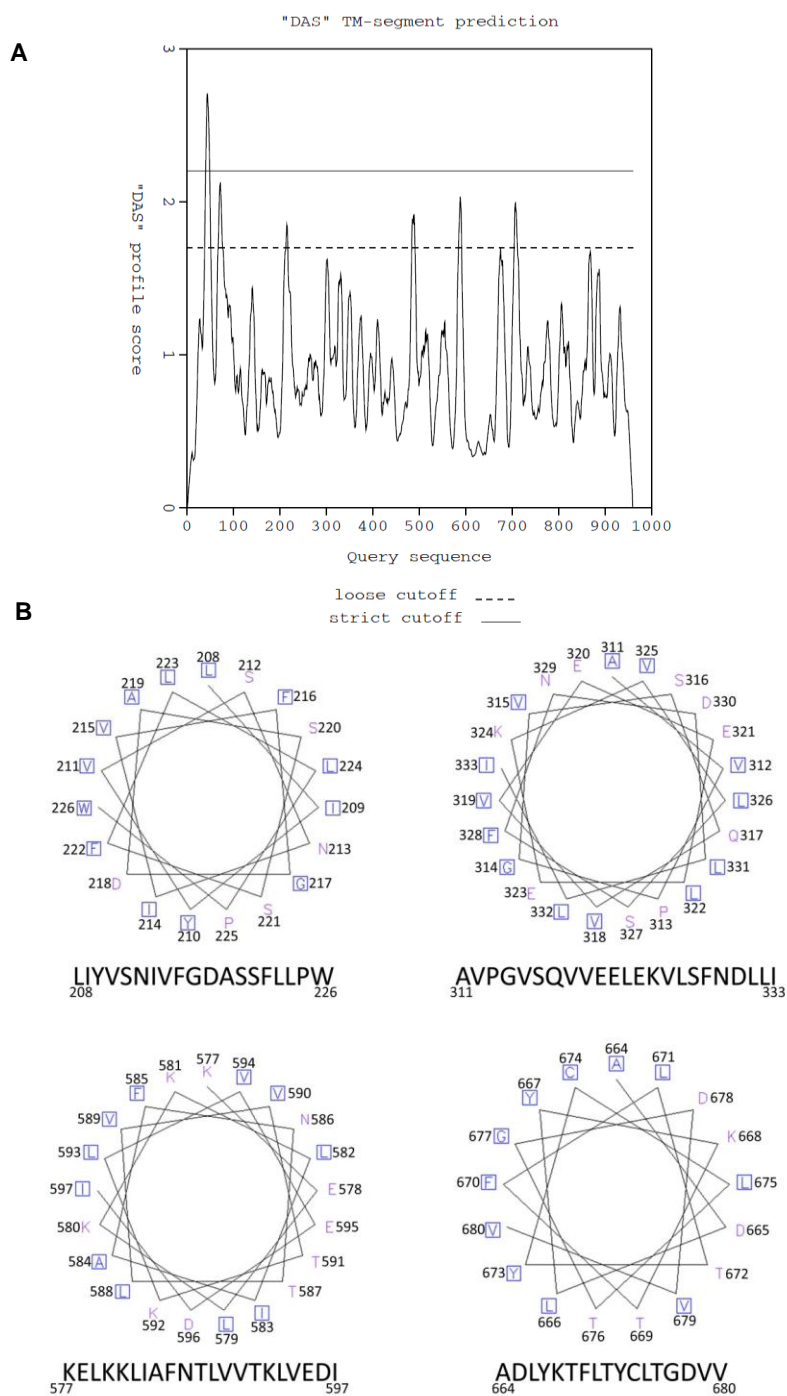


**Figure 5: Prediction analyses using the primary amino acid sequence of psTic110.**

**A:** Dense Alignment Surface method to predict hydrophobicity to identify putative transmembrane helices in the primary amino acid sequence of psTic110.

**B:** Helical wheel representation of the predicted amphipathic helices of Tic110. The primary sequence of psTic110 was analyzed by the emboss pepwheel program. The numbers refer to the amino acid position in the mature pea sequence. Hydrophobic and glycine residues are boxed.

## 4.2 *In situ* topology of the inner envelope protein Tic110

Large amounts of highly purified inner envelope membranes can be isolated from pea chloroplasts. These vesicles have a right-side-out orientation (Shingles and McCarty, 1995), thereby exposing peptide domains formerly oriented to the intermembrane space to the buffer media. This characteristic makes the vesicles suitable to either superficial protease treatment or selective biotinylation, subsequently followed by mass spectrometric-based sequencing, allowing to identify these exposed domains. In the following, trypsin digestion and selective biotinylation of isolated inner envelopes were used to identify peptides that were exposed to the surrounding buffer and thus orientated into the intermembrane space in intact chloroplasts to clarify the topology of Tic110 in an *in situ* assay.

### 4.2.1 Selective biotinylation of inner envelope membranes

To gain information on the topology of Tic110 in the inner envelope membrane three different chemicals with a biotin moiety were used: NHS-PEG<sub>4</sub>-Biotin, Sulfo-NHS-Biotin and Biotin-XX,SE (Figure 6). The succinimidyl ester reacts covalently with primary amino groups which exist at the accessible N-terminus and the  $\epsilon$ -amino from lysines, thereby adding the biotin group to the protein. This chemical reactivity towards overrepresented lysines in a polypeptide chain represents a suitable tool to study surface arrangements of a protein. Sites of covalent labeling in proteins can be identified using mass spectrometry by determining the change in mass of peptide fragments after labeling and by sequencing of the modified peptides in the mass spectrometer.

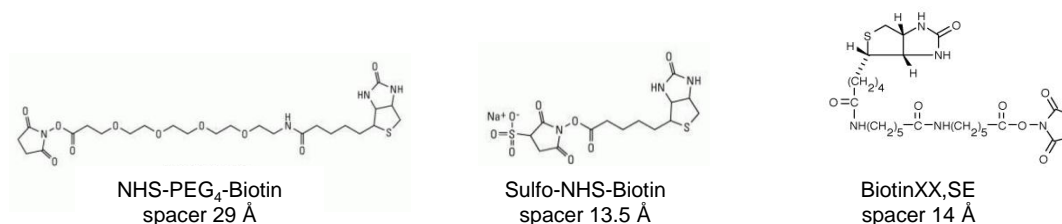


**Figure 6: Structures of three different cross-linkers that were used in this study:** NHS-PEG<sub>4</sub>-Biotin, Sulfo-NHS-Biotin and Biotin-XX,SE. Spacer lengths are indicated in Å.

All three chemicals were chosen because of their spacer length (to prevent diffusion through any pore proteins) and their membrane-impermeability to prevent membrane penetration. Isolated inner envelope membranes were biotinylated at their surface (4 °C, 10 min) and the reaction was quenched using 10 mM Tris/HCl pH 7.4. Samples were subjected to SDS-PAGE and to control the biotinylation, after transfer onto nitrocellulose membrane, tagged proteins were visualized using a avidin/biotin-horseradish peroxidase enzyme complex (VECTASTAIN ABC-HRP Kit). Figure 7 shows the SDS-PAGE analysis of 15 µg total protein

from isolated inner envelope membranes treated in the presence of NHS-PEG<sub>4</sub>-Biotin, Sulfo-NHS-Biotin and Biotin-XX,SE (Figure 7 A) and the biotin detection in each fraction following streptavidin reaction (Figure 7 B). Slight amounts of Tic110 are biotinylated, independently from the structure of cross-linker that was used. Besides, other proteins of the inner envelope membrane are also biotinylated proving that the reaction was successful and that only a few biotin residues were attached to Tic110. The bracket-marked band in the Coomassie-stained SDS-PAGE corresponding to Tic110 was excised and polypeptides were reduced, alkylated and trypsin-digested in-gel overnight at 37 °C. Tryptic peptides were analyzed by AG Carell (LMU, Munich). Identified peptides with found modifications were matched against the pea Tic110 sequence.

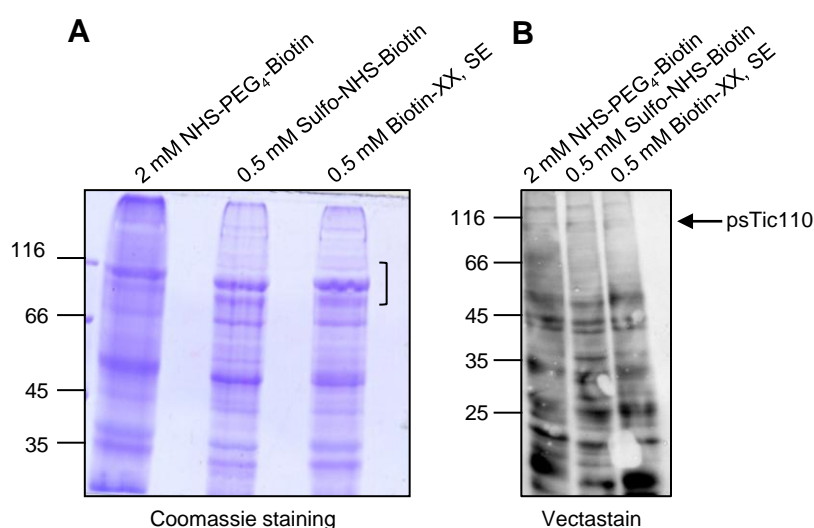


**Figure 7: Selective biotinylation of isolated inner envelope vesicles.**

Proteins from 15 µg biotinylated inner envelope vesicles separated by SDS-PAGE were either Coomassie stained or transferred onto nitrocellulose membrane.

**A:** Bracket-marked band in the Coomassie-stained SDS-PAGE corresponding to Tic110 was excised and polypeptides were reduced, alkylated and trypsin-digested in-gel overnight at 37 °C.

**B:** Biotinylation of inner envelope proteins was detected after reaction with streptavidin coupled to horse-radish peroxidase (VECTASTAIN ABC-HRP Kit).

Peptides from all parts of Tic110 could be detected, resulting in a high sequence coverage. Modifications resulting from the biotinylation could be found at nearly every lysine residue, however, the N-terminus was not modified. Consequently, selective biotinylation under the applied conditions is not useful to clarify the *in situ* topology of Tic110 in isolated inner envelope vesicles.

#### 4.2.2 Limited proteolysis of inner envelope membranes

Limited proteolysis is a biochemical technique that allows the degradation of (surface) exposed parts of proteins, thus providing information on accessible portions of the protein. It can be successfully applied to analyze conformational and topological features of a protein. Especially in combination with subsequent mass spectrometry this method specifically provides information about structural determinants down to the single amino acid level. Using isolated intact inner envelope vesicles with a right-side-out orientation (Waegemann et al., 1992) makes these formerly intermembrane space protruding domains accessible to the surrounding buffer and thus, to the protease of choice. By using moderate temperatures, low amounts of enzyme and short incubation times, it should be possible to "shave" the vesicles without risking that the protease enters or digest parts which are protected by the inner envelope membrane. Ultracentrifugation leads to the pelleting of proteolyzed vesicular membranes and the supernatant containing the soluble peptides, which can then be identified and sequenced with subsequent mass spectrometric analyses.

In the past it has been stated that degradation of Tic110 only occurs due to remaining protease-activity at post-protease treatment steps due to insufficient quenching of the protease (Jackson et al., 1998). Thus, a first step was to ensure efficient quenching conditions. For this, 10  $\mu$ g isolated inner envelope vesicles were treated with either  $\alpha$ -macroglobulin or excess soybean trypsin inhibitor prior to the incubation with 10 ng trypsin. After incubation with the protease for 90 s at room temperature, the degradation pattern of Tic110 was compared to untreated inner envelopes using Tic110-specific antiserum. No difference between quenched protease-treated and control samples could be observed, leading to the conclusion that the protease indeed can be adequately quenched (Figure 8 A). Two bands with a lower molecular weight could be observed in all three samples, however, as this degradation also occurred in the non-protease sample, it can be concluded that this occurred during sample preparation.

Treatment of 10  $\mu$ g total inner envelope membrane protein with 10 ng trypsin for 90 s at room temperature led to the typical degradation pattern observed in former experiments (Lübeck et al., 1996, Balsera et al., 2009). In contrast, selected control proteins, which are anchored in the inner envelope but do not expose domains to the intermembrane space, Tic62, Tic40 and IEP37, are not degraded, corroborating that these proteins are protected by the double lipid layer of the inner envelope membrane (Figure 8 B). To further exclude the possibility that trypsin might penetrate through the membrane and thereby achieves access to intra-vesicular domains, agarose beads with immobilized trypsin were used for limited proteolysis. Increasing amounts of trypsin-beads were used and the degradation pattern was compared with soluble trypsin treatment. As seen in Figure 8 C, no obvious differences in

degradation could be observed between immobilized and mobile trypsin, thus substantiating the assumption that trypsin cannot enter isolated right-side-out vesicles under the applied conditions and that Tic110 indeed exposes domains to the out-side of the vesicles.

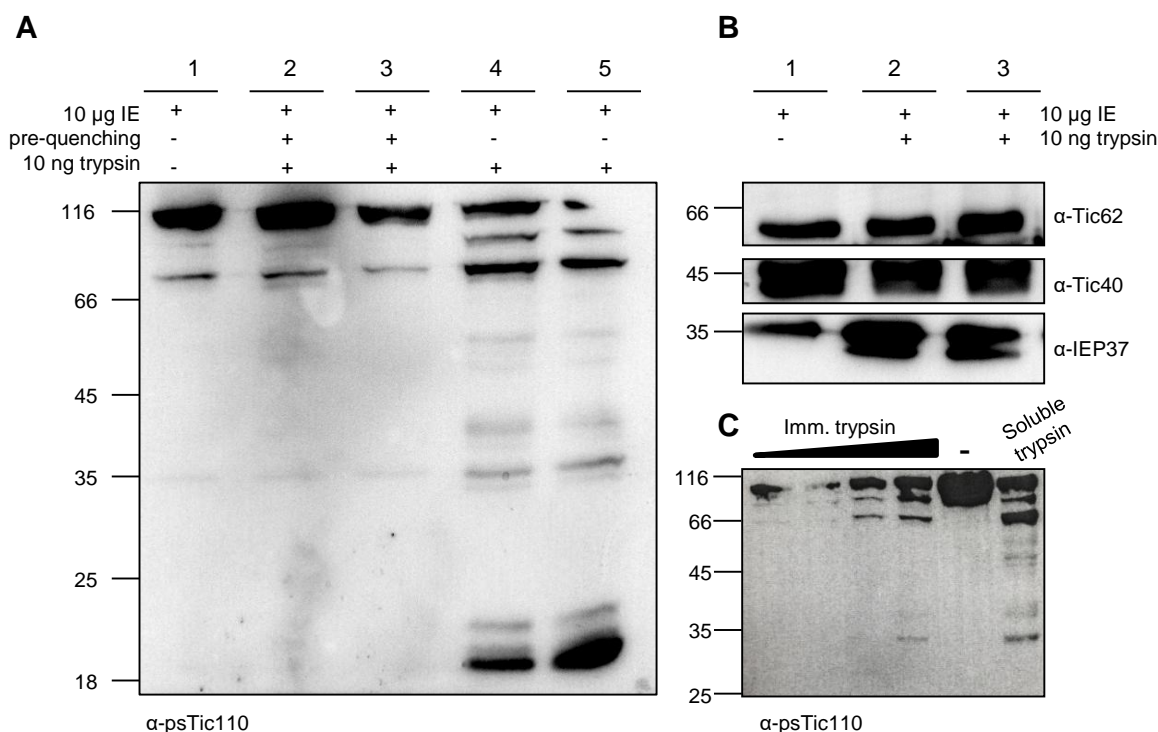


**Figure 8: Limited proteolysis of intact isolated inner envelope vesicles using the protease trypsin.**

**A:** Inner envelope vesicles (10 µg) were treated with and without 10 ng trypsin for 90 s at RT. Samples in lane 1 were not treated with protease, whereas samples in lane 2 and 3 were pretreated with protease inhibitor macroglobulin (2) or excess soybean trypsin inhibitor (3) to demonstrate optimal quenching of the protease. Two biological replicates in lane 4 and 5 were treated with 10 ng trypsin, followed by inhibition of the protease with excess soybean trypsin inhibitor. Treated and non-treated envelopes were collected via ultracentrifugation, resuspended in 2x SDS sample buffer, subjected to 10.5 % SDS-PAGE, blotted onto nitrocellulose and were immunodecorated using antiserum against psTic110.

**B:** As control proteins psTic62, psIEP37 and psTic40 were chosen. Same samples (1, 4 and 5) as in A were subjected to SDS-PAGE, transferred onto nitrocellulose membrane and immunodecorated using antisera as indicated.

**C:** Limited proteolysis using immobilized trypsin in comparison with soluble trypsin protease. Envelopes were collected via ultracentrifugation and analyzed on 10.5 % SDS-PAGE, followed by immunoblotting onto nitrocellulose and probing with psTic110-specific antiserum.

Three biological replicates of inner envelope vesicles were chosen for mass spectrometric analyses upon incubation with trypsin. 60 µg total membrane protein were proteolyzed with 75 ng of trypsin for 90 s at room temperature. The reaction was quenched by using excess soybean trypsin inhibitor. After ultracentrifugation the supernatant containing the released tryptic peptides was sent for mass spectrometric analysis, whereas the shaved envelopes were analyzed using SDS-PAGE and immunoblotting with Tic110-specific antiserum. Again,

degradation pattern was comparable as previously observed (Figure 9 A, Balsera et al., 2009).

Only peptides with high and medium quality score found in each replicate were matched against the sequence of psTic110. The representative result from three biological replicates is shown in Figure 9 B, which includes the indication of the four amphipathic helices (red boxes) and stromal and intermembrane space parts, respectively, to facilitate matching.

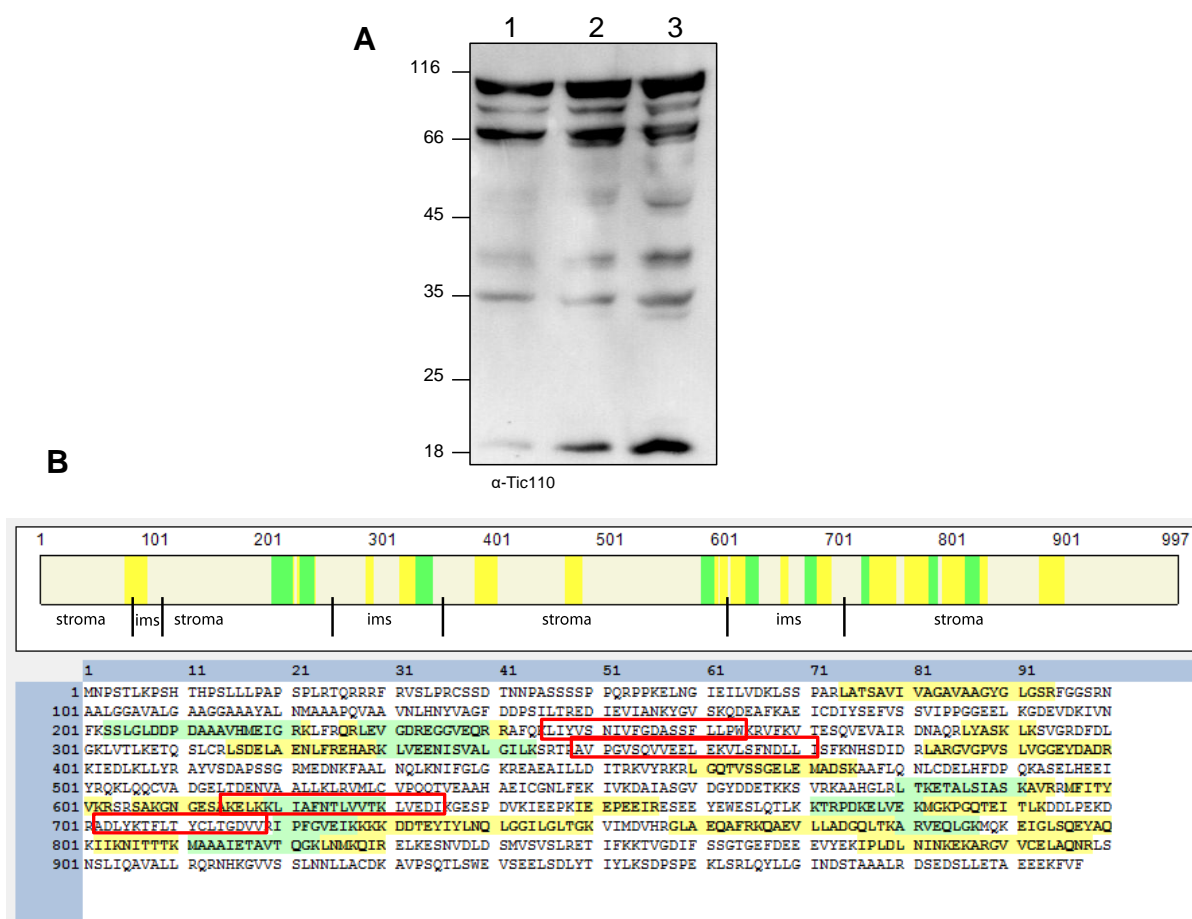


**Figure 9: Limited proteolysis of isolated inner envelopes for mass spectrometric analysis.**

**A:** Three biological replicates (1, 2 and 3) were chosen for mass spectrometric analysis. 60  $\mu$ g inner envelope proteins were superficially proteolyzed with 75 ng trypsin for 90 s at RT. The reaction was stopped by using excess trypsin inhibitor from soybean. After ultracentrifugation the supernatant containing the released tryptic peptides was sent for mass spectrometric analysis, whereas the shaved envelopes were analyzed using Tic110-specific antiserum.

**B:** Tryptic peptides found in each replicate were matched against the sequence of psTic110. Green peptides = high quality peptides, yellow peptides = medium quality peptides. Stromal parts and loops protruding into the intermembrane space are indicated and the four putative amphipathic helices are marked with red boxes.

No peptides could be found from the extreme N-terminus of the protein. The first N-terminal peptide found was LATSAVIVAGAGYCLGSR which represents one of the two N-terminal membrane anchors. The next identified peptides were shown to be located close to the first

amphipathic helix, however, these peptides matched to regions which are thought to reside in the stroma. Three peptides were identified from the first intermembrane space loop and two peptides in the large stromal loop between amphipathic helix 2 and 3. A variety of peptides was identified located in the region around helix 3 and 4, including both outer and inner parts. Again, no peptides could be identified at the very C-terminus of the protein. Overall, a variety of peptides were identified, which derive from both stromal and intermembrane space loops, thus it was not possible to exclusively identify peptides originating from outside-oriented loops and a reliable quantification process had to be established which will be explained in the next section.

#### **4.2.3 Tandem Mass Tag labeling and quantification of tryptic peptides**

In principle, identified peptides exhibit a variety of properties dramatically influencing their behaviour during ionization and thus, detection. No definitive conclusion can be drawn from the number of detection occurrence of a single peptide. A high value of identified peptide does not necessarily mean that this peptide was originally present at high numbers, but only that it reaches the detector more often than others. For example, hydrophobic peptides tend to be under presented during detection but unfortunately, quantification of identified peptides remained one of the outstanding problems in proteomics. To overcome this problem, isobaric labeling can be applied by using the so-called TMT labels (Tandem Mass Tag) (Thompson et al., 2003). Such structurally identical isobaric tags consist of three parts: (i) a reactive group, (ii) a reporter region and (iii) a normalizer residue (Figure 10). The reactive group is used to covalently react with the free N-terminus and  $\epsilon$ -amino group of lysine residues. Incorporation of heavy isotopes ( $^{13}\text{C}$  or  $^{15}\text{N}$ ) in the reporter group and heavy isotopes ( $^{13}\text{C}$  or  $^{15}\text{N}$ ) in the normalizer group provides tags with the same total mass. Once peptides are labeled, they are combined and analyzed using mass spectrometry. In a first MS spectrum, intact differentially labeled peptides are indistinguishable. However, since each tag variant contains a labile component with a different mass, reporter ions can be generated which will be recorded in a subsequent MS/MS spectrum. Intensities from each variant represent the relative abundances of the peptide in each sample. By varying the distribution of stable isotopes between the reporter and normalizer regions, a series of reporter ions with varying masses can be generated.



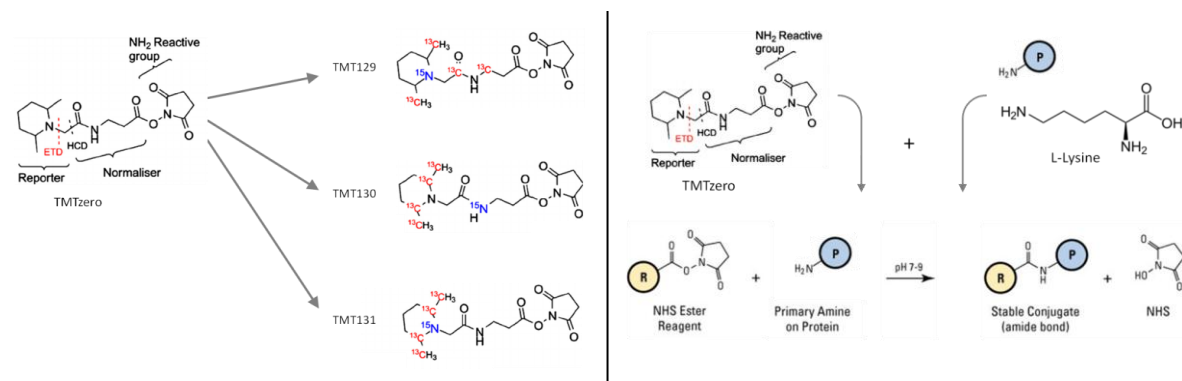


**Figure 10: Mechanism of TMT isobaric labeling.**

Structures, isotope positions, MS/MS fragmentation sites and collision-induced reporter ions for each reagent plus chemical reactions for the amine-reactive chemicals. The tags harbor three functional groups: an amine-reactive group and an isotopic reporter group linked by an isotopic normalizer group for the normalization of the total mass of the tags. The amine-reactive, NHS-ester-activated group reacts with N-terminal amine groups and  $\epsilon$ -amine groups of lysine residues to couple the tags to the peptides.

We made use of three labels (TMT129, TMT130 and TMT131), thus allowing us to analyze three different samples resulting from distinct origins (Figure 11 A). Sample 1A consisted of isolated inner envelope vesicles. These vesicles were labeled with TMT129 aiming at only labeling lysine residues from peptides exposed on the surface. After this short labeling step, envelopes were digested with trypsin resulting in short tryptic peptides carrying the label TMT129 only at previously exposed lysine residues. A subsequent labeling step using TMT131 was performed to label residual and previously non-accessible lysine residues and N-termini of peptides (sample 1B). Soluble Tic110 was used as a reference (Figure 11 B). This sample was trypsin-digested as sample 1B, but was labeled with TMT130, resulting in labeling of all accessible lysine residues and N-termini (sample 2). By comparing the abundances of the reporter ions, it was possible to relatively quantify the identified peptides, thereby giving information of peptides resulting from exposed domains.



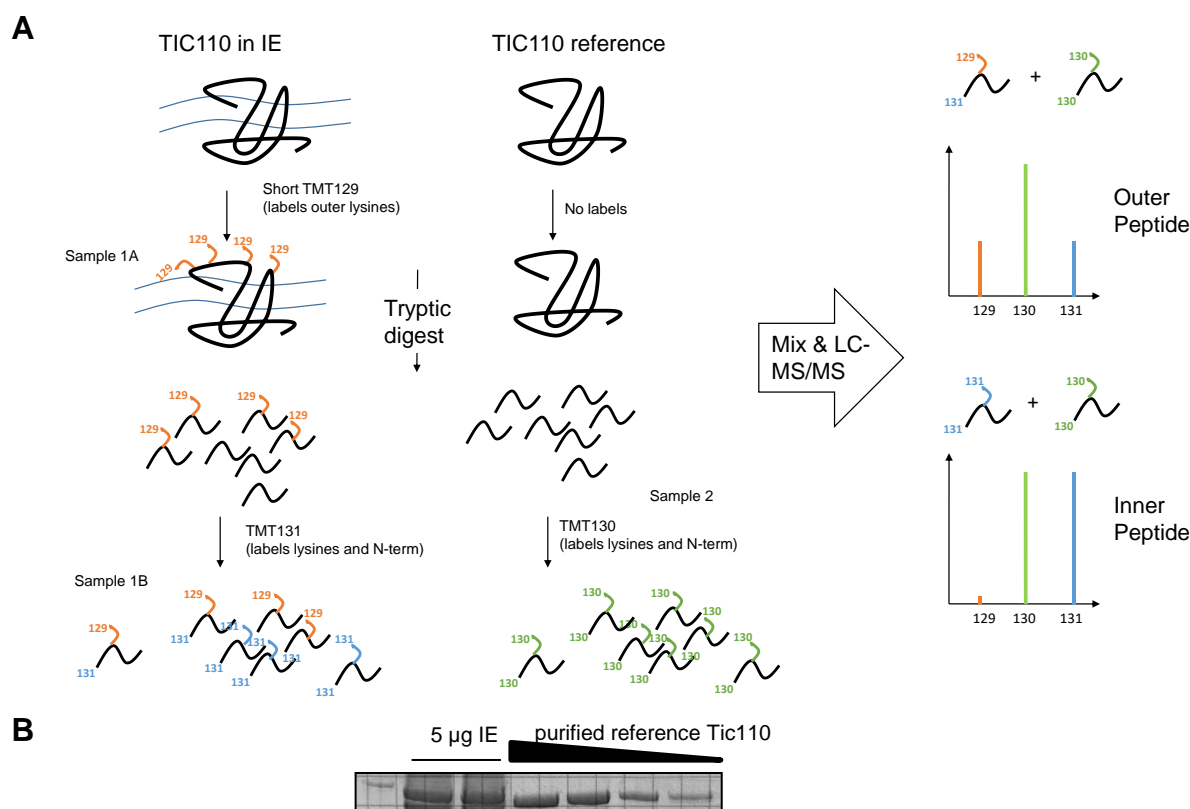


**Figure 11: Experimental outline for the TMT-labeling.**

**A:** Three labels TMT129, TMT130 and TMT131 were used for labeling of three samples of distinct biological origins (see text for details), mixed and subjected to LC MS/MS.

**B:** Equal amount of purified Tic110 (reference) and Tic110 in isolated inner envelope vesicles were subjected to 10.5 % SDS-PAGE. Finally, 10 µg of purified Tic110 and the respective amount of isolated inner envelopes were used for TMT analysis.

TMT labeling was carried out according to the manufacturer's recommendation, except that the first labeling of outer lysine residues was done for 10 min at 4 °C instead of 1 h at 37 °C. The differentially TMT-labeled samples were pooled and analyzed via LC-MS/MS. Raw data were analyzed with respect to the described conditions: First, ratio between 129/131 should be ~1 and ratio 130/131 >1. Application of these conditions revealed two peptides with the desired ratios, IEEPK and IVEDIK. Matching these peptides against the pea sequence of Tic110 displayed that peptides IEEPK and IVEDIK are originated from parts that are thought to be localized in the intermembrane space, namely between amphipathic helix 3 and 4. Although only two peptides with the desired ratios could be identified, the presented labeling strategy provides further insights into the topological model of Tic110 in isolated inner envelopes by identifying two peptides that have a high probability to be localized in the intermembrane space.

### 4.3 *In vivo* topology of Tic110: use of a genetically encoded tag for light and electron microscopy

In intact living cells proteins may exhibit native topological features that do not exist in purified form. Thus, it is of great importance to catch glimpses of structural organization of a protein in its native surroundings. Electron microscopy is the most powerful technique to resolve ultra-structural organization in tissues and cells. However, limitations exist concerning proteinogenic tags for specific protein detection during EM. Immunogold labeling is still the method of choice, but requires specific antibodies and their accessibility in fixed tissues. Recently, the genetically encoded tag miniSOG was shown to provide a major improvement in correlated light and electron microscopy (Shu et al., 2011). MiniSOG is a small fluorescent flavoprotein engineered from the LOV-domain of *Arabidopsis* with half the size of GFP and is originally from the plant protein phototropin 2. In nature, phototropin uses flavin mononucleotide (FMN) as a cofactor, a molecule responsible for transport and interchange of electrons in a variety of metabolic pathways. Benefiting from this capability of FMN, researchers have mutated the responsible amino acids of the FMN-interacting domain of phototropin, with the result that this protein uses the excitation energy of FMN to produce singlet oxygen (Figure 12 A, B). The resulting protein, miniSOG, provides a flexible method to determine the distribution of biologically relevant molecules in detail by EM and fluorescent microscopy at the same time (Shu et al., 2011). Illumination with blue light leads to the formation of singlet oxygen (= photooxidation) that locally catalyzes the polymerization of diaminobenzidine into an osmiophilic precipitate. During preparation for electron microscopy this precipitate gets visualized due to the reaction with osmium tetroxide. The mentioned specific characteristics make miniSOG a suitable tool to tag proteins without altering their localization and function, allowing to study the precise ultrastructural organization of a miniSOG-tagged protein in its cellular environment by using photooxidation.

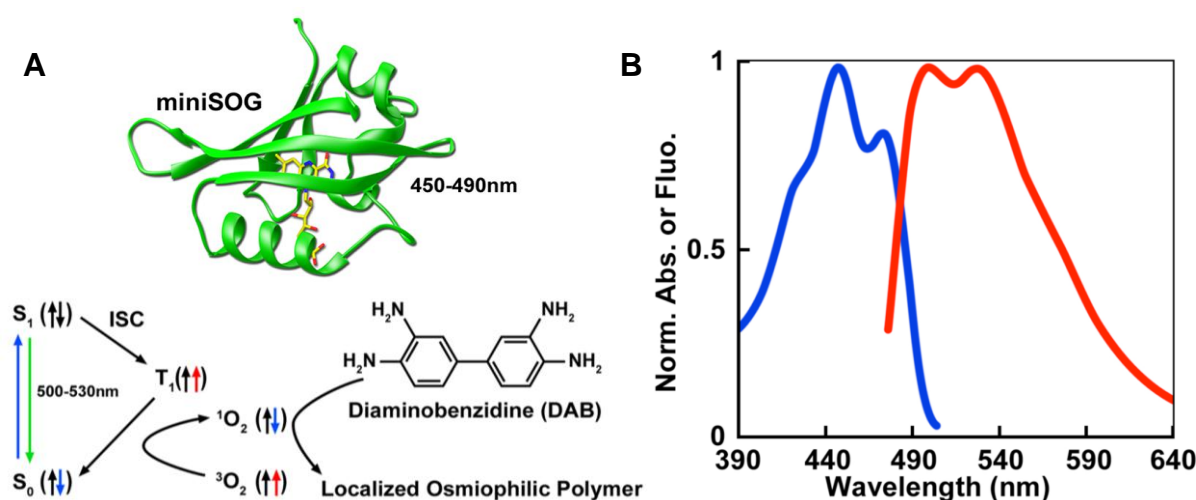


**Figure 12: Mechanism of miniSOG-induced singlet oxygen production.**

**A:** Schematic diagram of the mechanism of singlet oxygen production. Spin states are depicted by the arrow. ISC = intersystem crossing. Picture is taken from the publication (Shu et al., 2011).

**B:** Normalized absorbance (blue) and emission (red) spectra. Picture is taken from the publication (Shu et al., 2011).

MiniSOG has been successfully applied to demonstrate the correct localization of a variety of proteins by light and EM in cultured cells as well as mitochondria in *C. elegans* and in intact mouse brain (Shu et al., 2011). However, this is the first time that miniSOG was used in chloroplasts. We aimed to position miniSOG at specific positions of Tic110 which are localized, according to the current topological model, within the two intermembrane space loops. As a stromal control, miniSOG was also positioned at the C-proximal end of Tic110. With the resolution capacity of EM, it should be possible to discriminate between different sub-compartments of the chloroplast, namely outer envelope, intermembrane space, inner envelope and stroma. Thus, it is possible to identify osmiophilic precipitates exclusively found in distinct sub compartments.

According to the current topological model two loops ranging from residues 226 to 311 and 597 to 664 are protruding into the intermembrane space. Within these loops two amino acids (EY and DF at positions 257 and 622, respectively) were changed against “similar” amino acids EF via site-directed mutagenesis PCR using the complete plasmid pGEM5Zf(+) containing the open reading frame for preTic110 as a template. These exchanged bases generated a restriction cleavage site for the endonuclease type I EcoRI and did not change the overall character of the two amino acids allowing to assume that the function of the protein did not change due to the mutations. The coding region of miniSOG was cloned in-frame into the loops. The Tic110-miniSOG sequence was used as a template for PCR and was flanked with attB-sites to use the GATEWAY system. The fusion constructs were

eventually cloned in-frame into the destination vector pK7FWG2 with a 35S promoter and a C-terminal GFP tag. All constructs carried a stop codon at the C-terminal end to prohibit expression of vector-encoded GFP, however, also constructs were generated allowing the expression of GFP to facilitate tracking of the protein in case that technical issues should prevent tracking of the relatively low intensity of miniSOG's fluorescence (Figure 13).

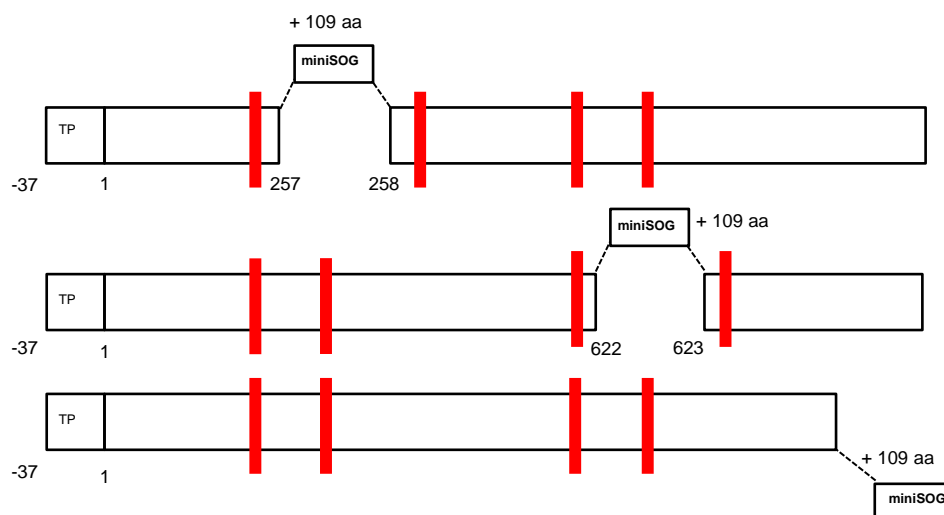


**Figure 13: Construction of various miniSOG-tagged Tic110 proteins.**

Schematic diagram of the constructs of miniSOG-tagged Tic110 proteins used in this thesis. Amphipathic helices are depicted by red lines. The numbers refer to the amino acid position of the Tic110 protein at which the miniSOG protein is positioned. Number 1 indicates the N-terminal amino acid excluding the transit peptide. TP = transit peptide, aa = amino acid.

### 4.3.1 Expression and localization of transiently expressed miniSOG-tagged Tic110 proteins

For specific tracking of expression and localization of miniSOG-fused proteins antisera were raised against the miniSOG protein. For this, the coding sequence of a synthesized miniSOG gene (Genscript, Piscataway, USA) was cloned in-frame into a pET21d(+) vector with a C-terminal 6xHisTag and the fusion protein was expressed heterologously in *E. coli*. Sufficient amounts of soluble miniSOG protein could be achieved within 3 h growth at 37 °C after induction with 1 mM IPTG even though the overexpressed protein was barely detectable on a Coomassie-stained SDS-PAGE (not shown). The crude bacterial cell extract containing the recombinant protein from a 1 l culture was subjected to Nickel-purification and a subsequent gel-filtration using a Superdex 200 (300/10) column and 500 µg of pure protein was used for antibody generation (Pineda, Berlin). Two bands could be observed in the Coomassie-stained SDS gel, representing monomeric and dimeric miniSOG (Figure 14 A). Serum after 61 days of immunization was used to test the specificity of the antibody against the antigen. For this, increasing amounts of pure protein was analyzed on 15 % SDS-PAGE followed by immunodecoration with the antiserum (1:1000).

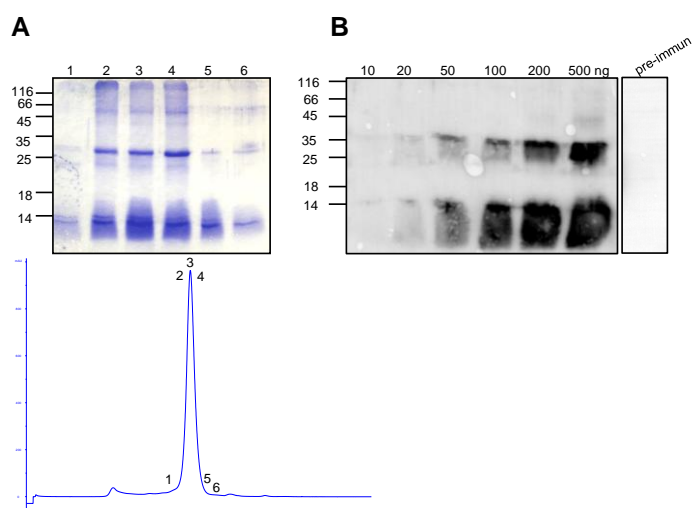


**Figure 14: Purification of miniSOG<sub>His6</sub> for antiserum production.**

**A:** After Nickel-purification proteins were further purified to homogeneity using gel filtration. Samples correspond to the peak as indicated in the chromatogram were analyzed on 15 % SDS-PAGE.

**B:** Increasing amounts of pure protein (10-500 ng) were separated on 15 % SDS-PAGE, transferred onto PVDF and immunodecorated with antiserum against miniSOG from one rabbit after 61 days of immunization. Antiserum detects both monomer and dimer.

As a result, the antiserum detects both monomer and dimer already at amounts of 20 ng of pure protein.

In a next step, to track if the miniSOG-tagged Tic110 proteins were targeted and localized correctly in the inner envelope of chloroplasts tobacco leaves were transiently infected with *Agrobacteria* carrying the respective plasmids coding for 35S::preTic110-miniSOG<sub>ims1</sub>, 35S::preTic110-miniSOG<sub>ims2</sub> and 35S::preTic110-miniSOG<sub>c-ter</sub>. Expression of proteins was allowed for three days in the greenhouse. Intact protoplasts and chloroplasts were isolated and subjected to fluorescence microscopy and/or to SDS-PAGE followed by immunoblotting using antisera against atTic110 and miniSOG. In a first try for detection of fluorescence constructs with the addition of GFP at the C-terminus were used. Figure 15 A shows the correct localization of a miniSOG-tagged Tic110<sub>ims1</sub> in the envelope of chloroplasts. Immunoblot analyses further supported this observation. Using the *Arabidopsis* Tic110-specific antiserum a band with a higher molecular weight could be observed for all three constructs in addition to the endogenously expressed native Tic110 (Figure 15 B). The size-shift is due to the addition of 12 kDa of miniSOG protein to Tic110. By using the antiserum against miniSOG this observation could be verified. The high molecular weight band could be specifically detected with the miniSOG antiserum, whereas the band corresponding to authentic Tic110 was not detected with the miniSOG specific antiserum (Figure 15 D).

Although miniSOG's fluorescence is modest compared to GFP (quantum yield of 0.37 versus 0.6) (Shu et al., 2011), microscopic analyses were also carried out using constructs without the expression of vector-encoded GFP using a spinning disc microscope (Zeiss, Oberkochen, Germany). Fluorescence microscopy revealed the correct localization of miniSOG-tagged Tic110<sub>ims2</sub> proteins in the envelope membrane of chloroplasts (Figure 15 C) by recording only miniSOG's fluorescence.

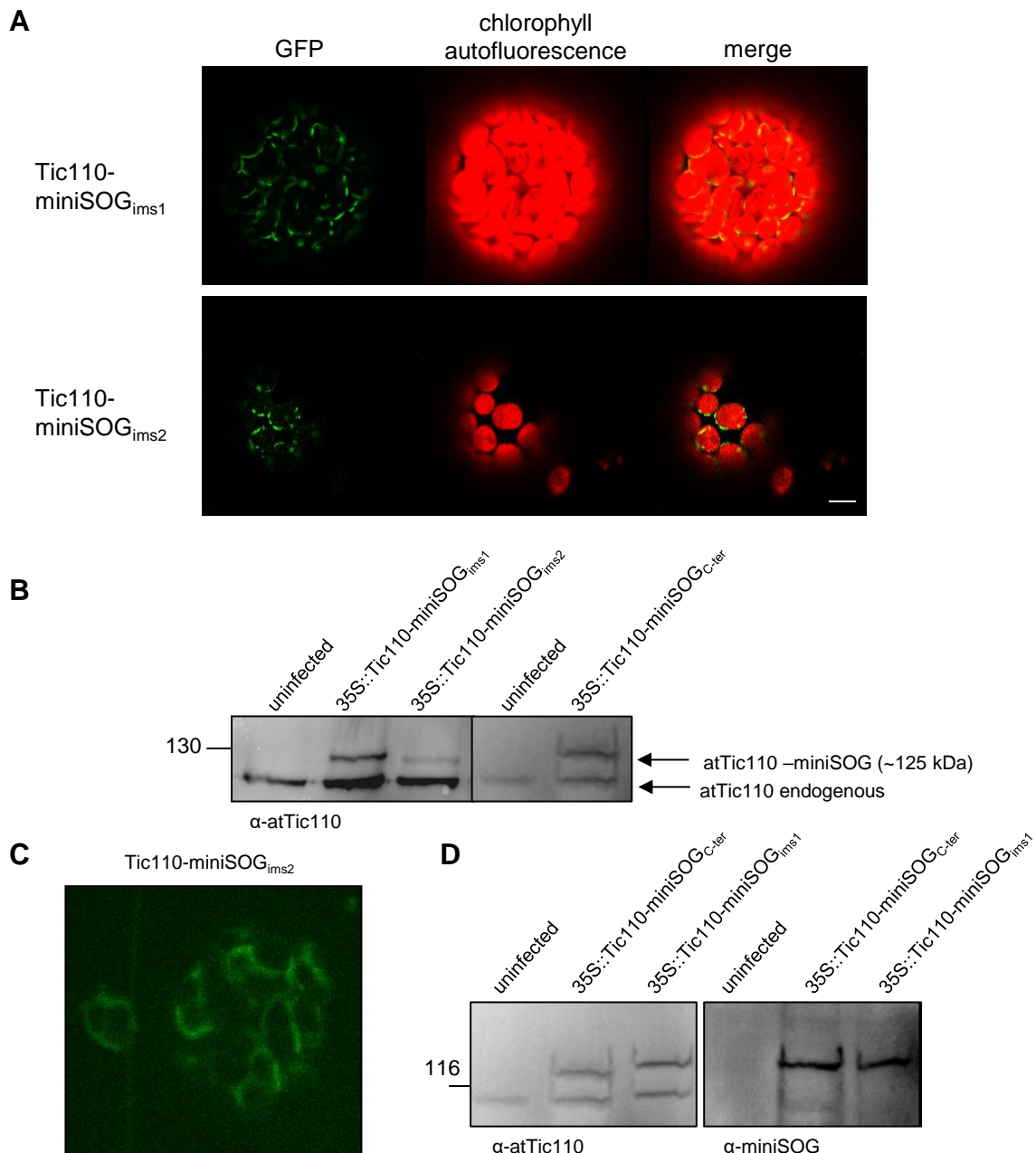


**Figure 15: Localization and expression of miniSOG-tagged Tic110 proteins under 35S promoter.**

**A:** Protoplasts were isolated from transiently expressing tobacco leaves (35S::preTic110-miniSOG<sub>ims1</sub> and 35S::preTic110-miniSOG<sub>ims2</sub>) and analyzed by confocal fluorescence microscopy. GFP fluorescence is recorded in parallel to the autofluorescence of chlorophyll. Please note that here the vector-encoded expression of GFP was allowed. Scalebar = 5  $\mu$ m.

**B:** Immunoblot analysis of isolated chloroplasts from tobacco leaves which express the miniSOG-tagged Tic110 proteins. Equal amount (10  $\mu$ g of chlorophyll) were loaded onto 8.5 % SDS-PAGE, transferred onto PVDF membrane and were probed with antiserum against atTic110. The arrows mark the endogenously expressed untagged Tic110 and the miniSOG-tagged Tic110 protein which has a higher molecular weight.

**C:** Protoplasts transiently expressing 35S::preTic110-miniSOG<sub>ims2</sub>. Please note that here the fluorescence of miniSOG was recorded and not of GFP. The autofluorescence of chlorophyll was blocked by a specific filter.

**D:** Immunoblot analysis of isolated chloroplasts from tobacco leaves which express the indicated miniSOG-tagged Tic110 proteins. Equal amount (10  $\mu$ g of chlorophyll) were loaded onto 8.5% SDS-PAGE, transferred onto PVDF membrane and were immunodecorated with antiserum against atTic110 and miniSOG.

These results confirmed that the introduced miniSOG in all three positions of Tic110 did not hamper correct targeting and localization of Tic110, allowing to assume that the topology is also not affected. Furthermore, as miniSOG's fluorescence could be recorded, it can be assumed that the specific properties of this small flavoprotein are maintained in the recombinant proteins, which is necessary for photooxidation.

#### **4.3.2 Photooxidation of chloroplasts expressing transiently miniSOG-tagged Tic110**

After confirming that the constructed miniSOG-tagged Tic110 proteins are targeted properly into their destination organelle - the chloroplast - experiments concerning photooxidation were carried out. 35S::preTic110-miniSOG<sub>ims1</sub> and 35S::preTic110-miniSOG<sub>ims2</sub> were transiently expressed in tobacco leaves using *A. tumefaciens* and expression was allowed for three days in the climate chamber under short day conditions. Transfected leaves were cut, fixed and blocked as described in method section 3.3.2 and then subjected to photooxidation. For this purpose, upon addition of a DAB solution (0.5 mg/ml) tissues were illuminated with blue light for several minutes using an inverted confocal microscope and standard FITC filter set. The DAB solution was exchanged four times. As a control, samples were photooxidized without the addition of DAB. After photooxidation, samples were further prepared for electron microscopy (AG Klingl, LMU Munich, method section 3.3.2). Figure 16 shows electron micrographs of leaves that were infected with preTic110-miniSOG<sub>ims1</sub> and were photooxidized with and without the addition of DAB. The ultrastructure of chloroplasts was preserved during sample preparation, resulting in an intact thylakoid network. By focusing on the area between outer and inner envelope at rare occasions a slight dark precipitate resembling dot-like structures could be observed in samples of plants transformed with 35S::preTic110-miniSOG<sub>ims1</sub> that were photooxidized in presence of DAB (Figure 16 A, zoom-in). These dots are not visible in samples using the same construct, but that were photooxidized without the addition of DAB (Figure 16 B). Here, the intermembrane space shows a clear background.



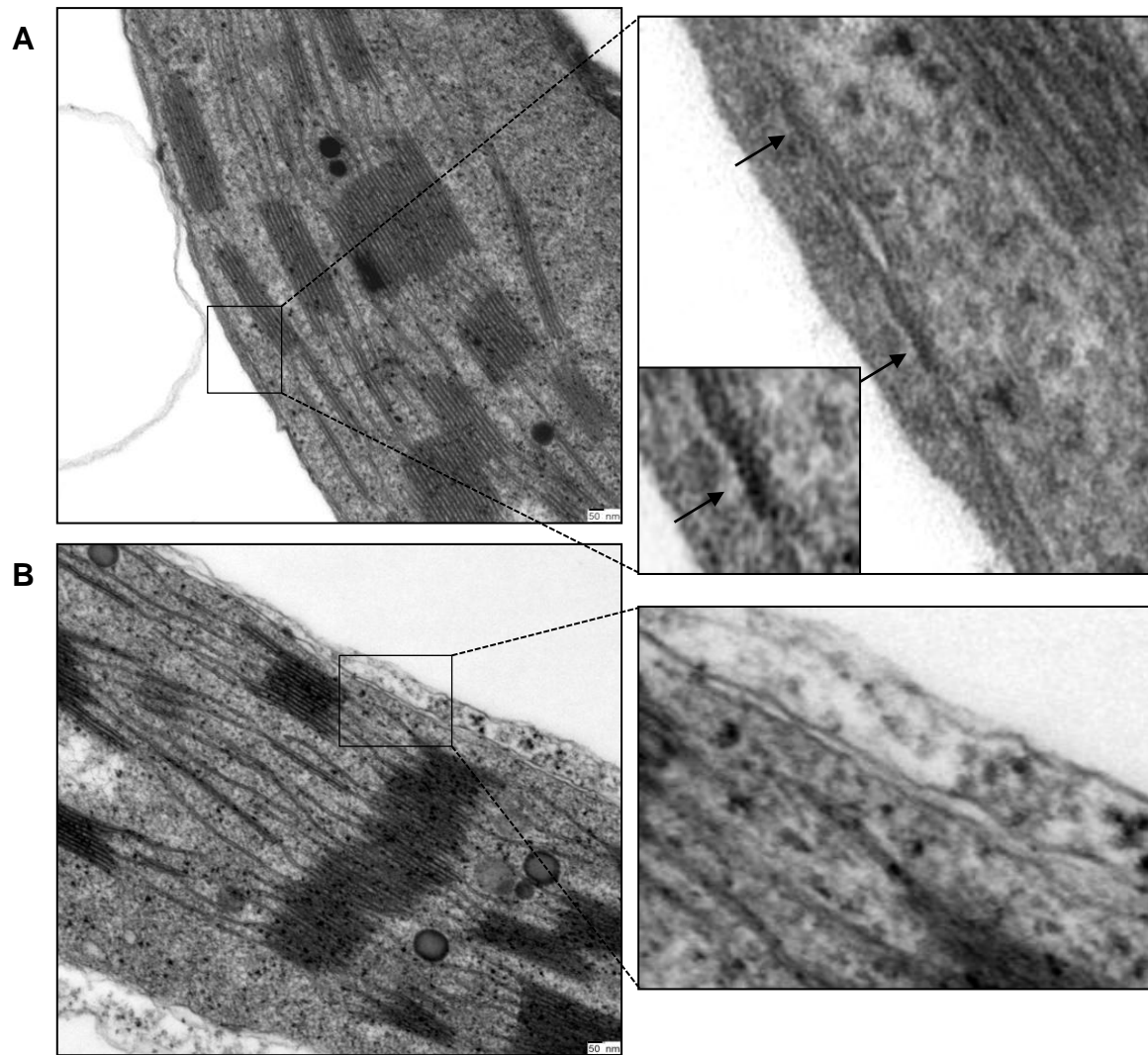


**Figure 16: Electron micrographs of photooxidized chloroplasts transiently expressing miniSOG-tagged Tic110<sub>ims1</sub> with and without the addition of diaminobenzidine.**

Leaf tissues transiently expressing 35S::preTic110-miniSOG<sub>ims1</sub> were photooxidized in the presence (A) or absence of DAB (B). Enlargement of the region boxed revealed dot-like structures, which is only present in samples containing DAB. Arrows indicate the dot-like structures. Scalebar = 50 nm.

However, these dot-like structures could so far only be observed in chloroplasts expressing Tic110-miniSOG<sub>ims1</sub> and more pictures have to be taken into account, but nonetheless, these data suggest that miniSOG-tagged Tic110<sub>ims1</sub> might produce an osmiophilic precipitate in the intermembrane space of chloroplasts upon photooxidation in the presence of DAB, indicating that the loop between amino acid 226 and 311 is protruding into the intermembrane space.



### 4.3.3 Functional *in vivo* analysis of miniSOG-tagged Tic110 proteins in heterozygous *TIC110/tic110* *Arabidopsis* plants

Correct functionality of a protein is connected with its topology. Although it has been shown that miniSOG-tagging did not influence envelope-targeting of Tic110 it could not be concluded from the previous experiments that the recombinant proteins were not affected in topology and thus function. To analyze this issue, heterozygous *TIC110/tic110* plants were transformed with the previously described tagged *TIC110*-miniSOG constructs and were analyzed regarding their complementation efficacy. Homozygous *tic110* null mutants are embryo lethal, and even heterozygous T-DNA mutants already show a pale green phenotype and reduced growth. If the complementation with miniSOG-tagged *TIC110* is successful, plants being homozygous for *tic110* should be present in the progeny. This of course requires expression and correct assembly of the protein into its channel-like structure in the inner envelope membrane. Expression of tagged constructs is driven by the 1800bp promoter region of native Tic110 to avoid silencing or artefacts due to overexpression under a 35S promoter. *atPro110::preTic110-miniSOG<sub>ims1</sub>*, *atPro110::preTic110-miniSOG<sub>ims2</sub>* and *atPro110::preTic110-miniSOG<sub>C-ter</sub>* were cloned into the pHGW vector. *atPro110::preTic110-miniSOG<sub>ims1</sub>* and *atPro110::preTic110-miniSOG<sub>ims2</sub>* were used for transient expression in tobacco leaves to analyze promoter activity using *A. tumefaciens* carrying the respective plasmids. Expression could be detected three days post infection using *atTic110* specific antiserum which resulted in the same band with a higher molecular weight as seen before. However, compared to 35S expression, expression is less (Figure 17).

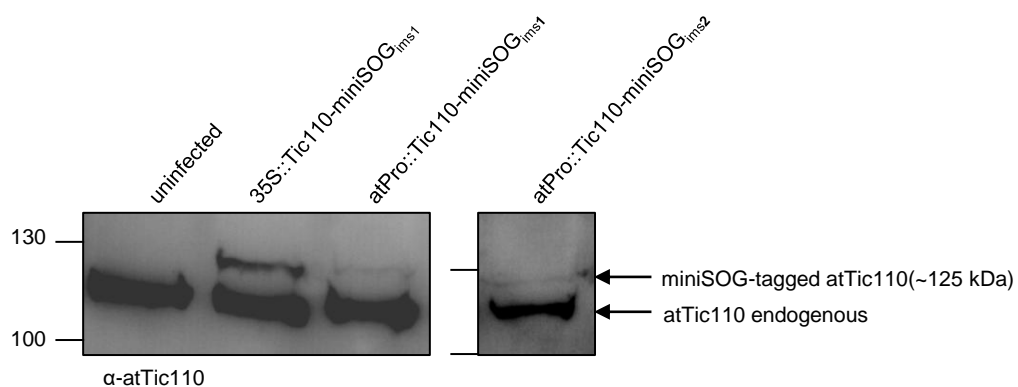


**Figure 17: Transient expression of miniSOG-tagged Tic110 proteins driven under Tic110-native promoter in tobacco leaves.** Immunoblot analyses of isolated chloroplasts from tobacco leaves that express the miniSOG-tagged Tic110 proteins Tic110-miniSOG<sub>ims1</sub> and Tic110-miniSOG<sub>ims2</sub>. Equal amount (10  $\mu$ g of chlorophyll) were loaded onto 8.5 % SDS-PAGE, transferred onto PVDF membrane and were probed with antiserum against atTic110. The arrows indicate the endogenously expressed untagged Tic110 and the miniSOG-tagged Tic110 protein which has a higher molecular weight.

After validating the activity of the endogenous promoter, heterozygous *TIC110/tic110* plants were transformed using the floral-dip method with *Agrobacteria* carrying *atPro::preTic110*-

miniSOG<sub>ims1</sub>, atPro::preTic110-miniSOG<sub>ims2</sub>, atPro::preTic110-miniSOG<sub>C-ter</sub> and transformed plants were selected on hygromycin-containing plates. Hygromycin-resistant plants were then analyzed on the DNA level by using primers for WT Tic110, T-DNA insertion and construct insertion (table 2, material section 2.4). The analysis of all three variants is ongoing, however, on a macroscopic level plants transformed with atPro::preTic110:miniSOG<sub>ims1</sub> exhibited a pale and yellowish phenotype, starting from the first days in young leaves and then spreading into all leaves (Figure 18 A). This is in slight contrast to *TIC110/tic110* plants, where the yellowish phenotype got weaker with period of time (Figure 18 A). The yellowish phenotype of transformed plants was more prominent when plants were grown on soil compared to growth on MS-plates supplemented with 0.5 % sugar (Figure 18 B). As no homozygous *tic110/tic110* plants could be isolated, seeds were analyzed. From 142 counted seeds 108 were mature whereas 34 dead seeds could be observed, resulting in a 24 % abortion rate. Thus, with a high probability, it is not possible to delete *TIC110* even in the presence of a miniSOG-tagged *TIC110*, indicating that the miniSOG-tagged Tic110<sub>ims1</sub> is not fully capable to fulfill the important import-related function of native Tic110 protein. To exclude that the phenotype was caused by insertion of the T-DNA at a random position in the genome two additional independent lines of transformed plants with atPro::preTic110-miniSOG<sub>ims1</sub> (#4 and #16) were analyzed. Indeed, both displayed the same phenotype (data not shown).

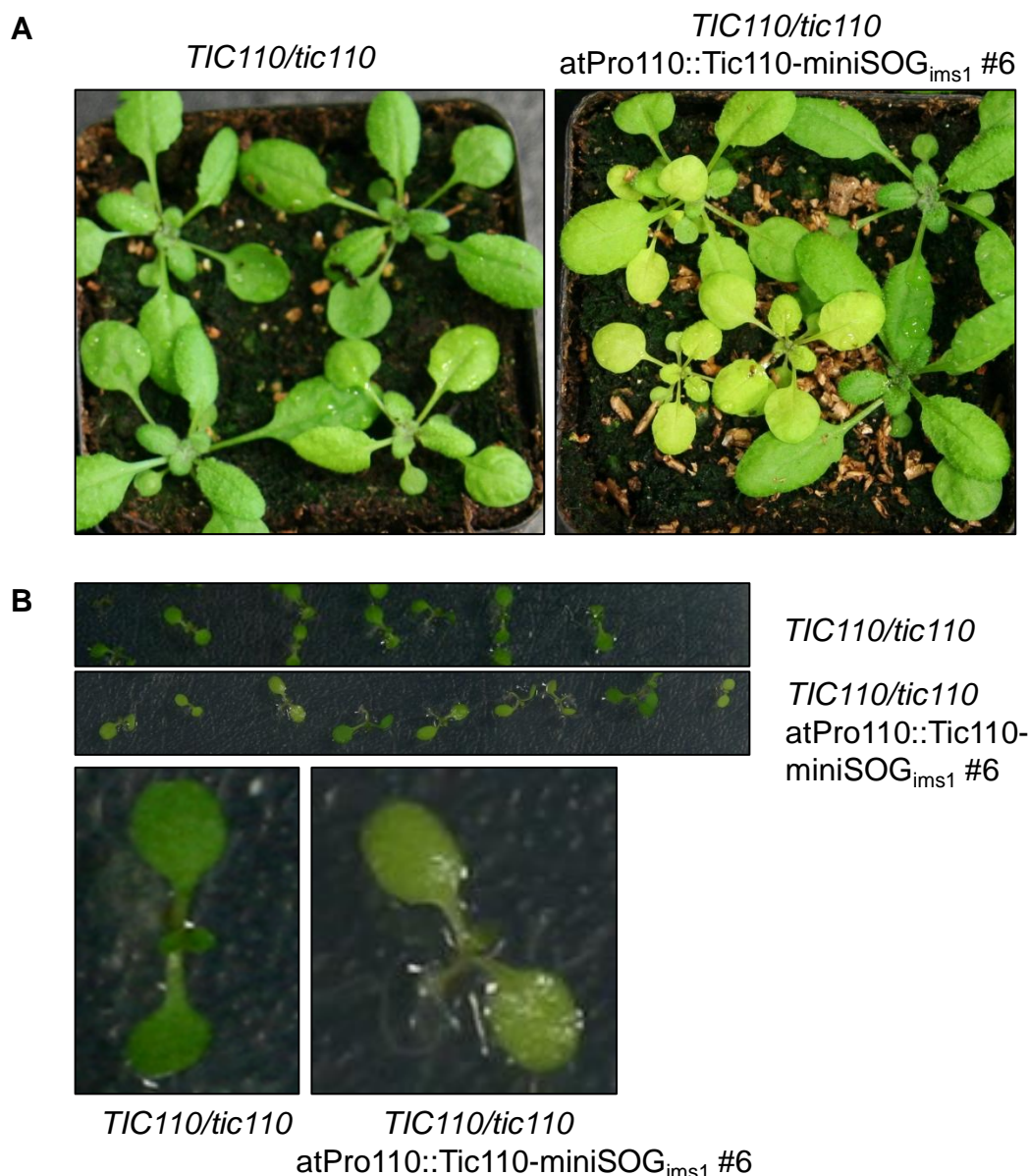


**Figure 18: Stable expression of miniSOG-tagged *atPro::Tic110<sub>ims1</sub>* in heterozygous *Arabidopsis TIC110/tic110* plants.**

**A:** Phenotype of 14-day-old *Arabidopsis TIC110/tic110* plants, either untransformed (left) or transformed with *atPro::preTic110-miniSOG<sub>ims1</sub>* (right). Plants were grown on soil under long-day conditions.

**B:** Phenotype of 7-day-old *Arabidopsis TIC110/tic110* plants, either untransformed (upper panel) or carrying *atPro::preTic110-miniSOG<sub>ims1</sub>* (lower panel). Plants were grown on ½ MS-media plates supplemented with 1 % sucrose. Enlargements of leaves from single plants are depicted at the bottom.

To examine the actual protein amount of Tic110 of *atPro::preTic110-miniSOG<sub>ims1</sub>* transformed plants, immunoblot analysis using *atTic110* specific antiserum was performed. This revealed that no significant reduction of authentic Tic110 could be observed in comparison to untransformed *TIC110/tic110* plants (Figure 19). Protein amount of Tic110 in heterozygous plants (transformed and untransformed) compared to WT is reduced, which is in line with previous observations (Inaba et al., 2005).

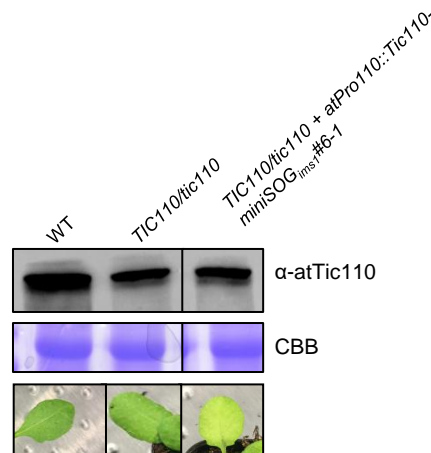


**Figure 19: Immunoblot analysis of total protein extracts.**

10 µg total protein from wild type plants (lane 1), *TIC110/tic110* (lane 2) and *TIC110/tic110* plants transformed with miniSOG-tagged atPro::preTic110<sub>ims1</sub> (lane 3) were separated on 10.5 % SDS-PAGE, transferred to PVDF membrane and immunodecorated with antiserum against atTic110. Samples for WT and *TIC110/tic110* were the same as in Figure 20 and unrelated lanes were cropped out. Loading control was visualized with CBB.

Taken together these data revealed that transformation of miniSOG-tagged atPro::preTic110<sub>ims1</sub> led to a pale phenotype which is even more drastic compared to *TIC110/tic110* plants, pointing towards a disturbed protein function of miniSOG-tagged Tic110<sub>ims1</sub>. However, protein amount of authentic Tic110 is unaffected, thus it remains to be established why these plants display such a strong chlorotic phenotype.

#### 4.3.4 Role of regulatory cysteines in Tic110 *in vivo*

Pea Tic110 contains nine cysteine residues, of which six are fully conserved in land plants: Cys134(190), Cys275, **Cys445(501)**, Cys470(526), **Cys492(548)**, **Cys506(562)**, **Cys674(728)** Cys854 and **Cys890 (944)** in pea sequence (in bold are cysteines that are conserved in all green lineages, numbers in brackets indicate the respective residue in *Arabidopsis*) (Balsera et al., 2009). Therefore, these residues are potential candidates for disulfide bridge formation or regulatory mechanisms during the import process. Previously performed *in vitro* analyses had revealed that mutation of Cys492 and deletion of the C-terminus of dNTic110 (involving Cys890) caused noticeable changes in the behavior of dNTic110 upon oxidation, thus regulatory functions concerning oxidation states are expected to exist. However, to study the *in vivo* role of the conserved cysteines complementation of heterozygous *Arabidopsis* *TIC110/tic110* mutants with Tic110 containing mutated cysteine residues was performed.

The coding sequence of atTic110 was used as a template and cysteines at residues 190, 501, 526, 548, 562, 728 and 944 (*Arabidopsis* sequence) were mutated to serine by site-

directed mutagenesis. After verification of the exchange, constructs were cloned into pHGW under the control of the native *Tic110* promoter and plasmids were transformed into *Agrobacterium* strain GV3101. *TIC110/tic110* plants were transformed using the floral-dip method and plants were selected on hygromycin-containing plates. The selection of the T2 generation is still ongoing, however, one prominent candidate was found. Transformed plants were heterozygous for *TIC110/tic110* but carried an additional *TIC110* variant with a mutation at C526 (Figure 20 A). These plants exhibited a faint yellowish phenotype, but interestingly protein levels were increased compared to untransformed *TIC110/tic110*. Protein amount was comparable to that of *Tic110* in wild type plants (Figure 20 B). However, more plants need to be analyzed to substantiate this observation and to analyze in detail the impact of the mutation at this position.

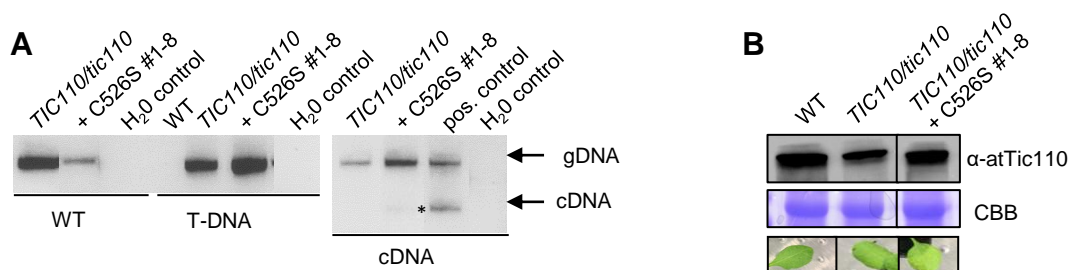


**Figure 20: Analysis of transformed plants on DNA and protein level.**

**A:** Genotyping of plants using primer for WT, T-DNA insertion and cDNA insertion. Primer are listed in table 2, material section 2.4. Asterisk marks the weak band corresponding to the introduced cDNA carrying the mutation C526S.

**B:** Immunoblot analysis of total protein extracts from wild type plants (lane 1), *TIC110/tic110* (lane 2) and plants transformed with *atPro::Tic110<sub>C526S</sub>* (lane 3). 10 µg total protein were separated on 10.5 % SDS-PAGE, transferred to PVDF membrane and immunodecorated with antiserum against *atTic110*. Samples for WT and *TIC110/tic110* were the same as in Figure 19 and unrelated lanes were cropped out. Loading control was visualized with CBB.

#### 4.4 Topology of Tic110 in a reconstituted proteoliposome system

Soluble Tic110 can be purified under non-denaturing conditions by removing the two N-terminal hydrophobic helices (in the following named as dNTic110). Although the protein behaves like a tetramer during size-exclusion chromatography (Balsera et al., 2009), BN-PAGE analysis suggested dimer formation as the protein was present at 200-250 kDa. It could be shown that the variant without the two N-terminal hydrophobic helices is still able to stably insert into liposomes as a dimer, proving that the C-terminal domain of Tic110 indeed contains membrane-affine regions (Figure 21 and Balsera et al., 2009). Reconstitution of dNTic110 into liposomes occurred bidirectionally and resulted in a cation-selective channel after fusion with a planar lipid bilayer (Balsera et al., 2009).

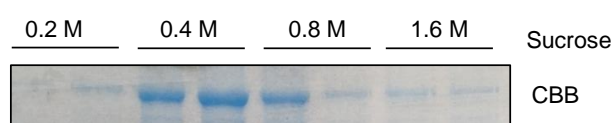


**Figure 21: Insertion of dNTic110 into liposomes.**

Flotation assay to confirm the insertion of dNTic110 into liposomes. Liposomes and pure dNTic110 were incubated as described in the method section 3.3.14. After dialysis, samples were adjusted to a sucrose concentration of 1.6 M sucrose and were placed in the bottom of a sucrose gradient containing steps of 0.8 M, 0.4 M and 0.2 M of sucrose. The gradient was centrifuged at 100000 g for 19 h at 4 °C and fractions were collected, with 10 % TCA precipitated and analyzed on 10.5 % SDS-PAGE.

This reconstituted liposomal system provides a tool to perform structural studies of dNTic110 in a minimal membrane-mimicking system without interference by other membrane components. dNTic110-proteoliposomes were used to investigate the channel composition and topology with three different experimental approaches:

Firstly, a cross-linking assay using a mass spectrometric-cleavable cross-linker was used to provide distance constraints. After reconstitution of dNTic110 in liposomes the application of the cross-linker should connect any peptide that is in close proximity. Identification of cross-linked peptides should provide distance parameters that aid in building the topological model of the reconstituted dNTic110 channel in proteoliposomes.

Secondly, a liposome leakage assay was conducted to study the channel-forming capability under different conditions.

Thirdly, single molecule observation of Förster resonance energy transfer (smFRET) can be used to provide insights into the structure and dynamics of proteins. To study the spatial arrangement of the amphipathic helices with respect to distance values between the involved helices upon channel formation several variants of specifically fluorophore-labeled monomeric dNTic110 proteins were generated in order to monitor a FRET signal between the helices in dNTic110-proteoliposomes.

#### 4.4.1 DSSO cross-linking of reconstituted dNTic110 in proteoliposomes

A novel powerful cross-linking strategy was developed to accurately identify cross-linked peptides of protein complexes (Kao et al., 2011). Here, a mass spectrometric-cleavable cross-linker, disuccinimidyl sulfoxide (DSSO) was used. This cross-linker contains two symmetric collision-induced dissociation (CID)-cleavable sites that allow accurate identification of DSSO-cross-linked peptides based on their distinct fragmentation pattern unique to cross-linking types (inter-link, intra-link, dead-end). DSSO contains amine-reactive N-hydroxysuccinimide (NHS) ester at each end of a 7-carbon spacer arm, thus reacting with lysine residues (Figure 22).

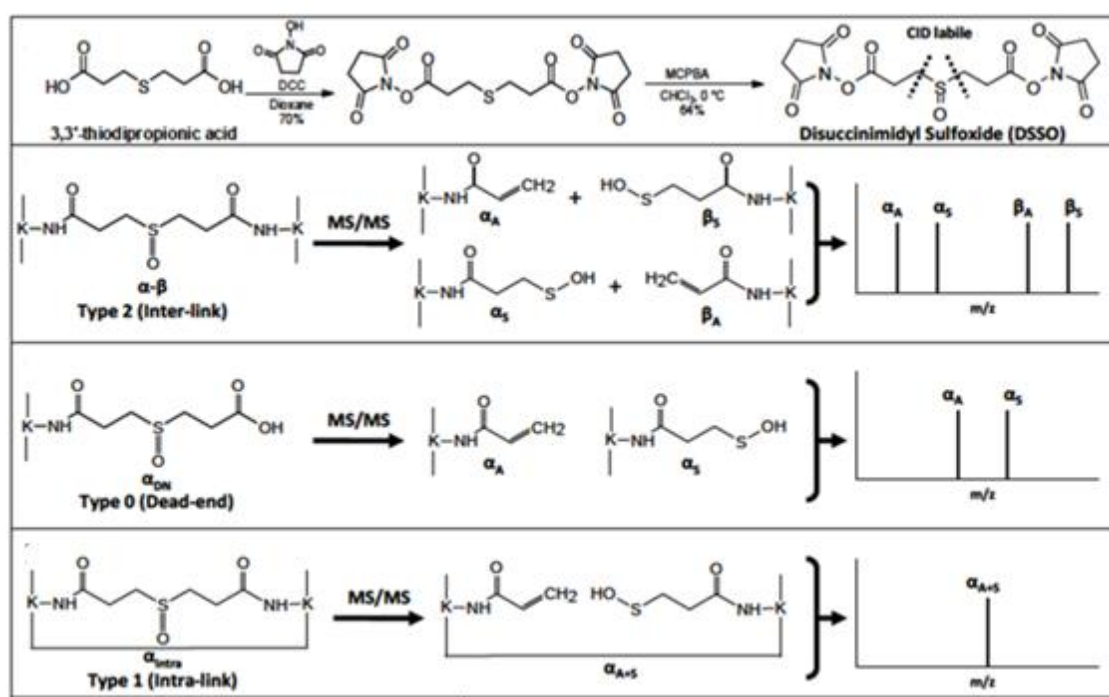


**Figure 22: DSSO synthesis and structure.** MS/MS fragmentation patterns of the three possible types of DSSO-cross-linked peptides: inter-linked, dead-end, and intra-linked. Figure is taken out from (Kao et al., 2011).

dNTic110-proteoliposomes were prepared as described in the methods section 3.3.14 except that the buffer was depleted from Tris to avoid quenching of the cross-linker. Instead, liposomes were prepared in 10 mM HEPES/KOH pH 7.6, 200 mM NaCl. Liposomes and freshly purified dNTic110 (~0.5 mg/ml) were mixed in a ratio 1:1 in the presence of 80 mM Nonanoyl-*N*-methylglucamide for 1.5 h at 4 °C. Detergent and residual Tris buffer from purified dNTic110 was removed by dialysis overnight at 4 °C against 10 mM HEPES/KOH pH 7.6, 200 mM NaCl without detergent. Samples were subjected to sucrose flotation and fractions containing proteoliposomes were pooled. Sucrose was removed by 1:8 dilution with



buffer 10 mM HEPES/KOH pH 7.6, 200 mM NaCl and pelleted proteoliposomes were resuspended in cross-linking buffer 10 mM HEPES/KOH pH 7.6, 200 mM NaCl and subjected to cross-linking. To this end, 1.5 mM of DSSO cross-linker was added two times for each 45 min at 4 °C. After this, proteoliposomes were acetone-precipitated and the air-dried pellet containing ~250 µg of protein was resuspended, reduced, alkylated and trypsin-digested. To enrich peptides, size-exclusion was performed using a Superdex Peptide 3.2/300 column. Measurements were done on a QExactive HF and for data analysis MaxQuant software was used (AG Carell, LMU Munich).

Table 3 shows the identified peptides; so far, only dead-end or intra-linked peptides could be identified, thus no distance-providing information could be gathered from this experiment.

**Table 3: Identified peptides of dNTic110 with dead-end or intra-linked cross-links.** (ds) indicates the attachment of the cross-linker to peptides.

| Link Type  | Modified sequences          | Number of detections |
|------------|-----------------------------|----------------------|
| Dead-end   | LTK(ds)ETALSIASK            | 4                    |
| Dead-end   | LVEDIK(ds)GESPDVK           | 4                    |
| Intra-link | IPLDLNINK(ds)EK(ds)AR       | 3                    |
| Intra-link | DAIASGVDGYDDETK(ds)K(ds)SVR | 3                    |
| Dead-end   | LNMK(ds)QIR                 | 1                    |
| Dead-end   | IIK(ds)NITTTK               | 2                    |
| Dead-end   | LASYLDK(ds)VR               | 1                    |
| Dead-end   | SDPSPEK(ds)LSR              | 3                    |
| Intra-link | GNGESAK(ds)ELK(ds)K         | 3                    |
| Intra-link | LYASK(ds)LK(ds)SVGR         | 2                    |
| Dead-end   | ETALSIASK(ds)AVR            | 2                    |
| Dead-end   | YGVSK(ds)QDEAFK             | 1                    |
| Intra-link | NK(ds)YEDEINK(ds)R          | 1                    |
| Dead-end   | IPLDLNINK(ds)EK             | 2                    |
| Intra-link | SAK(ds)GNGESAK(ds)ELK       | 3                    |
| Dead-end   | NSK(ds)IEISELNR             | 2                    |
| Dead-end   | GESPDVK(ds)IEEPK            | 1                    |
| Dead-end   | SK(ds)AEAESLYQSK            | 2                    |
| Dead-end   | DAIASGVDGYDDETK(ds)K        | 1                    |
| Dead-end   | QEYEQLIAK(ds)NR             | 1                    |
| Dead-end   | K(ds)QAEVLLADGQLTK          | 1                    |
| Intra-link | LTK(ds)ETALSIASK(ds)AVR     | 1                    |
| Intra-link | SAK(ds)GNGESAK(ds)ELK(ds)K  | 1                    |
| Dead-end   | QAEVLLADGQLTK(ds)AR         | 1                    |
| Intra-link | LVEDIK(ds)GESPDVK(ds)IEEPK  | 1                    |
| Dead-end   | VEQLGK(ds)MQK               | 2                    |



#### 4.4.2 Liposome leakage assay with dNTic110-containing proteoliposomes

In planar lipid bilayers, dNTic110 and native Tic110 form a voltage-dependent cation-selective channel (Balsera et al., 2009). However, as the electrodes are sensitive to oxidizing or reducing agents, it is difficult to measure the impact of oxidation or reduction of a protein on channel-activity by this method. Thus, we designed an *in vitro* assay in which we monitored indirectly the channel-forming capacity of dNTic110 by the measurement of a dye leaking out of vesicles induced by the formation of a channel consisting of dNTic110. Carboxyfluorescein's fluorescence is self-quenched at high concentration within vesicles due to the transfer of energy to non-fluorescent dimers (Chen and Knutson, 1988). Upon spontaneous insertion of any pore-forming protein, the dye is released into the surrounding buffer, leading to an increase of the quantum yield of the dye, and the resulting fluorescence can be measured with a fluorescence spectrometer.

Dye-encapsulated liposomes were prepared as described in the methods section 3.3.17 with a final concentration of 20 mM carboxyfluorescein. Unilamellar liposomes with a diameter of 200 nm were dialyzed overnight at 4 °C against buffer without dye to remove uncharged carboxyfluorescein. 5 µl of prepared liposomes were diluted in 995 µl 1x PBS pH 7.4 to reach a suitable fluorescence signal. After reaching the equilibrium, either freshly purified protein (5 µl of 1 mg/ml) or 5 µl buffer as a control was added and fluorescence was recorded with excitation at 494 nm and emission at 515 nm every ms for 300 or 600 s. After each measurement, 0.5 % Triton X-100 was added to the liposomes, which led to massive release of the dye out of the liposomes. This release was set to 100 % dequenching efficiency to normalize the obtained values.

The addition of 50 nM dNTic110 led to a constant increase of fluorescence over time, whereas the fluorescence of protein-free liposomes remained at a low level (Figure 23 A). To determine whether the channel-forming activity was triggered in a Tic110 concentration-dependent manner, different concentrations of dNTic110 were applied. The release of carboxyfluorescein increased with increasing dNTic110 concentrations (Figure 23 B), thus leading to the conclusion that pore-formation was indeed mediated by the applied dNTic110.

Pea Tic110 contains nine cysteines distributed throughout the polypeptide chain. It has been shown that Tic110 contains one or two regulatory disulfide bridges (Balsera et al., 2009). These intramolecular bridges could have a critical influence on the structure and function of the central TIC component. Switches between reduction and oxidation of these disulfide bridges could either lead to an open or closed formation of Tic110, respectively, and thereby limit the amount of incoming preproteins. To analyze the impact of oxidation and reduction on channel-formation, freshly purified dNTic110 was either oxidized by 50 µM CuCl<sub>2</sub> or

reduced with 10 mM DTT for 1 h at 20 °C. Again, 5 µl of treated protein (1 mg/ml) was used for dye-release measurements.

Upon oxidation with  $\text{CuCl}_2$  no significant increase of dye-release could be observed, moreover the signal remained low over time, comparable to the buffer control, indicating that the channel was closed after oxidation (Figure 23 C). Untreated dNTic110 showed a constant increase in fluorescence signal, as already observed before (Figure 23 A and B). Interestingly, treatment with DTT of dNTic110 led to a high increase of dye-release over time.

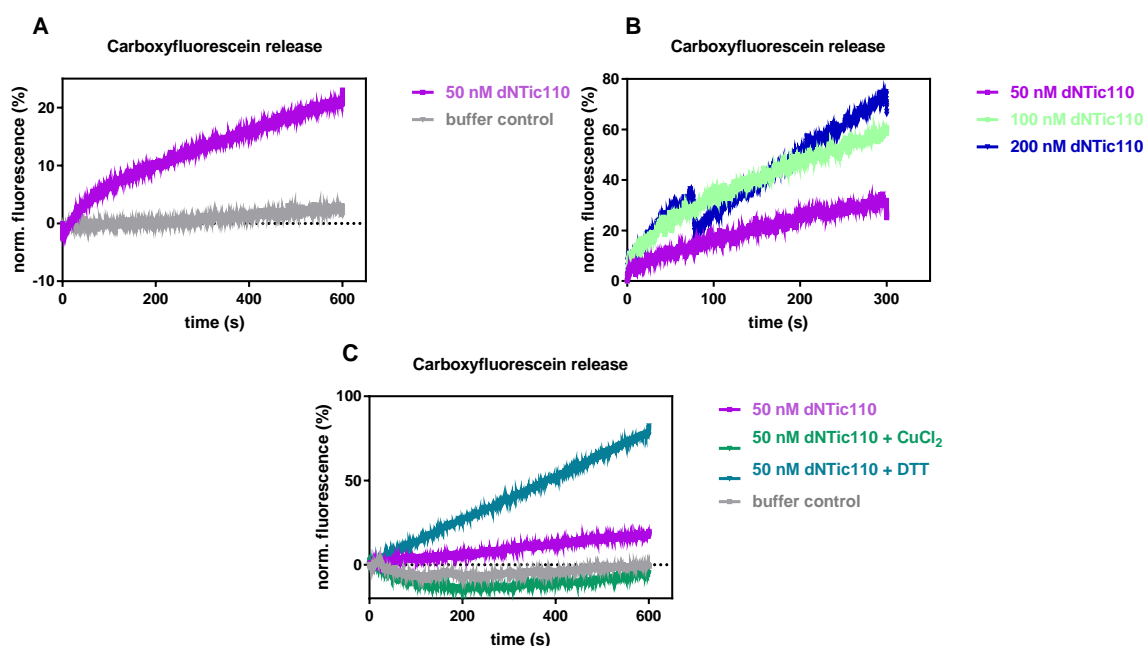


**Figure 23: dNTic110 channel-forming activity in carboxyfluorescein-encapsulated liposomes.**

Liposomes containing 20 mM carboxyfluorescein were incubated at room temperature in 995 µl 1x PBS (pH 7.4). The indicated concentrations of purified dNTic110 were added and the fluorescence was recorded every 1 ms (excitation at 494 nm and emission at 515 nm). Initial fluorescence was set to 0, whereas total liposome dequenching resulting from 0.5 % Triton X-100 was set to 100 %.

**A:** Carboxyfluorescein release upon addition of 50 nM purified dNTic110 in comparison to buffer.

**B:** Carboxyfluorescein release upon increasing concentrations of purified dNTic110 ranging from 50 nM to 200 nM.

**C:** dNTic110 was oxidized by 50 µM  $\text{CuCl}_2$  or reduced by 10 mM DTT for 1 h at 20 °C. 50 nM of pure protein was added to the liposomes.

To confirm that the increase of fluorescence signal indeed results from the channel-forming capacity of dNTic110 and not from membrane destruction, we made use of the well-established pore-forming activity of  $\alpha$ -hemolysin from *Staphylococcus aureus*. Using the same conditions as with dNTic110 a similar increase in fluorescence over time could be observed (data not shown).

Taken together, these results strongly support the model that reconstituted dNTic110 forms a concentration-dependent channel in liposomes and that this channel-forming capacity is negatively affected by oxidation and positively influenced upon reduction of the protein.

#### 4.4.3 Incorporation of the unnatural amino acid acetylphenylalanine at specific positions of dNTic110

The channel-forming capacity of dNTic110 has been demonstrated by means of a liposome leakage assay as shown above and by electrophysiology data (Balsera et al., 2009). However, structural insights in how the helices are arranged upon channel formation is missing. Therefore, we aimed to position fluorophores at strategic positions within the amphipathic helices for subsequent fluorophore-labeling and FRET analyses. Amine-reactive conjugates, such as succinimidyl-esters, can be used to label lysine residues or N-terminal amines. Virtually all proteins have lysine residues, and most have a free amine at the N-terminus, thus it is likely to attach many fluorophores to the protein. However, site-specific labeling is not possible. Instead, for site-specific labeling cysteines are used to covalently transfer a fluorescent dye to the protein, mainly because this amino acid is firstly underrepresented in proteins and thus, it is simple to generate single-cysteines proteins. Secondly, these single-cysteine proteins can be used for cysteine-maleimide chemistry which includes a wide range of fluorescent dyes. However, Tic110 harbors nine cysteines positioned throughout the polypeptide sequence and it has been shown that at least some cysteines play a regulatory role (Balsera et al., 2009). To avoid that cysteine mutations perturb the overall function or structure of Tic110 we decided to use the amber suppression system during translation in *E. coli* for the site-specific incorporation of a non-canonical amino acid into the protein without altering its structure. The system is based on the amber codon, which is the least used stop codon during translation in *E. coli*. By using a one-plasmid system encoding an engineered aminoacyl-tRNA synthetase (aaRS) and the orthogonal suppressor tRNA<sup>UAG</sup> the amber codon is converted into a coding triplet in translation (Reichert et al., 2015). This is achieved by aminoacylation of the complementary amber tRNA<sup>CUA</sup> by an orthogonal aminoacyl-tRNA synthetase that is specifically designed and optimized to accept the unnatural amino acid (UAA) acetylphenylalanine (Figure 24). The improved fidelity of the highly specific aa-tRNA synthetase/tRNA pair towards the non-canonical amino acid acetylphenylalanine leads to relatively high amounts of expressible proteins carrying the desired UAA at designated locations. The mentioned UAA acetylphenylalanine (in short: Apa) offers a keto-group which is (i) absent in polypeptides and (ii) does not cross-react with other components in the polypeptide backbone or cellular environments (Reichert et al., 2015). The application of hydroxylamine-derivatives of the commercially available fluorescent chemicals allows post-translational and site-specific protein-dye conjugations, which can subsequently be used for FRET-based analyses.

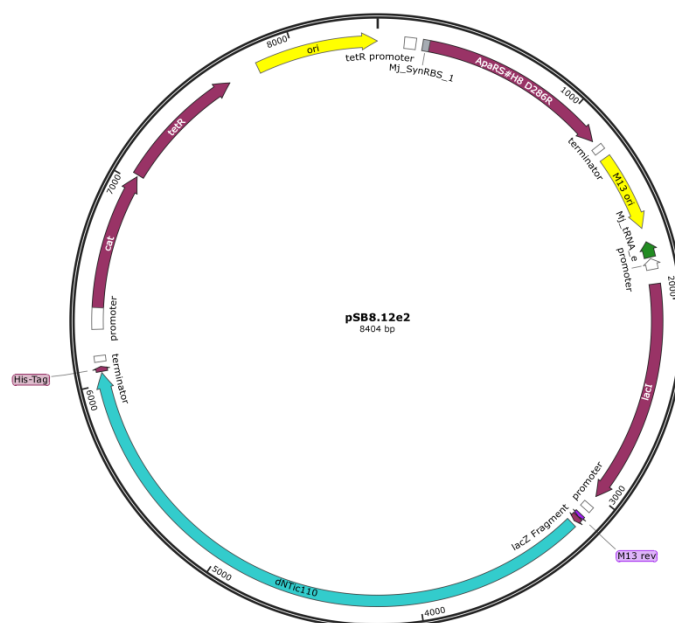


**Figure 24: Vector map of the one-plasmid amber suppression system pSB8.12e2 used in this study.** One-plasmid system of the pSB8.12e2 vector coding for the tRNA synthetase (ApaRS#HB8 286R), tRNA and the gene of interest. Courtesy of A. Reichert (AG Skerra, TU Munich). Expression of tRNA synthetase can be controlled by the addition of tetracycline, whereas expression of gene of interest (dNTic110) is IPTG-inducible.

#### 4.4.3.1 Expression of dNTic110 carrying acetylphenylalanine

First, we determined suitable positions for the fluorophores within the four potential amphipathic helices of dNTic110. The codons for phenylalanine of dNTic110 were exchanged against UAG, the amber codon, by site-directed mutagenesis. Phenylalanine was chosen because of its similarity to the unnatural amino acid and with the aim not to perturb the overall amphipathic character of the helices. Constructs with amber codons at positions F216, F222, F328, F585 and F670 were cloned with XbaI/AfeI into pSB8.12e2 (Figure 25) and plasmids were transformed into BL21 (DE3).

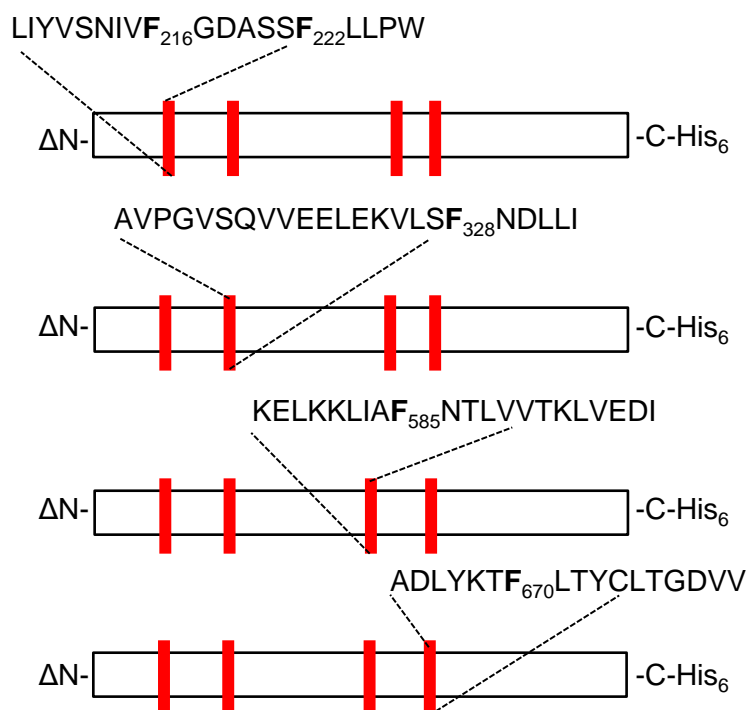


**Figure 25: Schematic representation of different dNTic110 mutants used in this study.**

Constructions of dNTic110 proteins carrying amber codons at residues 216, 222, 328, 585, 670. Red lines represent the four amphipathic helices and the numbers indicate the position of the phenylalanine whose bases were exchanged against the amber codon (UAG). ΔN represents the loss of the two hydrophobic N-terminal helices.

The addition of 1 mM acetylphenylalanine during expression of Tic110-585<sub>amb</sub> led to the production of full-length dNTic110 16 h post induction at 30 °C (Figure 26). Immunoblot analysis using psTic110-specific antiserum revealed that the band visible in the Coomassie-stained SDS-PAGE indeed corresponded to full-length Tic110 (Figure 26).

Soluble dNTic110 can be expressed using low amounts of IPTG (0.5 mM) and low temperature (12 °C) overnight. However, for sufficient efficiency of amber suppression, elevated temperatures were used for expression (30 °C). Unfortunately, this did result in higher levels of insoluble protein expression, which was unwanted. Consequently, expression of soluble dNTic110-Apa was carried out following the established protocol for soluble expression of dNTic110, except that the temperature was shifted to 18 °C and the incubation time was prolonged to 36 h after induction to obtain sufficient amounts of soluble Apa-Tic110 protein.

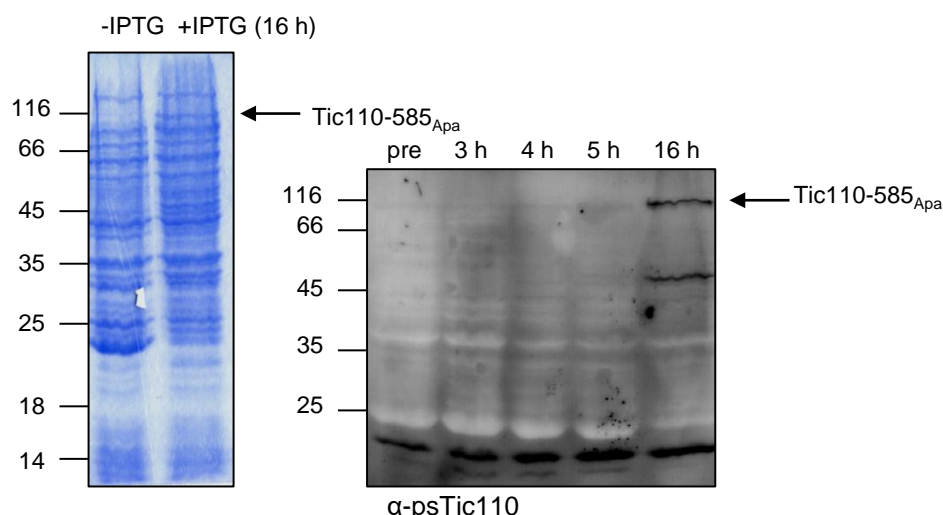


**Figure 26: Co-translational incorporation of the unnatural amino acid acetylphenylalanine into dNTic110 mediated by *E. coli*.** Addition of Apa during translation led to successful incorporation of it at residue 585 after 16 h of expression at 30 °C, resulting in full-length dNTic110. Immunoblot analysis using psTic110 antiserum specifically recognized the full-length protein.

#### 4.4.3.2 Purification of dNTic110 featuring acetylphenylalanine and reactivity test

dNTic110-328<sub>Apa</sub> was used to perform purification steps. Purification of Apa-containing dNTic110 was carried out following the protocol developed by Balsera et al. except that the crude bacterial pellet was subjected to batch-purification using Ni-NTA beads in the presence of 500 mM Urea. For wash and elution 20 mM Tris/HCl pH 8.0, 200 mM NaCl without and with 400 mM imidazole was used, respectively. Elutions were pooled and the protein was further purified using an Superdex 200 column equilibrated with 20 mM Tris/HCl pH 8, 200 mM NaCl. Peaks fractions were analyzed on 10.5 % SDS-PAGE (Figure 27 A). Fractions from peak 2 and peak 3 contained dNTic110-328<sub>Apa</sub> and were concentrated using an Amicon-filter with a cutoff of 30 kDa. At the end, 180 µl with a concentration of 0.7 mg/ml of dNTic110 was obtained. To analyze the liposome affinity of this mutant protein, proteoliposomes were prepared as described in methods section 3.3.14 except that the applied concentration of dNTic110-328<sub>Apa</sub> was lower. Figure 27 B shows that a low amount of Tic110-328<sub>Apa</sub> indeed stably integrated into liposomes.

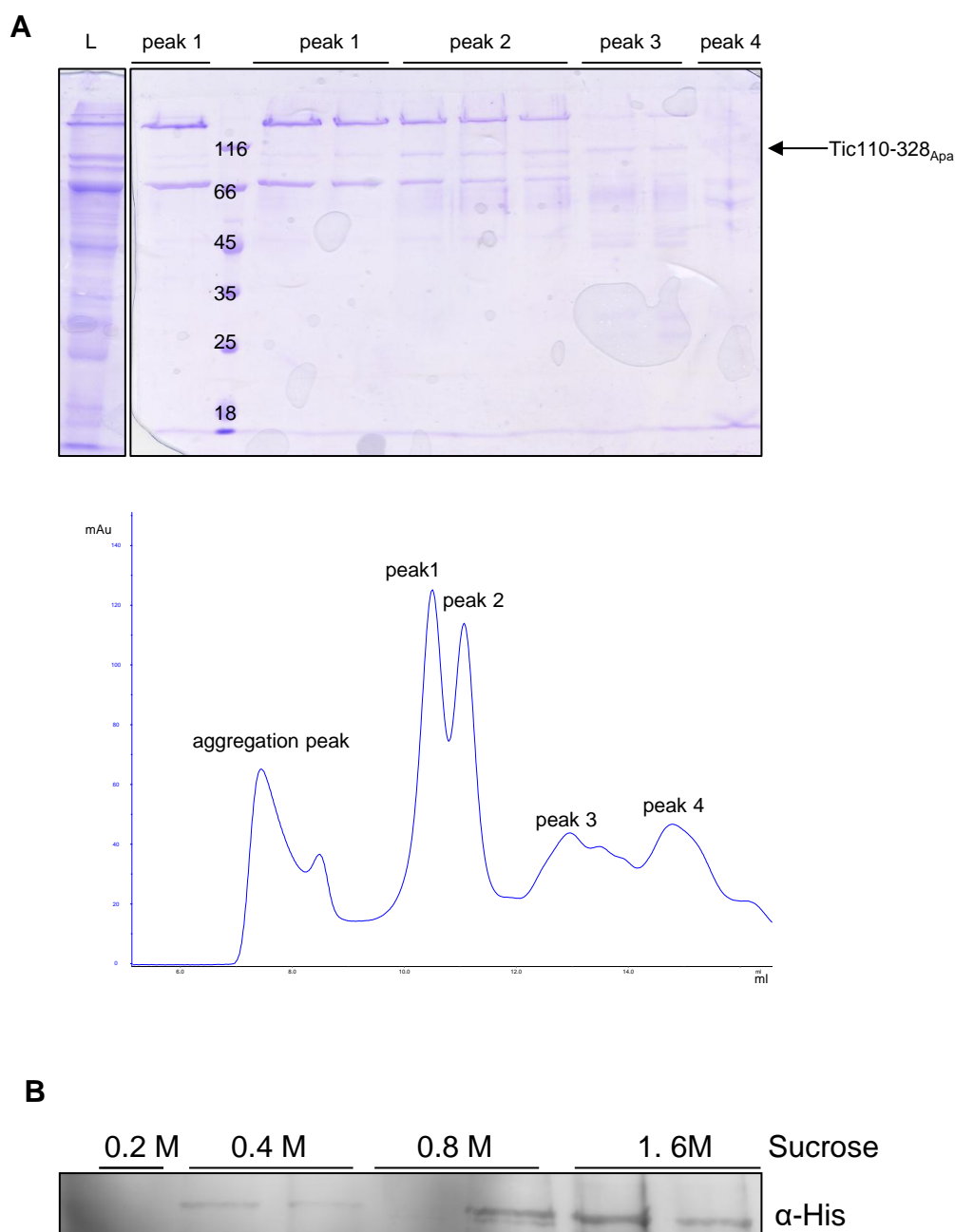


**Figure 27: Purification of dNTic110-328<sub>Apa</sub> and insertion into liposomes.**

**A:** SDS-PAGE of the four peaks taken from the gel filtration as indicated in the chromatogram. L = load.

**B:** Flotation assay to confirm the insertion of dNTic110-328<sub>Apa</sub> into liposomes. Prepared liposomes and purified dNTic110-328<sub>Apa</sub> were incubated as described in the method section 3.3.14. After dialysis, samples were adjusted to a sucrose concentration of 1.6 M sucrose and were loaded on the bottom of a sucrose gradient containing steps of 0.8 M, 0.4 M and 0.2 M of sucrose. The gradient was centrifuged at 100000 g for 19 h at 4 °C and fractions were collected, with 10 % TCA precipitated and analyzed on 10.5 % SDS-PAGE, followed by immunoblotting using anti-His antibody to detect the His-Tag of dNTic110-328<sub>Apa</sub>.

For reactivity tests of the keto-group a higher amount of protein was required. For this purpose, dNTic110-670<sub>Apa</sub> was overexpressed at elevated temperatures and was extracted from inclusion bodies. After Ni-NTA batch-purification under denaturing conditions, the pure protein was refolded in 20 mM Tris pH 8, 200 mM NaCl overnight. To test the reactivity of the keto-group the protein was labeled with hydroxylamine-Alexa Fluor488. 2 µl of a 50 mM stock solution was added to 160 µl of protein (0.6 mg/ml). Labeling was carried out at 4 °C overnight. Excess dye was removed by dialysis overnight at 4 °C against buffer without dye. Labeling efficiency was calculated as mentioned in method section 3.3.16 and was found to be 9.9 %.

Taken together it can be concluded that very low amounts of soluble dNTic110 could be produced that contained the unnatural amino acid at position 328 resulting from effective amber suppression during translation in *E. coli*. This protein stably integrated into liposomes, substantiating the supposition that the unnatural amino acid did not disturb the behaviour of dNTic110 in a membrane-mimicking environment.

The introduced keto-group of the protein at residue 670 could be site-specifically labeled with a hydroxylamine derivative of Alexa Fluor488 with a labeling efficiency of ~10 %. Thus, preliminary work was successful and future FRET-based experiments can now reveal information about the spatial arrangements of the four amphipathic helices in a proteoliposomal system.

#### 4.5 Electron microscopy analysis of purified dNTic110

dNTic110 was purified to homogeneity using the established protocol. The pure protein was diluted to a final concentration of 19 µg/ml. 0.02 % of LDAO and 0.2 % of glutaraldehyde was added, the protein was negatively stained and applied to thin carbon films. Data were collected using a 100-kV Morgagni routine transmission electron microscope (AG Beckmann, LMU Munich). Preliminary pictures of single dNTic110 particles are depicted in Figure 28.



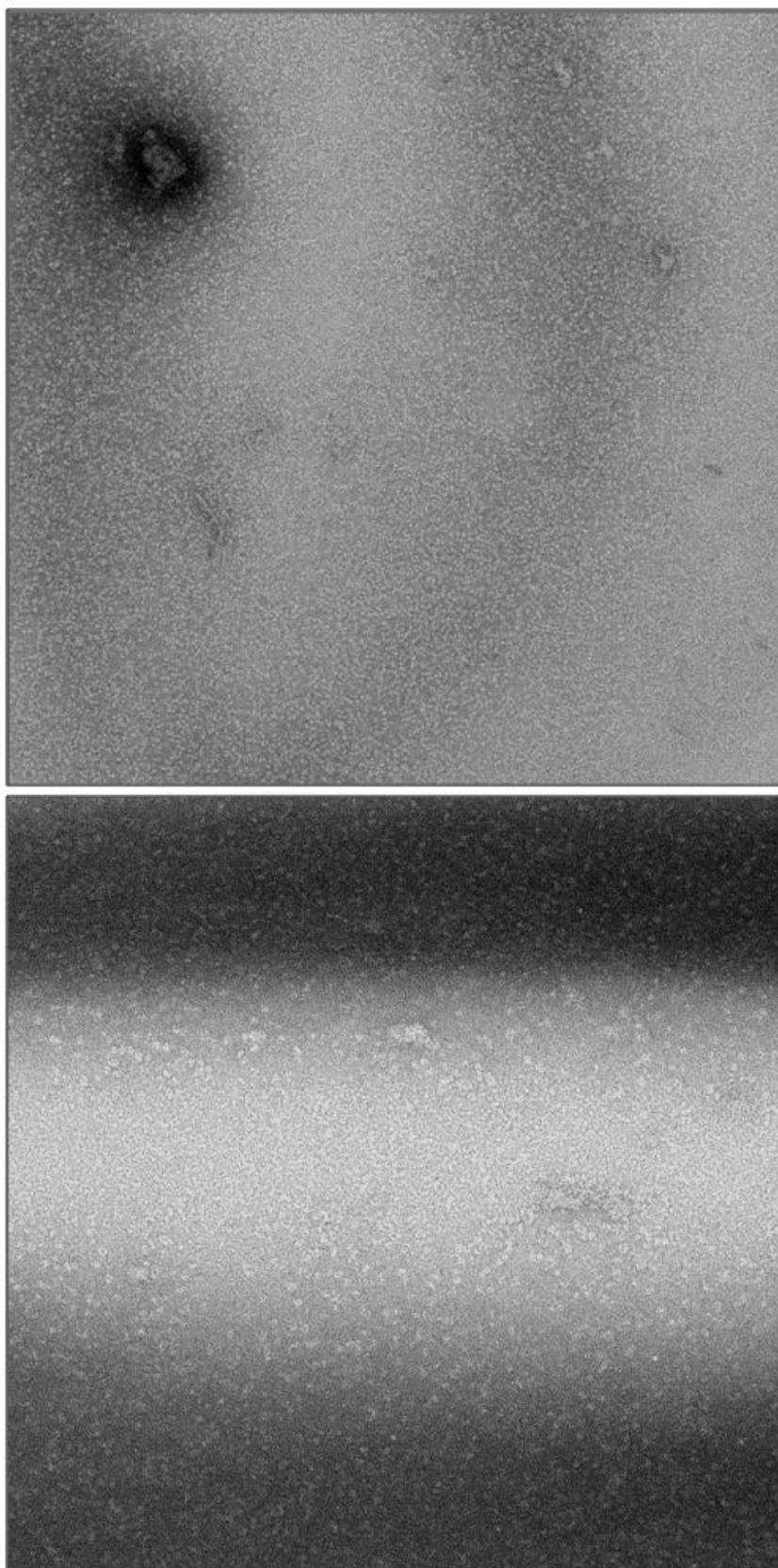


**Figure 28: Electron micrographs of single dNTic110 particles.**

## 5. Discussion

From previously reported results a topological model concerning Tic110 was created which included all data so far available on Tic110. The protein is anchored via its two hydrophobic helices into the inner envelope membrane. Parts of the large C-terminus are protruding into the intermembrane space, thereby allowing the interaction with both TOC complex and incoming preproteins. The topological model is based on distinct facts:

- (i) Tic110 is susceptible to proteases that cannot cross the inner envelope under controlled conditions (Lübeck et al., 1996; Balsera et al., 2009; this work).
- (ii) dNTic110, which lacks the two hydrophobic transmembrane helices, still integrates into liposomes (Balsera et al., 2009; this work).
- (iii) dNTic110-proteoliposomes show channel-forming capacity *in vitro* (Heins et al., 2002; Balsera et al., 2009; this work).
- (iv) The Tic110 sequence contains helices with predicted amphipathic features which might build up the channel.

In the present study, the model was re-addressed by state-of-the-art methods to complete the current understanding of topology and function of the inner envelope protein Tic110.

### 5.1 *In situ* topology of Tic110

Isolated inner envelope membranes provide a great tool for *in situ* topological studies. The vesicles have a right-side-out orientation (Shingles and McCarty, 1995), leading to regions formerly oriented to the intermembrane space that are now exposed to the surrounding medium. The vesicles can be used for limited protease treatment or selective biotinylation, subsequently followed by mass spectrometric-based sequencing, allowing to identify these external domains.

Three different chemicals were utilized for selective labeling, all of them with a biotin moiety that chemically reacts with the  $\epsilon$ -amino-group of lysine residues or the free N-terminus of a polypeptide chain. By applying cross-linkers with variable and long spacer lengths it was aimed to avoid passive diffusion into the vesicles. Furthermore, incubation time and temperature were reduced (10 min at 4 °C) to ensure only surface labeling of the isolated vesicles. Immunoblot analyses detecting biotin residues revealed that biotinylation of Tic110 in isolated inner envelope vesicles indeed only occurred at surface exposed regions. However, mass spectrometric analyses showed that nearly every single lysine of Tic110 was labeled by all three cross-linkers. Thus, it is highly tempting to speculate that despite their proposed membrane impermeability and long spacer length the applied cross-linkers somehow entered the vesicles, probably directly by diffusion through the Tic110

translocation pore. The shortest cross-linkers were Sulfo-NHS-Biotin and Biotin-XX,SE; both had a spacer length of 13.5 Å and 14 Å, respectively. The longest spacer was found in NHS-PEG<sub>4</sub>-Biotin with 29 Å. Considering that Tic110 has a pore size between 15 and 30 Å (Heins et al., 2002), the pore might be still big enough for even the longest cross-linker used in this study, which had a linker length of 29 Å. It had to be concluded that under the applied conditions selective biotinylation is not a suitable tool for surface labeling of isolated vesicles.

As an alternative method to exclusively identify peptides from loops protruding into the surrounding buffer trypsin was applied under conditions that only allow degradation of peptides exposed to the buffer medium. Degradation of Tic110 occurred very rapidly, in contrast to selected control proteins which were not degraded at all. Unfortunately, with mass spectrometric analyses not only peptides from the external domains but also a high number of peptides could be identified that are presumably located in the inner part of the vesicle, meaning that they originally are found in the stroma. This observation can be explained in different ways. To exclude that trypsin crossed the membrane and thereby had access to internal protein domains adequate control proteins were analyzed. It was shown that neither Tic62, nor Tic40 nor IEP37 were degraded at all, leading to the conclusion that these proteins were indeed protected by the inner envelope membrane during the protease treatments. Moreover, by using trypsin-immobilized beads as a comparison it was ensured that no soluble trypsin is present in the buffer, thus providing a technical control for non-entrance of trypsin. Using trypsin-immobilized beads led to the same degradation pattern of Tic110, indicating that only surface exposed parts of Tic110 are degraded by externally added trypsin.

Although the isolation according to the protocol leads to right-side-out vesicles, which is also substantiated by the non-degradation of control-proteins, it cannot be excluded that a very small amount (~5 %) of produced vesicles turned into wrong-side-out vesicles during preparation. This would mean that loops or domains that are normally localized in the chloroplast stroma are now exposed to the buffer and hence are susceptible to proteolytic degradation. In this scenario Tic62, Tic40 and IEP37 should also be degraded to some extent, which is apparently not the case. Possibly, these potential degradation products of control proteins were below the detection level in immunoblot assays, whereas mass spectrometric analyses are so sensitive that a single peptide is already detectable which could result in false positives.

Alternatively, tryptic degradation might have triggered a conformational change of the residual protein in the membrane upon cleavage. This could result in a drastic conformational change of the residual protein, leading to more trypsin-susceptible parts, which are normally not accessible.

Since the previous approaches were not successful in establishing a topology of Tic110 a reliable quantification assay had to be established to get a better idea of which peptides are more abundant in the sample than others. Quantification is still a bottleneck in proteomics, however by using isobaric labels it is possible to obtain reliable data. We made use of three different TMT labels to compare the relative abundance of peptides. We could identify two peptides that have a high probability to be at the outside of the inner envelope vesicles. These two peptides are matched to a region which is according to our current topological model oriented towards the intermembrane space (between amphipathic helix 3 and 4).

One possibility to substantiate these results would be the generation of either a monoclonal antibody against the N- or C-terminus of Tic110 or by use of a peptide-sensitive antibody using the identified peptide from loop 2 as the antigen. With this, it would be possible to “track” the degradation of susceptible regions, namely the loop exposed to the out-side of the vesicles will occur faster than the degradation of other parts.

## **5.2 *In vivo* topology and function of Tic110**

The *in vivo* topology of Tic110 was analyzed using the genetically encoded tag miniSOG. MiniSOG is capable of producing singlet oxygen, that in presence of diaminobenzidine leads to the production of an osmiophilic precipitate and can be visualized during electron microscopy.

Three distinct miniSOG-tagged Tic110 proteins were generated. MiniSOG was placed in both external loops that are protruding into the intermembrane space as well as at the very C-terminus as a control for stromal localization. It was possible to successfully target and express all miniSOG-tagged variants transiently in tobacco chloroplasts, which was confirmed by either fluorescence microscopy or immunoblot analyses by using antisera against atTic110 and miniSOG. Immunoblot analyses could confirm successful expression under the control of both promoters (35S and endogenous Tic110), although expression was higher using the 35S promoter. Photooxidation was carried out using transiently infected tobacco leave tissues and in some cases, a dot-like structure in the intermembrane space could be observed that might indicate a specific reaction of Tic110-miniSOG (residues 226-311) generated singlet oxygen with DAB.

Due to our technical setup it was not possible to visually control the photooxidation process. However, as the ultra-structure of chloroplasts was still preserved, it could be argued that blue light illumination had no detrimental effect on the tissue. To get a stronger signal a possibility would be to create tandem-miniSOG fusion proteins. However, this would increase the risk of interference of the tag with the structure and/or function of the tagged protein. So far, the miniSOG-tagging method has been established in a variety of organisms

or tissues (cell cultures, *C. elegans*, brain tissue of mouse). None of these organisms contain chlorophyll which absorbs predominantly blue (400 nm - 500 nm) as well as the red (600 nm - 700 nm) light. These wavelengths partially overlap with the absorption maximum of miniSOG. Thus, it cannot be excluded that the presence of chlorophyll interferes with the blue light mediated singlet oxygen production by miniSOG. One possibility to avoid that drawback is to use etioplasts. Etioplasts derive from plants that have not been exposed to light. However, as Tic110 is present in all kinds of plastids it should remain possible to perform a photooxidation experiment with a functionally expressed Tic110. Even though the detection of an unambiguous precipitate in the intermembrane space will remain problematic, it should be possible to discriminate between stroma and intermembrane space. By using the C-terminal control it should be possible to clearly identify parts that are located in the stroma, which are not visible by using intermembrane space-tagged Tic110.

Improvements could be achieved by analyzing how much DAB reagent is required for image detection. This has to be considered very carefully, avoiding under- and over-labeling of the tissue, and multiple parameters, such as protein expression level, labeling density, fixation conditions, heavy metal staining and microscope settings play a role in the EM visualization of the labeled product. All these parameters must be carefully addressed before further experiments can lead to promising results.

The correct function of a protein is affiliated with its native topology. Although it could be shown that targeting to the chloroplast is not impaired by inserting miniSOG in various parts of Tic110 it cannot be excluded that its native topology is altered. To confirm the correct assembly of the channel-like structure, complementation lines of heterozygous *TIC110/tic110 Arabidopsis* plants with the various miniSOG-tagged Tic110 constructs under the control of its native promoter were generated. Only if the variants can complement the phenotype of heterozygous mutant plants, it can be deduced that topology and thus function is not impaired in transgenic plants. To this end, *TIC110/tic110* plants were transformed with all three constructs, however so far no homozygous progeny plants could be isolated. Furthermore, in case of transformation with miniSOG at residue 257, the plants look even more chlorotic than their heterozygous parents. The plants look obviously chlorotic and yellowish, which implies that the import machinery is not functioning properly, and required photosynthetic compounds are not assembled correctly. This effect became even more prominent when plants were grown on soil and not on sugar-containing plates. At this stage, miniSOG-tagged Tic110<sub>ims1</sub> transformed plants are hampered in assembling a fully working photosynthetic machinery. So far it is not clear whether this chlorotic phenotype is due to the absence (non-expression of protein) of miniSOG-tagged Tic110<sub>ims1</sub> or dominant negative effects. Especially regarding the fact that close to this region the proposed transit peptide of

preproteins binding domain is localized (Inaba et al., 2005), one can speculate that due to competition with intrinsic Tic110 interaction with incoming preproteins is negatively affected. It has been shown by others with different truncated constructs that they have a dominant negative effect on intrinsic Tic110 (Inaba et al., 2005). In this case, immunoblot analysis showed that intrinsic Tic110 is not reduced in transgenic plants, although plants look more chlorotic. However, the dominant negative effect is still more likely as the absence of miniSOG-tagged proteins simply should result in a heterozygous Tic110-like phenotype because no interference is expected, although it cannot be excluded that regulations on the RNA level occurred, leading to feedback mechanisms. So far, detection of miniSOG-tagged Tic110 with antiserum against miniSOG in stable *Arabidopsis* lines was not successful, thus no conclusion about protein levels of the recombinant protein can be drawn yet.

It would be interesting to see if the actual amount of some photosynthetic precursors such as pSSU in the chloroplast is reduced in transgenic plants compared to untransformed heterozygous plants.

As these complementation studies do not allow to draw reliable conclusion concerning correct topology of the Tic110 fusion proteins, another idea would be to perform limited proteolysis with intact chloroplasts from transgenic plants or transiently expressing tobacco leaves. Trypsin can penetrate the outer envelope but not the inner envelope. The degradation pattern can now be tracked with the miniSOG specific antibody, at least for transiently expressing tobacco leaves. The signal of domains of the intermembrane space loops carrying miniSOG should be disappear very early during protease treatment, whereas the signal using the construct with miniSOG at the C-terminus should remain stable even with increasing trypsin concentrations, as miniSOG at that position is protected by the inner membrane.

Beside genetic tagging, the *in vivo* topology of Tic110 could also be addressed by spatially restricted enzymatic tagging. Ascorbate peroxidase (Apex) can be used, which normally catalyses the reduction of  $H_2O_2$  and the simultaneous oxidation of ascorbate. However, upon mutation of the active centre the enzyme also accepts other substrates, e.g. biotin-phenol (Rhee et al., 2013). In the presence of  $H_2O_2$  the mutated Apex (mApex) will covalently transfer biotin-phenol to electron rich amino acids like tyrosine or histidine to every peptide in close proximity. Modified amino acids can be identified by mass spectrometry. This approach was performed by Rhee et al. who targeted mApex to different mitochondrial sub-compartments and solved the topology of many outer and inner mitochondrial membrane proteins (Rhee et al., 2013). Recently, this approach was even more improved by applying desthiobiotin as a substrate for mAPEX (Lee et al., 2017). By targeting mApex to different sub-compartments of the chloroplast – equivalent to the mitochondria – namely stroma,

inner envelope membrane or intermembrane space, it will be possible to tag Tic110 from different orientations which should result in differentially labeled pattern identified with mass spectrometry. This experimental approach would not only allow to determine the topology of a single membrane-spanning protein like Tic110, but offers also great applicability to map the architecture of chloroplast membrane proteins in living cells in a high throughput manner.

Tic110 contains six fully conserved cysteines which might be involved in disulfide bridge formation. *In vitro* data showed that mutation of at least two of them influenced the behavior of the protein in solution. To analyze the role of the cysteines *in vivo*, heterozygous *TIC110/tic110* plants were transformed with various mutated cysteine variants. To this end, the presence of a construct having a mutated cysteine at position 526 in a heterozygous background led to a chlorotic phenotype, although the total amount of Tic110 was unaffected compared to wild type plants. It has to be mentioned that this cysteine is not among the six fully conserved ones, nevertheless, it is present in many plant species. Interestingly, the protein amount of Tic110 in plants transformed with the construct carrying C526S was higher than in the heterozygous parent plants, suggesting that the mutated protein is indeed expressed at normal levels. It remains to be established if this mutation has an impact on e.g. protein import or interaction with other proteins. Furthermore, the *in vivo* role of this cysteine under stress conditions could also be addressed.

### 5.3 Topology of dNTic110 in a reconstituted proteoliposome system

Reconstituted proteoliposomal systems provide a platform to perform structural studies of dNTic110 in a minimal membrane-mimicking system without interference by other membrane components. dNTic110 proteoliposomes were used to investigate the channel composition/topology with three different experimental approaches.

Using chemical cross-linking coupled with mass spectrometry provides a great tool to study structures of protein complexes to understand their functions and regulations. However, this method has been challenging because of technical difficulties in unambiguous identification of cross-linked peptides and determination of cross-linked sites by MS analysis. Cross-linkers that dissociate under collision-induced dissociation (CID) conditions in the mass spectrometer may be applied to facilitate the identification of cross-linked products based on the characteristic fragment ions and constant neutral losses in MS/MS spectra. We made use of the DSSO cross-linker, which contains a CID-labile group (a sulfoxide) that can create characteristic marker ions upon ionization. On the basis of these marker ions it is possible to discriminate inter- and intrapeptide cross-links from dead-end cross-links (Kao et al., 2011).

It was possible to reconstitute dNTic110 successfully into liposomes to generate proteoliposomes for cross-linking. However, only intra or dead-end cross-links could be identified which did not provide any information about distance constraints between domains. One explanation could be the increased complexity in comparison to other experimental setups. DSSO cross-linking was successfully applied for cytochrome c or ubiquitin, both pure proteins in solution (Kao et al., 2011). It cannot be excluded that the presence of lipids did reduce the efficiency of DSSO cross-linking. Another explanation would be that cross-linking was carried out at 4 °C and not at 37 °C, to prevent proteolysis of dNTic110 proteoliposomes. It is likely that this resulted in reduced reactivity of the cross-linker. Further experiments have to be performed in order to establish optimal cross-linking conditions.

A liposome leakage assay was conducted to demonstrate channel-activity of dNTic110 as an alternative to the data obtained from electrophysiology. It could be shown that dNTic110 triggered the dye-release from carboxyfluorescein-charged liposomes in a concentration dependent manner. The presented results suggest that the channel consisting of dNTic110 is closed upon oxidation and open upon reduction. This has also been demonstrated for the second channel, Tic20, by swelling assays (Kovács-Bogdán et al., 2011). Reduction of Tic110 with physiological reducing agents, such as Trxs, pointed out that Tic110 could be a target for Trx regulation. Tic110 is the second demonstrated Trx target in the TIC translocon (after Tic55), further suggesting multiple ways of regulation of protein import at the level of the TIC translocon (Balsera et al., 2009). The impact of that kind of regulation concerning channel activity can now be analyzed in more detail with the liposome leakage assay. Besides analyzing the impact of oxidation or reduction, the liposome leakage assay is an optimal tool to study the effect of any mutations on channel-formation properties due to its relatively simple experimental setup. The pore size of Tic110 reconstituted into liposomes was estimated using the polymer size exclusion method (Krasilnikov et al., 1992). The size of the narrowest and the widest opening state was obtained by the application of differently sized non-electrolyte polyethylene glycol (PEG) molecules (Krasilnikov et al., 1992; Smart et al., 1997). If small PEG molecules were gradually excluded from the pore, this resulted in reduction of the current passing through the channel. In contrast, applying larger PEG molecules, which are completely excluded from the pore, the conductance of the channel was not affected. With this method it was estimated that the Tic110 channel has at least a diameter of 15 Å and at its most open form a diameter of 31 Å, indicating that the channel does not have a uniform cylinder-like shape (Heins et al., 2002). However, the narrowest opening of 15 Å would be sufficient to allow the translocation of a partially folded protein (Heins et al., 2002). Alternatively, fluorochromes coupled to large dextran molecules can be



encapsulated to estimate pore dimensions (Vandenbossche et al., 1991). Thereby it would not be only possible to estimate the pore size in general, but also to track opening changes upon oxidation or reduction. It would be interesting to see whether oxidation really has a conformational effect on Tic110, leading to a reduced pore size or if it is just an all-or-nothing-response (open or close). Recently, another way for pore size estimation has been applied by probing the translocation channels with particles of fixed diameter and the translocons are found to be larger than 25 Å (Ganesan et al., 2017). The authors concluded that TOC and TIC are bigger than the mitochondrial counterparts, TOM and TIM. However, although this in organellar assay has a lot of advantages over *in vitro* assays, the TOC pore size could not be determined independently of TIC, thus it is not able to reflect translocation pores alone. Here, with the abovementioned liposome leakage assay, it would be possible to analyze TOC and TIC components independent from each other, although it remains *in vitro*.

To improve this experimental approach a single liposome assay could be performed. As single-patch clamp analyses are difficult to conduct, a membrane pore could theoretically be detectable at concentrations as low as to 1-2 pores per liposome by means of fluorescence spectroscopy. So far, detailed mechanistic studies of membrane transport are typically analyzed by macroscopic measurements. Small vesicles and high protein-to-lipid ratios are required to obtain a good signal-to-noise ratio, which makes it difficult to calculate transport rates. In a study conducted by Zollmann et al. they developed a method called dual-color fluorescence-burst analysis to analyze peptide transport into single liposomes with, on average, one to three protein complexes per vesicle (Zollmann et al., 2015).

Studies of protein structure and function using single-molecule Förster resonance energy transfer (smFRET) benefit from the ability to site-specifically label proteins with small fluorescent dyes. Genetically encoding the unnatural amino acid acetylphenylalanine is an efficient way to introduce commercially available fluorescent tags with high yield and specificity (e.g. with hydroxylamine derivatives of Alexa Fluor488 and 647).

It could be shown that detectable amounts of soluble Tic110 carrying Apa at position F328 could be expressed via the amber suppression system in *E. coli* and purified resulting in 600 µg protein/l culture. In contrast, using GFP as a protein to study amber suppression efficiency, the 10-fold amount of expressed protein could be achieved (Reichert et al., 2015). However, it has to be taken into account that Tic110 is a large protein, probably this fact alone results in lower expression levels. Besides, GFP-Apa was expressed at 30 °C for 20 h, whereas Tic110 was expressed at 18 °C for 36 h. Effective amber suppression depends on the expression of the respective aa-tRNA synthetase that transfers the unnatural amino acid onto the respective tRNA. Most likely the expression of aa-tRNA synthetase is likewise

reduced under low temperatures, consequently leading to reduced amounts of aminoacylated tRNAs.

The synthesized protein was labeled with hydroxylamine-Alexa Fluor488, reaching a labeling efficiency of 5-10 %. Optimal labeling conditions for the reactivity between the keto-group and the hydroxylamine derivative were reported to be: (i) high temperature (37 °C), (ii) long incubation time (18 h), (iii) high protein concentrations (around 200 µM) and (iv) buffer with a pH around 5 (Brustad et al., 2008). These conditions cannot be applied for Tic110 due to several reasons. Tic110 has an isoelectric point of pH 5.7, thereby increasing the risk to form precipitates in buffers with a low pH. As Tic110 is protease-sensitive, temperature must be kept low and as sufficient amount of proteins could not be produced, lower concentrations had to be used which also reduced the labeling efficiency. One possibility to increase the labeling efficiency is to use an aniline-based catalyst. By using phenylendiamine it has been shown that labeling increases even in the presence of a buffer with physiological pH (Mahmoodi et al., 2015). It remains to be established if this is also the case for labeling of Tic110. However, literature searches revealed that also other proteins are difficult to label. In their experiments, the authors used several days for each step, eventually gaining labeling efficiencies of 20 % (Ratzke et al., 2014). Nonetheless, smFRET studies require only little amounts of protein and the established expression of dNTic110 carrying Apa at specific positions can be used for further analyses in order to gain information about spatial arrangements between the helices.

## 5.4 Conclusions

A variety of state-of-the art approaches were applied in order to address the topology and function of Tic110 *in situ*, *in vivo* and *in vitro*. The obtained data could convincingly demonstrate that Tic110's topology consists of both intermembrane space- and stroma-orientated regions. The data indicate that both regions have precise and specific functions in the import process, e.g. interaction with incoming preproteins and regulative features concerning the channel's open state to limit the amount of incoming preproteins. These features are probably controlled and coordinated by cellular responses. However, resolving the three-dimensional structure is still the final goal to identify structure-function relationships of proteins. By using the generated site-specific fluorophore-labeled Tic110 variants for FRET analyses, it will be probably possible to gain structural information; together with the data resulting from electron microscopy analysis, which provides for the first time material for structural analyses on Tic110, it will be possible to finally resolve the structure-function relationship of Tic110 in the future.

## 6. List of references

- Agne, B., Infanger, S., Wang, F., Hofstetter, V., Rahim, G., Martin, M., Lee, D.W., Hwang, I., Schnell, D., and Kessler, F. (2009). A *toc159* import receptor mutant, defective in hydrolysis of GTP, supports preprotein import into chloroplasts. *J. Biol. Chem.* **284**, 8670–8679.
- Akita, M., Nielsen, E., and Keegstra, K. (1997). Identification of Protein Transport Complexes in the Chloroplastic Envelope Membranes via Chemical Cross-Linking. *J. Cell Biol.* **136**, 983–994.
- Arnon, D.I. (1949). COPPER ENZYMES IN ISOLATED CHLOROPLASTS. POLYPHENOLOXIDASE IN BETA VULGARIS. *Plant Physiol.* **24**, 1–15.
- Aronsson, H., Combe, J., Patel, R., Agne, B., Martin, M., Kessler, F., and Jarvis, P. (2010). Nucleotide binding and dimerization at the chloroplast pre-protein import receptor, *atToc33*, are not essential in vivo but do increase import efficiency. *Plant J. Cell Mol. Biol.* **63**, 297–311.
- Balsera, M., Goetze, T.A., Kovács-Bogdán, E., Schürmann, P., Wagner, R., Buchanan, B.B., Soll, J., and Bölter, B. (2009). Characterization of *Tic110*, a channel-forming protein at the inner envelope membrane of chloroplasts, unveils a response to  $\text{Ca}^{2+}$  and a stromal regulatory disulfide bridge. *J. Biol. Chem.* **284**, 2603–2616.
- Becker, T., Jelic, M., Vojta, A., Radunz, A., Soll, J., and Schleiff, E. (2004). Preprotein recognition by the Toc complex. *EMBO J.* **23**, 520–530.
- Bölter, B., and Soll, J. (2016). *Ycf1/Tic214* Is Not Essential for the Accumulation of Plastid Proteins. *Mol. Plant* **9**.
- Bölter, B., May, T., and Soll, J. (1998a). A protein import receptor in pea chloroplasts, *Toc86*, is only a proteolytic fragment of a larger polypeptide. *FEBS Lett.* **441**, 59–62.
- Bölter, B., Soll, J., Schulz, A., Hinnah, S., and Wagner, R. (1998b). Origin of a chloroplast protein importer. *Proc. Natl. Acad. Sci. U. S. A.* **95**, 15831–15836.
- Bruce, B.D. (2001). The paradox of plastid transit peptides: conservation of function despite divergence in primary structure. *Biochim. Biophys. Acta* **1541**, 2–21.
- Brustad, E.M., Lemke, E.A., Schultz, P.G., and Deniz, A.A. (2008). A General and Efficient Method for the Site-Specific Dual-Labeling of Proteins for Single Molecule Fluorescence Resonance Energy Transfer. *J. Am. Chem. Soc.* **130**, 17664–17665.
- Chen, R.F., and Knutson, J.R. (1988). Mechanism of fluorescence concentration quenching of carboxyfluorescein in liposomes: energy transfer to nonfluorescent dimers. *Anal. Biochem.* **172**, 61–77.
- Chen, K., Chen, X., and Schnell, D.J. (2000). Initial Binding of Preproteins Involving the *Toc159* Receptor Can Be Bypassed during Protein Import into Chloroplasts. *Plant Physiol.* **122**, 813–822.
- Chen, X., Smith, M.D., Fitzpatrick, L., and Schnell, D.J. (2002). In vivo analysis of the role of *atTic20* in protein import into chloroplasts. *Plant Cell* **14**, 641–654.

- Chen, Y.-L., Chen, L.-J., and Li, H.-M. (2016). Polypeptide Transport-Associated Domains of the Toc75 Channel Protein Are Located in the Intermembrane Space of Chloroplasts. *Plant Physiol.* 172, 235–243.
- Chew, O., Lister, R., Qbadou, S., Heazlewood, J.L., Soll, J., Schleiff, E., Millar, A.H., and Whelan, J. (2004). A plant outer mitochondrial membrane protein with high amino acid sequence identity to a chloroplast protein import receptor. *FEBS Lett.* 557, 109–114.
- Chou, M.-L., Chu, C.-C., Chen, L.-J., Akita, M., and Li, H. (2006). Stimulation of transit-peptide release and ATP hydrolysis by a cochaperone during protein import into chloroplasts. *J. Cell Biol.* 175, 893–900.
- Clantin, B., Delattre, A.-S., Rucktooa, P., Saint, N., Méli, A.C., Loch, C., Jacob-Dubuisson, F., and Villeret, V. (2007). Structure of the membrane protein FhaC: a member of the Omp85-TpsB transporter superfamily. *Science* 317, 957–961.
- Cserző, M., Wallin, E., Simon, I., von Heijne, G., and Elofsson, A. (1997). Prediction of transmembrane alpha-helices in prokaryotic membrane proteins: the dense alignment surface method. *Protein Eng.* 10, 673–676.
- Drescher, A., Ruf, S., Calsa, T., Carrer, H., and Bock, R. (2000). The two largest chloroplast genome-encoded open reading frames of higher plants are essential genes. *Plant J.* 22, 97–104.
- Dudek, J., Rehling, P., and van der Laan, M. (2013). Mitochondrial protein import: common principles and physiological networks. *Biochim. Biophys. Acta* 1833, 274–285.
- Fellerer, C., Schweiger, R., Schöngruber, K., Soll, J., and Schwenkert, S. (2011). Cytosolic HSP90 cochaperones HOP and FKBP interact with freshly synthesized chloroplast preproteins of Arabidopsis. *Mol. Plant* 4, 1133–1145.
- Flores-Pérez, Ú., Bédard, J., Tanabe, N., Lymperopoulos, P., Clarke, A.K., and Jarvis, P. (2016). Functional Analysis of the Hsp93/ClpC Chaperone at the Chloroplast Envelope. *Plant Physiol.* 170, 147–162.
- Ganesan, I., Shi, L.-X., Labs, M., and Theg, S.M. (2017). Evaluating the Functional Pore Size of Chloroplast TOC and TIC Protein Translocons. *bioRxiv* 188052.
- Glaser, S., van Dooren, G.G., Agrawal, S., Brooks, C.F., McFadden, G.I., Striepen, B., and Higgins, M.K. (2012). Tic22 is an essential chaperone required for protein import into the apicoplast. *J. Biol. Chem.* 287, 39505–39512.
- Goloubinoff, P., Christeller, J.T., Gatenby, A.A., and Lorimer, G.H. (1989). Reconstitution of active dimeric ribulose biphosphate carboxylase from an unfolded state depends on two chaperonin proteins and Mg-ATP. *Nature* 342, 884–889.
- Gross, J., and Bhattacharya, D. (2009). Reevaluating the evolution of the Toc and Tic protein translocons. *Trends Plant Sci.* 14, 13–20.
- Heins, L., Mehrle, A., Hemmler, R., Wagner, R., Küchler, M., Hörmann, F., Sveshnikov, D., and Soll, J. (2002). The preprotein conducting channel at the inner envelope membrane of plastids. *EMBO J.* 21, 2616–2625.
- Hinnah, S.C., Hill, K., Wagner, R., Schlicher, T., and Soll, J. (1997). Reconstitution of a chloroplast protein import channel. *EMBO J.* 16, 7351–7360.

- Hinnah, S.C., Wagner, R., Sveshnikova, N., Harrer, R., and Soll, J. (2002). The chloroplast protein import channel Toc75: pore properties and interaction with transit peptides. *Biophys. J.* 83, 899–911.
- Hörmann, F., Kuchler, M., Sveshnikov, D., Oppermann, U., Li, Y., and Soll, J. (2004). Tic32, an essential component in chloroplast biogenesis. *J. Biol. Chem.* 279, 34756–34762.
- Huang, P.-K., Chan, P.-T., Su, P.-H., Chen, L.-J., and Li, H. (2015). Chloroplast Hsp93 directly binds to transit peptides at an early stage of the preprotein import process. *Plant Physiol.* pp.01830.2015.
- Inaba, T., Li, M., Alvarez-Huerta, M., Kessler, F., and Schnell, D.J. (2003). atTic110 functions as a scaffold for coordinating the stromal events of protein import into chloroplasts. *J. Biol. Chem.* 278, 38617–38627.
- Inaba, T., Alvarez-Huerta, M., Li, M., Bauer, J., Ewers, C., Kessler, F., and Schnell, D.J. (2005). Arabidopsis tic110 is essential for the assembly and function of the protein import machinery of plastids. *Plant Cell* 17, 1482–1496.
- Inoue, H., Li, M., and Schnell, D.J. (2013). An essential role for chloroplast heat shock protein 90 (Hsp90C) in protein import into chloroplasts. *Proc. Natl. Acad. Sci. U. S. A.* 110, 3173–3178.
- Inoue, K., Baldwin, A.J., Shipman, R.L., Matsui, K., Theg, S.M., and Ohme-Takagi, M. (2005). Complete maturation of the plastid protein translocation channel requires a type I signal peptidase. *J. Cell Biol.* 171, 425–430.
- Jackson, D.T., Froehlich, J.E., and Keegstra, K. (1998). The Hydrophilic Domain of Tic110, an Inner Envelope Membrane Component of the Chloroplastic Protein Translocation Apparatus, Faces the Stromal Compartment. *J. Biol. Chem.* 273, 16583–16588.
- Jackson-Constan, D., and Keegstra, K. (2001). Arabidopsis genes encoding components of the chloroplastic protein import apparatus. *Plant Physiol.* 125, 1567–1576.
- Jelic, M., Soll, J., and Schleiff, E. (2003). Two Toc34 homologues with different properties. *Biochemistry (Mosc.)* 42, 5906–5916.
- Kao, A., Chiu, C., Vellucci, D., Yang, Y., Patel, V.R., Guan, S., Randall, A., Baldi, P., Rychnovsky, S.D., and Huang, L. (2011). Development of a Novel Cross-linking Strategy for Fast and Accurate Identification of Cross-linked Peptides of Protein Complexes. *Mol. Cell. Proteomics* 10, M110.002212.
- Kasmati, A.R., Töpel, M., Khan, N.Z., Patel, R., Ling, Q., Karim, S., Aronsson, H., and Jarvis, P. (2013). Evolutionary, molecular and genetic analyses of Tic22 homologues in Arabidopsis thaliana chloroplasts. *PloS One* 8, e63863.
- Kessler, F., and Blobel, G. (1996). Interaction of the protein import and folding machineries of the chloroplast. *Proc. Natl. Acad. Sci.* 93, 7684–7689.
- Kessler, F., and Schnell, D. (2009). Chloroplast biogenesis: diversity and regulation of the protein import apparatus. *Curr. Opin. Cell Biol.* 21, 494–500.
- Kikuchi, S., Bédard, J., Hirano, M., Hirabayashi, Y., Oishi, M., Imai, M., Takase, M., Ide, T., and Nakai, M. (2013). Uncovering the protein translocon at the chloroplast inner envelope membrane. *Science* 339, 571–574.

- Köhler, D., Montandon, C., Hause, G., Majovsky, P., Kessler, F., Baginsky, S., and Agne, B. (2015). Characterization of chloroplast protein import without Tic56, a component of the 1-megadalton translocon at the inner envelope membrane of chloroplasts. *Plant Physiol.* 167, 972–990.
- Köhler, D., Helm, S., Agne, B., and Baginsky, S. (2016). Importance of translocon subunit Tic56 for rRNA processing and chloroplast ribosome assembly. *Plant Physiol.*
- Kouranov, A., and Schnell, D.J. (1997). Analysis of the Interactions of Preproteins with the Import Machinery over the Course of Protein Import into Chloroplasts. *J. Cell Biol.* 139, 1677–1685.
- Kouranov, A., Chen, X., Fuks, B., and Schnell, D.J. (1998). Tic20 and Tic22 Are New Components of the Protein Import Apparatus at the Chloroplast Inner Envelope Membrane. *J. Cell Biol.* 143, 991–1002.
- Kovacheva, S., Bédard, J., Patel, R., Dudley, P., Twell, D., Ríos, G., Koncz, C., and Jarvis, P. (2005). In vivo studies on the roles of Tic110, Tic40 and Hsp93 during chloroplast protein import. *Plant J. Cell Mol. Biol.* 41, 412–428.
- Kovács-Bogdán, E., Benz, J.P., Soll, J., and Bölder, B. (2011). Tic20 forms a channel independent of Tic110 in chloroplasts. *BMC Plant Biol.* 11, 133.
- Krasilnikov, O.V., Sabirov, R.Z., Ternovsky, V.I., Merzliak, P.G., and Muratkhodjaev, J.N. (1992). A simple method for the determination of the pore radius of ion channels in planar lipid bilayer membranes. *FEMS Microbiol. Immunol.* 5, 93–100.
- Laemmli, U.K. (1970). Cleavage of Structural Proteins during the Assembly of the Head of Bacteriophage T4. *Nature* 227, 680.
- Lamberti, G., Gügel, I.L., Meurer, J., Soll, J., and Schwenkert, S. (2011). The cytosolic kinases STY8, STY17, and STY46 are involved in chloroplast differentiation in Arabidopsis. *Plant Physiol.* 157, 70–85.
- Lee, K.H., Kim, S.J., Lee, Y.J., Jin, J.B., and Hwang, I. (2003). The M Domain of atToc159 Plays an Essential Role in the Import of Proteins into Chloroplasts and Chloroplast Biogenesis. *J. Biol. Chem.* 278, 36794–36805.
- Lee, S.-Y., Kang, M.-G., Shin, S., Kwak, C., Kwon, T., Seo, J.K., Kim, J.-S., and Rhee, H.-W. (2017). Architecture Mapping of the Inner Mitochondrial Membrane Proteome by Chemical Tools in Live Cells. *J. Am. Chem. Soc.* 139, 3651–3662.
- Leister, D. (2003). Chloroplast research in the genomic age. *Trends Genet. TIG* 19, 47–56.
- Li, H., and Teng, Y.-S. (2013). Transit peptide design and plastid import regulation. *Trends Plant Sci.* 18, 360–366.
- Lübeck, J., Soll, J., Akita, M., Nielsen, E., and Keegstra, K. (1996). Topology of IEP110, a component of the chloroplastic protein import machinery present in the inner envelope membrane. *EMBO J.* 15, 4230–4238.
- Mahmoodi, M.M., Rashidian, M., Zhang, Y., and Distefano, M.D. (2015). Application of meta- and para- phenylenediamine as enhanced oxime ligation catalysts for protein labeling, PEGylation, immobilization and release. *Curr. Protoc. Protein Sci.* Editor. Board John E Coligan AI 79, 15.4.1-15.4.28.

- Martin, W., Rujan, T., Richly, E., Hansen, A., Cornelsen, S., Lins, T., Leister, D., Stoebe, B., Hasegawa, M., and Penny, D. (2002). Evolutionary analysis of Arabidopsis, cyanobacterial, and chloroplast genomes reveals plastid phylogeny and thousands of cyanobacterial genes in the nucleus. *Proc. Natl. Acad. Sci. U. S. A.* 99, 12246–12251.
- May, T., and Soll, J. (2000). 14-3-3 proteins form a guidance complex with chloroplast precursor proteins in plants. *Plant Cell* 12, 53–64.
- Moore, T., and Keegstra, K. (1993). Characterization of a cDNA clone encoding a chloroplast-targeted Clp homologue. *Plant Mol. Biol.* 21, 525–537.
- Nakamoto, H., Fujita, K., Ohtaki, A., Watanabe, S., Narumi, S., Maruyama, T., Suenaga, E., Misono, T.S., Kumar, P.K.R., Goloubinoff, P., et al. (2014). Physical interaction between bacterial heat shock protein (Hsp) 90 and Hsp70 chaperones mediates their cooperative action to refold denatured proteins. *J. Biol. Chem.* 289, 6110–6119.
- Nakrieko, K.-A., Mould, R.M., and Smith, A.G. (2004). Fidelity of targeting to chloroplasts is not affected by removal of the phosphorylation site from the transit peptide. *Eur. J. Biochem.* 271, 509–516.
- Nickel, C., Soll, J., and Schwenkert, S. (2015). Phosphomimicking within the transit peptide of pHCF136 leads to reduced photosystem II accumulation in vivo. *FEBS Lett.* 589, 1301–1307.
- Nielsen, E., Akita, M., Davila-Aponte, J., and Keegstra, K. (1997). Stable association of chloroplastic precursors with protein translocation complexes that contain proteins from both envelope membranes and a stromal Hsp100 molecular chaperone. *EMBO J.* 16, 935–946.
- Oreb, M., Zoryan, M., Vojta, A., Maier, U.G., Eichacker, L.A., and Schleiff, E. (2007). Phospho-mimicry mutant of atToc33 affects early development of Arabidopsis thaliana. *FEBS Lett.* 581, 5945–5951.
- Paila, Y.D., Richardson, L.G., Inoue, H., Parks, E.S., McMahon, J., Inoue, K., and Schnell, D.J. (2016). Multi-functional roles for the polypeptide transport associated domains of Toc75 in chloroplast protein import. *eLife* 5, e12631.
- Pain, D., and Blobel, G. (1987). Protein import into chloroplasts requires a chloroplast ATPase. *Proc. Natl. Acad. Sci. U. S. A.* 84, 3288–3292.
- Park, E., and Rapoport, T.A. (2012). Mechanisms of Sec61/SecY-mediated protein translocation across membranes. *Annu. Rev. Biophys.* 41, 21–40.
- Qbadou, S., Becker, T., Mirus, O., Tews, I., Soll, J., and Schleiff, E. (2006). The molecular chaperone Hsp90 delivers precursor proteins to the chloroplast import receptor Toc64. *EMBO J.* 25, 1836–1847.
- Ratnayake, R.M.U., Inoue, H., Nonami, H., and Akita, M. (2008). Alternative processing of Arabidopsis Hsp70 precursors during protein import into chloroplasts. *Biosci. Biotechnol. Biochem.* 72, 2926–2935.
- Ratzke, C., Hellenkamp, B., and Hugel, T. (2014). Four-colour FRET reveals directionality in the Hsp90 multicomponent machinery. *Nat. Commun.* 5, 4192.

- Reichert, A.J., Poxleitner, G., Dauner, M., and Skerra, A. (2015). Optimisation of a system for the co-translational incorporation of a keto amino acid and its application to a tumour-specific Anticalin. *Protein Eng. Des. Sel. PEDS* 28, 553–565.
- Reumann, null, and Keegstra, null (1999). The endosymbiotic origin of the protein import machinery of chloroplastic envelope membranes. *Trends Plant Sci.* 4, 302–307.
- Reumann, S., Inoue, K., and Keegstra, K. (2005). Evolution of the general protein import pathway of plastids (Review). *Mol. Membr. Biol.* 22, 73–86.
- Rhee, H.-W., Zou, P., Udeshi, N.D., Martell, J.D., Mootha, V.K., Carr, S.A., and Ting, A.Y. (2013). Proteomic Mapping of Mitochondria in Living Cells via Spatially-Restricted Enzymatic Tagging. *Science* 339, 1328–1331.
- Rial, D.V., Arakaki, A.K., and Ceccarelli, E.A. (2000). Interaction of the targeting sequence of chloroplast precursors with Hsp70 molecular chaperones. *Eur. J. Biochem.* 267, 6239–6248.
- Richardson, L.G., Jelokhani-Niaraki, M., and Smith, M.D. (2009). The acidic domains of the Toc159 chloroplast preprotein receptor family are intrinsically disordered protein domains. *BMC Biochem.* 10, 35.
- Richter, S., and Lamppa, G.K. (1998). A chloroplast processing enzyme functions as the general stromal processing peptidase. *Proc. Natl. Acad. Sci.* 95, 7463–7468.
- Rosano, G.L., Bruch, E.M., and Ceccarelli, E.A. (2011). Insights into the CLP/HSP100 Chaperone System from Chloroplasts of *Arabidopsis thaliana*. *J. Biol. Chem.* 286, 29671–29680.
- Rudolf, M., Machettira, A.B., Groß, L.E., Weber, K.L., Bolte, K., Bionda, T., Sommer, M.S., Maier, U.G., Weber, A.P.M., Schleiff, E., et al. (2013). In vivo function of Tic22, a protein import component of the intermembrane space of chloroplasts. *Mol. Plant* 6, 817–829.
- Sambrook, J., Maniatis, T., Fritsch, E.F., and Laboratory, C.S.H. (1987). *Molecular cloning : a laboratory manual* (Cold Spring Harbor, N.Y. : Cold Spring Harbor Laboratory Press).
- Schleiff, E., Soll, J., Küchler, M., Kühlbrandt, W., and Harrer, R. (2003). Characterization of the translocon of the outer envelope of chloroplasts. *J. Cell Biol.* 160, 541–551.
- Schnell, D.J., and Blobel, G. (1993). Identification of intermediates in the pathway of protein import into chloroplasts and their localization to envelope contact sites. *J. Cell Biol.* 120, 103–115.
- Schnell, D.J., Kessler, F., and Blobel, G. (1994). Isolation of components of the chloroplast protein import machinery. *Science* 266, 1007–1012.
- Schünemann, D. (2007). Mechanisms of protein import into thylakoids of chloroplasts. *Biol. Chem.* 388, 907–915.
- Schweiger, R., Müller, N.C., Schmitt, M.J., Soll, J., and Schwenkert, S. (2012). AtTPR7 is a chaperone-docking protein of the Sec translocon in *Arabidopsis*. *J. Cell Sci.* 125, 5196–5207.
- Shi, L.-X., and Theg, S.M. (2010). A stromal heat shock protein 70 system functions in protein import into chloroplasts in the moss *Physcomitrella patens*. *Plant Cell* 22, 205–220.



- Shingles, R., and McCarty, R.E. (1995). Production of membrane vesicles by extrusion: size distribution, enzyme activity, and orientation of plasma membrane and chloroplast inner-envelope membrane vesicles. *Anal. Biochem.* 229, 92–98.
- Shu, X., Lev-Ram, V., Deerinck, T.J., Qi, Y., Ramko, E.B., Davidson, M.W., Jin, Y., Ellisman, M.H., and Tsien, R.Y. (2011). A Genetically Encoded Tag for Correlated Light and Electron Microscopy of Intact Cells, Tissues, and Organisms. *PLOS Biol.* 9, e1001041.
- Sjuts, I., Soll, J., and Bölter, B. (2017). Import of Soluble Proteins into Chloroplasts and Potential Regulatory Mechanisms. *Front. Plant Sci.* 8.
- Smart, O.S., Breed, J., Smith, G.R., and Sansom, M.S. (1997). A novel method for structure-based prediction of ion channel conductance properties. *Biophys. J.* 72, 1109–1126.
- Sohrt, K., and Soll, J. (2000). Toc64, a new component of the protein translocon of chloroplasts. *J. Cell Biol.* 148, 1213–1221.
- Sommer, M., Rudolf, M., Tillmann, B., Tripp, J., Sommer, M.S., and Schleiff, E. (2013). Toc33 and Toc64-III cooperate in precursor protein import into the chloroplasts of *Arabidopsis thaliana*. *Plant Cell Environ.* 36, 970–983.
- Sommer, M.S., Daum, B., Gross, L.E., Weis, B.L.M., Mirus, O., Abram, L., Maier, U.-G., Kühlbrandt, W., and Schleiff, E. (2011). Chloroplast Omp85 proteins change orientation during evolution. *Proc. Natl. Acad. Sci. U. S. A.* 108, 13841–13846.
- Stahl, T., Glockmann, C., Soll, J., and Heins, L. (1999). Tic40, a new “old” subunit of the chloroplast protein import translocon. *J. Biol. Chem.* 274, 37467–37472.
- Stengel, A., Benz, J.P., Buchanan, B.B., Soll, J., and Bölter, B. (2009). Preprotein import into chloroplasts via the Toc and Tic complexes is regulated by redox signals in *Pisum sativum*. *Mol. Plant* 2, 1181–1197.
- Su, P.-H., and Li, H. (2010). Stromal Hsp70 is important for protein translocation into pea and *Arabidopsis* chloroplasts. *Plant Cell* 22, 1516–1531.
- Sugiura, M. (1989). The chloroplast chromosomes in land plants. *Annu. Rev. Cell Biol.* 5, 51–70.
- Sun, Y.-J., Forouhar, F., Li Hm, H., Tu, S.-L., Yeh, Y.-H., Kao, S., Shr, H.-L., Chou, C.-C., Chen, C., and Hsiao, C.-D. (2002). Crystal structure of pea Toc34, a novel GTPase of the chloroplast protein translocon. *Nat. Struct. Biol.* 9, 95–100.
- Thompson, A., Schäfer, J., Kuhn, K., Kienle, S., Schwarz, J., Schmidt, G., Neumann, T., and Hamon, C. (2003). Tandem Mass Tags: A Novel Quantification Strategy for Comparative Analysis of Complex Protein Mixtures by MS/MS. *Anal. Chem.* 75, 1895–1904.
- Timmis, J.N., Ayliffe, M.A., Huang, C.Y., and Martin, W. (2004). Endosymbiotic gene transfer: organelle genomes forge eukaryotic chromosomes. *Nat. Rev. Genet.* 5, 123–135.
- Tranel, P.J., Froehlich, J., Goyal, A., and Keegstra, K. (1995). A component of the chloroplastic protein import apparatus is targeted to the outer envelope membrane via a novel pathway. *EMBO J.* 14, 2436–2446.

- Trösch, R., and Jarvis, P. (2011). The stromal processing peptidase of chloroplasts is essential in *Arabidopsis*, with knockout mutations causing embryo arrest after the 16-cell stage. *PloS One* 6, e23039.
- Tsai, J.-Y., Chu, C.-C., Yeh, Y.-H., Chen, L.-J., Li, H.-M., and Hsiao, C.-D. (2013). Structural characterizations of the chloroplast translocon protein Tic110. *Plant J. Cell Mol. Biol.* 75, 847–857.
- Vandenbossche, G.M.R., Van Oostveldt, P., and Remon, J.P. (1991). A fluorescence method for the determination of the molecular weight cut-off of alginate-polylysine microcapsules. *J. Pharm. Pharmacol.* 43, 275–277.
- Vojta, L., Soll, J., and Bölter, B. (2007). Protein transport in chloroplasts - targeting to the intermembrane space. *FEBS J.* 274, 5043–5054.
- de Vries, J., Sousa, F.L., Bölter, B., Soll, J., and Gould, S.B. (2015). YCF1: A Green TIC? *Plant Cell* 27, 1827–1833.
- Waegemann, K., and Soll, J. (1996). Phosphorylation of the transit sequence of chloroplast precursor proteins. *J. Biol. Chem.* 271, 6545–6554.
- Waegemann, K., Eichacker, S., and Soll, J. (1992). Outer envelope membranes from chloroplasts are isolated as right-side-out vesicles. *Planta* 187, 89–94.
- Wirmer, J., and Westhof, E. (2006). Molecular contacts between antibiotics and the 30S ribosomal particle. *Methods Enzymol.* 415, 180–202.
- Yang, X.-F., Wang, Y.-T., Chen, S.-T., Li, J.-K., Shen, H.-T., and Guo, F.-Q. (2016). PBR1 selectively controls biogenesis of photosynthetic complexes by modulating translation of the large chloroplast gene *Ycf1* in *Arabidopsis*. *Cell Discov.* 2.
- Young, J.C., Hoogenraad, N.J., and Hartl, F.U. (2003). Molecular chaperones Hsp90 and Hsp70 deliver preproteins to the mitochondrial import receptor Tom70. *Cell* 112, 41–50.
- Young, M.E., Keegstra, K., and Froehlich, J.E. (1999). GTP promotes the formation of early-import intermediates but is not required during the translocation step of protein import into chloroplasts. *Plant Physiol.* 121, 237–244.
- Zollmann, T., Moiset, G., Tumulka, F., Tampé, R., Poolman, B., and Abele, R. (2015). Single liposome analysis of peptide translocation by the ABC transporter TAPL. *Proc. Natl. Acad. Sci.* 112, 2046–2051.

## Curriculum Vitae

### Personal data

Family name: Sjuts

First name: Inga

### Education

- |                 |   |
|-----------------|---|
| since 04/2014   | PhD student, Plant Biochemistry<br>Ludwig-Maximilians-University, Munich, Germany<br>PhD thesis: Topology and function of the inner envelope protein<br>Tic110  |
| 10/2011-01/2014 | Master of Science in Microbiology and Biochemistry<br>Georg-August-University, Göttingen, Germany<br>Master thesis: Natural diversity of the <i>Arabidopsis-Verticillium</i><br>interaction                                   |
| 10/2008-07/2011 | Bachelor of Science in Biochemistry<br>University of Ulm, Ulm, Germany<br>Bachelor thesis: Investigation of selected protein-protein interactions<br>with a fluorescence-based Split-Ubiquitin-System in <i>S. cerevisiae</i> |
| 09/2007-07/2008 | Language schools Società Dante Alighieri and Casa Italiana, Rom   |
| 09/2000-06/2007 | German Abitur<br>Ubbo-Emmius-Gymnasium, Leer, Germany   |

### Publications

Sjuts I, Soll J and Bölder B (2017). Import of Soluble Proteins into Chloroplasts and Potential Regulatory Mechanisms. *Front. Plant Sci.*8:168. doi: 10.3389/fpls.2017.00168

## **Poster**

Sjuts I, de Vries J, Soll J, Gould S, Bölter B: Tic110: still the main translocation channel in protein import into chloroplasts.

EMBO Conference - Mechanisms and Regulation of Protein Translocation.

March 21 - 25, 2015, Dubrovnik, Croatia.

68. Mosbacher Kolloquium - Cell Organelles - Origin, Dynamics and Communication

March 29 - April 1, 2017, Mosbach, Germany.

## **Talks**

Protein Translocases in the Inner Envelope Membrane of Chloroplasts

Gordon Research Conference - Organellar Channels and Transporters

July 30 - August 4, 2017, Vermont, USA.

## **Eidesstattliche Versicherung**

Ich versichere hiermit an Eides statt, dass die vorgelegte Dissertation von mir selbständig und nur unter Verwendung der angegebenen Hilfsmittel und Quellen angefertigt wurde.

München, den 8.5.2018

---

Inga Sjuts

## **Erklärung**

Hiermit erkläre ich, dass ich zuvor nicht versucht habe, anderweitig eine Dissertation einzureichen oder mich einer Doktorprüfung zu unterziehen. Die vorliegende Dissertation wurde keiner weiteren Prüfungskommission weder in Teilen noch als Ganzes vorgelegt.

München, den 8.5.2018

---

Inga Sjuts

## Versicherung der Co-Autoren

Hiermit wird im Namen aller Co-Autoren versichert, dass sämtliche Passagen dieser Arbeit, die wörtlich oder nahezu wörtlich aus der unten aufgeführten Veröffentlichung entnommen wurden, vom Autor dieser Dissertation selbst stammen.

München, den 8.5.2018

---

Jürgen Soll

Siuts I, Soll J and Bölter B (2017). Import of Soluble Proteins into Chloroplasts and Potential Regulatory Mechanisms. *Front. Plant Sci.*8:168. doi: 10.3389/fpls.2017.00168

Das Copyright des Verlags wird dadurch gewahrt, dass es sich in der vorliegenden Dissertation um eine akademische, nicht-kommerzielle Veröffentlichung handelt und die entsprechenden Originalartikel ordnungsgemäß zitiert werden.

## **Danksagung**

Die Danksagung wurde aus Datenschutzgründen entfernt.